THE UNIVERSITY OF ALBERTA

PRELIMINARY STUDY OF THE USE OF LASER DOPPLER ANAEMOMETRY IN PUMP SUMP DESIGN

by

© SIDNEY J. LODEWYK

A THESIS

SUBMITTED TO THE FACULTY OF GRADUATE STUDIES AND RESEARCH

IN PARTIAL FULFILMENT OF THE REQUIREMENTS FOR THE DEGREE

OF MASTER OF SCIENCE

DEPARTMENT OF CIVIL ENGINEERING

EDMONTON, ALBERTA

FALL, 1986

Permission has been granted to the National Library of Canada to microfilm this thesis and to lend or sell copies of the film.

The author (copyright owner) has reserved other publication rights, and neither the thesis nor extensive extracts from it may be printed or otherwise reproduced without his/her written permission.

L'autorisation a été accordée à la Bibliothèque nationale du Canada de microfilmer cette thèse et de prêter ou de vendre des exemplaires du film.

L'auteur (titulaire du droit d'auteur) se réserve les autres droits de publication; ni la thèse ni de longs extraits de celle-ci ne doivent être imprimés ou autrement reproduits sans son autorisation écrite.

ISBN 0-315-32385-X

THE UNIVERSITY OF ALBERTA

RELEASE FORM

NAME OF AUTHOR SIDNEY J. LODEWYK

TITLE OF THESIS PRELIMINARY STUDY OF THE USE OF LASER DOPPLER ANAEMOMETRY IN PUMP SUMP DESIGN

DEGREE FOR WHICH THESIS WAS PRESENTED MASTER OF SCIENCE

YEAR THIS DEGREE GRANTED FALL, 1986

Permission is hereby granted to THE UNIVERSITY OF ALBERTA LIBRARY to reproduce single copies of this thesis and to lend or sell such copies for private, scholarly or scientific research purposes only.

The author reserves other publication rights, and neither the thesis nor extensive extracts from it may be printed or otherwise reproduced without the author's written permission.

(SIGNED) Sid Lodewyk

PERMANENT ADDRESS:

7-10620 83 Ave.

Edmonton, Alta.

T6E 2E2

DATED July 30 1986

THE UNIVERSITY OF ALBERTA

FACULTY OF GRADUATE STUDIES AND RESEARCH

The undersigned certify that they have read, and recommend to the Faculty of Graduate Studies and Research, for acceptance, a thesis entitled PRELIMINARY STUDY OF THE USE OF LASER DOPPLER ANAEMOMETRY IN PUMP SUMP DESIGN submitted by SIDNEY J. LODEWYK in partial fulfilment of the requirements for the degree of MASTER OF SCIENCE in CIVIL ENGINEERING.

.....

Supervisor

.....

.....

Date.....July 28/86.....

ABSTRACT

The hydraulic design of pump sumps is a common and difficult task. The flow patterns in a sump are too complex for theoretical analysis, and empirical rules will not guarantee success. A hydraulic model study is required to ensure that the installed sump will perform adequately. However, even a model study is not completely reliable, as there is no firm concensus as to what criteria should be used to size the model.

This thesis first reviews the literature on the design of pump sumps. The major aspects of good and poor sump designs are discussed, and the arguments for and against the use of Reynolds and Froude criteria in modelling sumps are presented. The paper goes on to present an experimental study of the flow structure in a pump sump. The many merits of laser Doppler anaemometry in the hydraulic design of sump models are brought forward as a superior alternative to other design methods.

ACKNOWLEDGEMENTS

The Author would like to thank Dr. N. Rajaratnam and Prof. A.W. Peterson for their support and guidance in this study. The assistance of Dr. P. Steffler with the Laser Doppler Anaemometer was invaluable. The assistance of S. Lovell and L. Flint-Petersen, staff at the T. Blench Hydraulics Laboratory, in setting up the experimental apparatus is also greatly appreciated. Financial support for this study was provided by the Natural Sciences and Engineering Research Council by means of grants to Dr. N. Rajaratnam and Prof. A.W. Peterson. This support is gratefully acknowledged.

Table of Contents

Chapter — Page

1. PART ONE: LITERATURE REVIEW 1

1.1 INTRODUCTION 1

1.2 General Aspects of Sump Design 1

1.2.1 Why Modelling is Important in Pump Sump Design 1

1.2.2 Applications of Pump Sumps 2

1.2.3 Hydraulic Problems in Pump Sumps 3

1.2.4 Hydraulic Features of Pump Sumps 4

1.3 Modelling flow in Pump Sumps 5

1.4 Relaxing Surface Tension Similarity 8

1.4.1 Reynolds Criteria Relaxation 10

1.4.2 Modelling using the Froude Criteria 12

1.5 Factors to Consider in Pump Sump Design 13

1.5.1 Evaluating Pump Sump Performance 15

1.5.2 Minimum Sump Volumes 18

1.5.3 Aspects of Good Sump Design 19

1.5.4 Aspects of Poor Sump Design 20

1.5.5 Sources of Vorticity 23

1.5.6 Improving Poor Sump Designs 25

1.5.6.1 Surface Vortex Elimination 25

1.5.6.2 Supression of Floor Vorticies 26

1.5.6.3 Supression of Wall Vorticies 27

1.5.6.4 Sump Dividing Walls 28

1.6 Conclusions 28

2. PART TWO: EXPERIMENTAL STUDY 33

2.1 INTRODUCTION 33

2.2 Laser Doppler Anaemometry 34

2.2.1 Some Physics of LDA Flow Measurement 34

2.2.2 LDA Equipment Used in Tests 35

2.3 Experimental Arrangement 39

2.4 Experimental Procedure 39

2.4.1 Measuring Flow Velocities in the Sump 43

2.4.2 Percent of Flow in the Study Zone 44

2.4.3 Checks on the LDA Velocities 45

2.4.4 Visualizing the Flow 46

2.5 Vorticity Meter 47

2.6 Structure of Flow in the Unimproved Sump 48

2.6.1 The Main Sump 53

2.6.2 Structure of Flow Under the Intake Bell ...61

2.6.3 Inside the Intake Pipes 77

2.7 Structure of Flow in the Improved Sump 85

2.7.1 The Main Sump 90

2.7.2 Structure of Flow Under the Bell 95

2.7.3 Flow in the Intake Cylinders 112

3. Conclusions 124

3.1 Comparing the Two Sump Designs 124

3.2 The Usefulness of LDA measurements in Pump Sump Design 125

3.3 Recommendations for Further Study 134

4. References 135

5. APPENDIX A: Velocities from the propeller probe. ...143

6. APPENDIX B: Data for the unimproved sump. 145

7. APPENDIX C: Data for the improved sump. 158

LIST OF FIGURES

FIGURE PAGE

1. Definition Sketch of Pump Sump.....6
2. Variation of Vortex Type with Reynolds and Froude Numbers.....14
3. Vortex Classification System.....16
4. Typical Intake Bellmouth Detail.....21
5. Good Sump Designs.....22
6. Poor Sump Designs.....24
7. Draft Tube Sump Intake.....29
8. Sump Improvement Devices.....30
9. Flow Improvement Devices.....31
10. Schematic Diagram of the Laser Doppler Anaemometer....37
11. Overall view of the Sump set up.....40
12. Plan view of the unimproved sump showing dimensions...41
13. Plan view of improved sump showing dimensions of the improvements.....42
14. Side view of sump showing operating conditions.....49
15. Patterns of flow in the unimproved sump. Results of the dye test.....50
16. Plan view of the glass floor section of the sump indicating the locations of the cross-sections where data was taken. 51
17. Longitudinal velocity profiles for the first section in the unimproved sump.....52
18. Longitudinal velocity profiles for the second section in

the unimproved sump.....54
19. Longitudinal velocity profiles for the third section in the unimproved sump.....55
20. Longitudinal velocity profiles for the area on the south side of the south intake in the unimproved sump.....56
21. Longitudinal velocity profiles for the area on the north side of the north intake in the unimproved sump.....57
22. Longitudinal velocity profiles for the section between the bells of the improved sump.....59
23. Longitudinal velocity profiles for the section near the back wall of the unimproved sump.....60
24. Longitudinal turbulent velocity fluctuations for the first section in unimproved sump.....62
25. Longitudinal turbulent velocity fluctuations for the second section in unimproved sump.....63
26. Longitudinal turbulent velocity fluctuations for the third section in unimproved sump.....64
27. Longitudinal turbulent velocity fluctuations for the section between the bells of the unimproved sump.....65
28. Longitudinal turbulent velocity fluctuations for the section near the back wall of the unimproved sump....66
29. Longitudinal velocity profiles for the area under the north bell, section 1 in the area xubels of figure 16.....67
30. Longitudinal velocity profiles for the area under the north bell, section 2 in the area xubels of figure 16.....68

31. Longitudinal velocity profiles for the area under the north bell, section 3 in the area xubels of figure 16.....69
32. Longitudinal velocity profiles for the area under the north bell, section 4 in the area xubels of figure 16.....70
33. Longitudinal velocity profiles for the area under the north bell, section 5 in the area xubels of figure 16.....71
34. Longitudinal turbulent velocity fluctuations for the area under the north bell, section 1 in the area xubels of figure 16.....72
35. Longitudinal turbulent velocity fluctuations for the area under the north bell, section 2 in the area xubels of figure 16.....73
36. Longitudinal turbulent velocity fluctuations for the area under the north bell, section 3 in the area xubels of figure 16.....74
37. Longitudinal turbulent velocity fluctuations for the area under the north bell, section 4 in the area xubels of figure 16.....75
38. Longitudinal turbulent velocity fluctuations for the area under the north bell, section 5 in the area xubels of figure 16.....76
39. Vertical profiles of the transverse velocity under the north bell of the unimproved sump, profiles at y = 0 in the area xubels.....78

40. Vertical profiles of the transverse velocity under the north bell of the unimproved sump, profiles at y = 35 in the area xubels.....79
41. Vertical profiles of the transverse velocity under the north bell of the unimproved sump, profiles at y = 70 in the area xubels.....80
42. Vertical profiles of the transverse velocity under the north bell of the unimproved sump, profiles at y = 105 in the area xubels.....81
43. Vertical profiles of the transverse velocity under the north bell of the unimproved sump, profiles at y = 140 in the area xubels.....82
44. Vertical velocity profiles taken at one quarter of the pipe diameter from the inside wall of the south intake pipe.....83
45. Vertical velocity profiles taken at one quarter of the pipe diameter from the inside wall of the north intake pipe.....84
46. Patterns of flow in the improved sump. Results of the dye test.....88
47. Plan view of the glass floor section of the improved sump indicating the locations of the cross-sections where data was taken.....89
48. Longitudinal velocity profiles for the first section in the improved sump.....91
49. Longitudinal velocity profiles for the second section in the improved sump.....92

50. Longitudinal velocity profiles for the third section in the improved sump.....94
51. Longitudinal velocity profiles for the area on the south side of the south intake in the improved sump.....96
52. Longitudinal velocity profiles for the area on the north side of the north intake in the unimproved sump.....97
53. Longitudinal velocity profiles for the section between the bells of the improved sump.....98
54. Longitudinal velocity profiles for the section near the back wall of the improved sump.....99
55. Longitudinal turbulent velocity fluctuations for the first section in improved sump.....100
56. Longitudinal turbulent velocity fluctuations for the second section in improved sump.....101
57. Longitudinal turbulent velocity fluctuations for the third section in improved sump.....102
58. Longitudinal turbulent velocity fluctuations for the section between the bells of the improved sump.....103
59. Longitudinal turbulent velocity fluctuations for the section near the back wall of the improved sump.....104
60. Longitudinal velocity profiles for the area under the north bell, section 1 in the area xubels of figure 47. 105
61. Longitudinal velocity profiles for the area under the north bell, section 2 in the area xubels of figure 47.....106
62. Longitudinal velocity profiles for the area under the

north bell, section 3 in the area xubels of figure 47.....108
63. Longitudinal velocity profiles for the area under the north bell, section 4 in the area xubels of figure 47.....109
64. Longitudinal velocity profiles for the area under the north bell, section 5 at in the area xubels of figure 47.....110
65. Longitudinal turbulent velocity fluctuations for the area under the north bell, section 1 in the area xubels of figure 47.....111
66. Longitudinal turbulent velocity fluctuations for the area under the north bell, section 2 in the area xubels of figure 47.....113
67. Longitudinal turbulent velocity fluctuations for the area under the north bell, section 3 in the area xubels of figure 47.....114
68. Longitudinal turbulent velocity fluctuations for the area under the north bell, section 4 in the area xubels of figure 47.....115
69. Longitudinal turbulent velocity fluctuations for the area under the north bell, section 5 in the area xubels of figure 47.....116
70. Vertical profiles of the transverse velocity under the north bell of the improved sump in the area xubels..117
71. Vertical profiles of the transverse velocity under the north bell of the improved sump in the area xubels..118

72. Vertical profiles of the transverse velocity under the north bell of the improved sump in the area xubels..119
73. Vertical profiles of the transverse velocity under the north bell of the improved sump in the area xubels..120
74. Vertical velocity profiles taken at one quarter of the pipe diameter from the inside wall of the south intake pipe.....121
75. Vertical velocity profiles taken at one quarter of the pipe diameter from the inside wall of the north intake pipe.....122
76. Comparison of velocity profiles of the two sump designs in the main sump.....126
77. Velocity vectors under the bell of the unimproved sump.....127
78. Velocity vectors under the bell of the improved sump showing the near radial flow into the intake.....128
79. Comparison of the velocity profiles inside the intake for the two sump designs.....129
80. Velocity vectors in the unimproved sump.....130
81. Velocity vectors in the improved sump.....131
82. Velocity vectors near the floor of the unimproved sump.....132
83. Velocity vectors near the floor of the improved sump.133
A1. View of the sump showing where the velocity measurements were taken with the propeller probe.....143

LIST OF PLATES

1. Laser Doppler anaemometer set up under the sump showing traverse, laser source (lower left), and front lens (top). 38
2. View of laser beams penetrating the floor of the sump. The location where the velocity is read is at the interrsection of the beams.....38
3. Cavitation core of the bell to bell vortex is visable as a white line of air bubbles. Note that for plates 3, 5 and 6 the flows have been increased by 2.4 l/s, and the submergence decreased by 6 cm to allow photographs of the flow problems to be taken. 86
4. Strong cavitation core is visible in the floor vortex below the intake bell. This picture taken at design flows in the unimproved sump.....86
5. Surface dimple in severe flows illustrates how vorticies are created by being shed from the intake cylinders. 87
6. Wall to bell vortex is revealed by its cavitation core, the white line connecting the bell to the wall. View is from below the sump.....87

List of Symbols

U - Average velocity in the longitudinal, or x direction.

V - Average velocity in the transverse, or y direction.

$\overline{u'^2}$ - Turbulent fluctuations of the x direction velocity.

$\overline{v'^2}$ - Turbulent fluctuations of the y direction velocity.

$\overline{u'v'}$ - Turbulent shear stress.

xsect1 - The section in the main sump where data was taken, refer to figures 16 and 47 for locations of this and the following sections.

xsect2 - The centre main sump section where data was taken.

xsect3 - The third section in the main sump where data was taken, this section is nearest the entrance.

xback - A section near the back wall where data was taken.

xbbels - A section where data was taken between the bells.

xsside - The section on the south side of the bell.

xnside - The section on the north side of the bell.

xubels - The area under the north bell consisting of five sections, one through five with section one closest to the backwall.

NOTE: Where other author's equations are used, variables in the equations are defined in the text.

1. PART ONE: LITERATURE REVIEW

1.1 INTRODUCTION

Pump sumps are a necessary feature in most operations that use fluids. The hydraulic design of a pumping station involves the flow through the pump, the discharge system, as well as the channelling of the fluid into the pump (the pump sump). The trend for pumping stations in recent years has been towards larger capacity pumps. As pumps become larger, the casing wall and support structure rigidity does not increase in proportion to the size, making large facilities more susceptable to vibration. To prevent vibration problems and achieve adequate performance in large pumps, better entrance and sump conditions are required. This increased need for high performance in sumps has led to the intense study of flow problems in pump sumps. The first part of this thesis presents a summary of the work done in this area to date.

1.2 General Aspects of Sump Design

1.2.1 Why Modelling is Important in Pump Sump Design

The complex nature of the flow patterns in pump sump limits the method of design to the use of a hydraulic model. Analytical solutions are impossible due to the complex nature of the problem, and empirical rules cannot eliminate all possible hydraulic problems. The model must reproduce

any flow separation, air entrainment, and development of vorticies and eddies that occur in the prototype under scaled conditions. The model should allow for the conditions where one of a series of several pumps in a sump is shut down or operating at a lower capacity. The entrance conditions as well as the sump itself have a large influence on the overall performance and should be modelled carefully.

1.2.2 Applications of Pump Sumps

Pump sumps are used in too many areas to be listed here, but a few applications in the field of Civil Engineering are listed below.

Irrigation - In this application water is pumped from a river or reservoir into a system of pipes or canals. The water is usually untreated.

Water Supply - This is similar to the Irrigation application except that the water may or may not be treated.

Storm Water - This involves the pumping of untreated water from a culvert or sump into another culvert.

Sewage - This involves the transferring of water to and from sewage works.

Dewatering - This is important in ship drydocks, farming and navigation locks.

Cooling Water - This is very important in both Nuclear and Thermoelectric power generation, and involves the pumping of water into the cooling system of the plant.

The importance of reliable supplies of cooling water in the Nuclear power industry is a large factor behind the recent interest in sump design. Because nuclear power plants cannot shut down quickly, the need for a trouble free source of cooling water is paramount.

1.2.3 Hydraulic Problems in Pump Sumps

Following Tullis (1979), the problems associated with the operation of sumps can be separated into six categories, but almost all have to do with fluid rotation in the sump itself. This fluid rotation may result from unsymmetrical sump layouts or sharp corners that cause separation of the flow. Solutions to these problems will be discussed in the third section.

1. *Surface Vorticies* - When severe enough, these may draw air from the surface into the pump causing imbalanced impeller loading, vibration and cavitation. The strength of a vortex is often rated as shown in figure 3.
2. *Subsurface Vorticies* - These emanate from the floor, side walls or back walls and enter the pump causing vibration and cavitation.
3. *Prerotation of flow entering Intake* - This will change the angle of attack on the impeller blades and reduce efficiency.
4. *Uneven Distribution of Flow entering the Pump Throat* -

This will result in imbalanced loading of the impeller blades and vibration.

5. *Fluctuations in Velocities at Pump Throat* - This may cause vibration and cavitation.
6. *Separation of Flow from the Intake Lip* — This is more a problem of pump design, but can also lead to severe vibration and cavitation.

The above list covers the basic problems in sump design. A more detailed list is given by Prosser, 1977. These problems can be very serious, and correcting them may entail plant shut-down.

1.2.4 Hydraulic Features of Pump Sumps

Prosser describes a typical pump sump as consisting of four separate zones. The first zone, the inlet, is where the water is channelled into the sump either through a pipe, or as free surface flow. There may be several inlet channels. The final entry into the sump is often through a control structure such as a weir.

The second zone, the approach flow area, contains items such as screens to remove debris, flow straighteners, and dividing walls that direct the flow into separate sumps.

The third zone is the sump itself. The sump is generally rectangular with a flat floor, and may serve more than one pump. The intake for the pump may be suspended, or

built either partially or completely into the wall or floor. The primary purpose of the sump is to provide stored fluid for the pump, and to damp out any flow problems originating in the second zone.

The fourth zone is the portion of pipe between the intake and the pump impeller. This zone must always be full of water to ensure that no cavitation and imbalanced impeller loading occurs in the pump. If this zone is too long, a large pressure drop may exist between the pump and the intake, increasing the risk of cavitation. These zones are illustrated in figure 1.

1.3 Modelling flow in Pump Sumps

The question of what criteria should be used when modelling the complex flows of pump sumps can be clarified using some theory. Hecker (1984) and others have shown, from dimensional analysis or consideration of the Reynolds equations, that the formation of a vortex of a certain type (VT) is dependent on five variables. These five variables are the relative submergence (s/r), the circulation number (ΓN), the Froude number (F), the Reynolds number (R), and the Weber number (W).

$$VT = f(s/r, \Gamma N, F, R, W) \text{ where,}$$

$$\Gamma N = \Gamma r/Q$$

$$F = Q/(rs)/(gs)^{0.5}$$

$$R = Q/(\nu s)$$

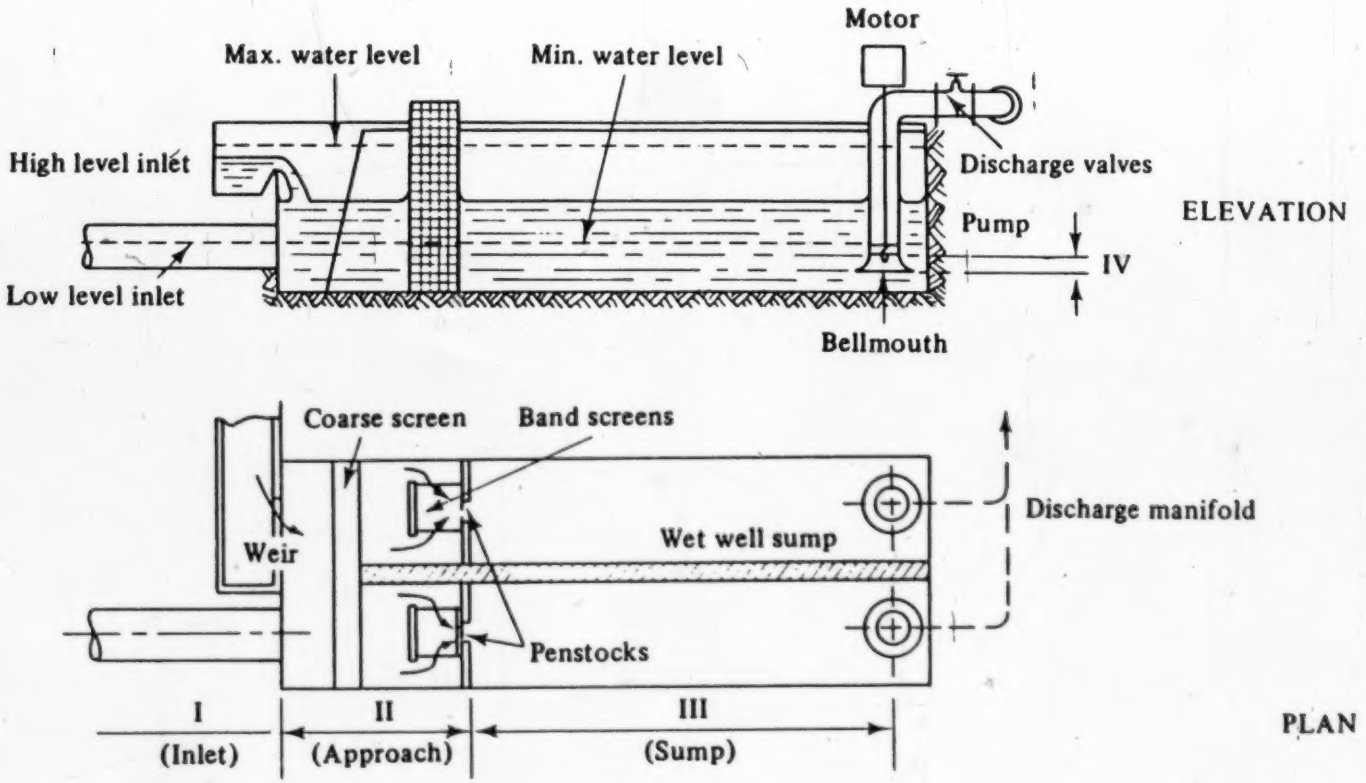

Figure 1. Definition Sketch of Pump Sump. (adapted from Prosser, 1977)

$W = \rho u^2 d/\sigma$

or $W_2 = \rho s Q^2/(A^2\sigma)$

f = a function dependant on the geometry and roughness of the intake.

And, s = submergence of intake.

r = radius of intake pipe.

d = diameter of intake pipe.

σ = surface tension.

Γ = circulation.

Q = discharge.

ρ = fluid density.

ν = kinematic viscosity.

g = gravitational acceleration.

u = fluid velocity.

These equations are useful in that they define the important parameters, but the presence of vorticies and other flow problems cannot be predicted from them.

Dynamic similarity requires that all five of these parameters have the same value in the model and prototype. To reduce the physical scale in the model several of these parameters must be neglected, since the only way complete similarity can be achieved using water is at full scale. For free surface models, the most important requirement is the similarity of the Froude number. This is also the case in

pump sump models, but the swirling flows and air core vorticies cause other parameters to be important as well. The two parameters most often neglected or 'relaxed' are the Weber number and the Reynolds number, for reasons that will be examined in the following text.

1.4 Relaxing Surface Tension Similarity

The similarity of surface tension phenomena is achieved when the Weber numbers are the same in the model and prototype. There is no real consensus on how well flow is modelled when the similarity of surface tension is neglected, or on how to allow for the scale effects. Daggett and Keulegan (1974) used different fluids to investigate the effects of surface tension on model size. They found that surface tension did not affect scaled vortex flow significantly, and that the scaled critical intake submergence was modeled correctly. Other researchers will not go this far in neglecting surface tension.

Guidelines are given by some researchers on how to take scale effects into account. Anwar (1965) states that while the air core size is not modeled correctly with the froude criteria, the prototype vortex size may be calculated from the correctly scaled circulation. He later found (1977) that as long the Weber number (W_2) was 1×10^4 or larger there were no surface tension scale effects. Jain *et al* (1978) found that as long as the weber number W was greater than 120 no scale effects were present. McCorquodale (1968) also

found that vortex sizes were not modeled correctly by Froude criteria and that the relative size of the air core was smaller in small models due to the stronger surface tension. He found that the scale effects became significant when the intake orifice was less than 2 inches in diameter, but were negligible when the orifice was larger.

Odgaard (1984) is another proponent of limiting the values of certain parameters to justify neglecting surface tension scale effects. He developed two equations of surface tension parameters from theory. When these 'surface tension factors' S_1 and S_2 are below a limiting value, surface tension effects become negligible.

$$S_1 = 0.335\sigma(g/(cH^2\nu^2))^{0.2}/(\gamma H)$$

$$S_2 = 147\sigma(cH^2\nu^2/g)^{0.2}/(\rho\Gamma^2)$$

where, σ = surface tension.

ν = kinematic viscosity.

H = air core depth.

c = shear drag coefficient.

Γ = circulation.

γ = unit weight.

ρ = fluid density.

g = acceleration due to gravity.

Yildrim and Jain (1981) indicate that surface tension effects may be more important than is generally thought.

They state that the effects of surface tension increase with decreasing depths and decreasing circulation. Hecker (1981) found that in Froude models of a fairly large size surface tension effects were significant for deep air core vorticies.

To define a general guide from the above research is not easy since enough is not yet known about the problem. It seems that if a model is operated at a Weber number W larger than 120 and is large enough so that the intake orifice is larger than 2 inches, the model will be free from surface tension scale effects except for inside the vortex core.

1.4.1 Reynolds Criteria Relaxation

The similarity of viscous phenomena in fluid flows is governed by the Reynolds number. Some researchers believe that when the Reynolds number is larger than a certain limiting value, there are no scale effects in Froude scaled flows. This limiting Reynolds number is approximately 3×10^4. Daggett and Keulegan (1974) found this number to be the limit for the pipe Reynolds number, Anwar (1978) found this number to hold for the radial reynolds number, and Padmanabhan and Hecker (1984) found this number to be the limit for the approach flow Reynolds number as well. Following this idea, as long as the model is operated above this limiting Reynolds number, the actual value of the Reynolds numbers do not have to match in model and prototype.

The Reynolds number is the ratio of inertial to viscous forces in fluid flows. Sweeny and Rockwell (1982) recommend the location of the maximum bell diameter as a representative location for the definition of the reynolds number, but many definitions are used. For the study of flow in pump sumps, three major formulations of the Reynolds number have been used. These are:

Pipe Reynolds number - $R_1 = vd/\nu$

Radial Reynolds number - $R_2 = Q/(\nu s)$

Approach flow Reynolds number - $R_3 = (v_3\ s_3)/\nu$

where, d = diameter of pump intake pipe.

s = the submergence of the intake.

s_3 = depth of approach flow.

v_3 = velocity of approach flow.

v = velocity at the location of d.

Froude scaling is not accepted by everyone however, and many of the detractors believe in speeding up the model above Froude scaled speeds to overcome scale efects. Fraser, Denny, and Young have all proposed the use of model intake velocities equal to that of the prototype. Dhillon *et al* (1981) however, have shown that the use of this equal velocity concept can be misleading. His work shows that the use of equal intake velocities can produce highly exaggerated vorticies that do not represent the prototype

situation. Babb and Mih (1984) indicate, in apparent contradiction, that increased intake velocities are desirable to limit scale effects, but should not be so large that surface waves are created since this will inhibit vortex formation. Durgin and Hecker (1978) give an approach to increasing velocities above Froude scaled values, and a technique to allow the application of the results to the prototype. Padmanabhan and Hecker (1984) conclude from their model - prototype comparisons that there is no need for higher than Froude scaled velocities. Models should be operated at Froude scaled flows or just slightly higher, if the latter researcher's work is followed.

Following the arguments of the majority of recent researchers then, a model may be said to be free of viscous scale effects if it is operated at Froude scaled flows and the Reynolds number is larger than 3×10^4. The speed of the flow may be increased to bring on vorticies supressed by scale effects, but should not be speeded up a large amount for general model observation and measurement.

1.4.2 Modelling using the Froude Criteria

After the relaxation of the Reynolds and Weber number constraints as indicated above, the flow in a pump sump model is a function of the Froude number, the circulation number, and the submergence only. Padmanabhan and Hecker (1984) found that Froude models correctly model the persistance of a vortex, the length of time it exists, and

the circulation in the sump. They also noted an increase in vortex type for similar Froude numbers when the flow near the entrance was partially blocked. This should be expected however, since the blocking will produce high local velocities and increased local Froude numbers. The Froude numbers used may not be comparable with those used elsewhere, depending on the factors used to define the Froude number and the type of blocking. Haindl (1956) found that Froude similarity did not hold for vortex phenomena, but he was more concerned with the core of very strong, long filament vorticies.

Anwar (1965) recommends a maximum scale of 1:20, and Dhillon found this to be valid as well. This limit would likely be covered by the 2 inch minimum intake diameter, except in models of very large sumps. The independence of the vortex type from the Reynold's number, and its dependance on the Froude number is shown in figure 2. Since the flow is a function of the Froude number alone, pump sumps should be scaled according to Froude criteria. Wijdieks (1984) gives some guidelines for pump sump modelling when the Weber and Reynolds number limits cannot be met due to size considerations.

1.5 Factors to Consider in Pump Sump Design

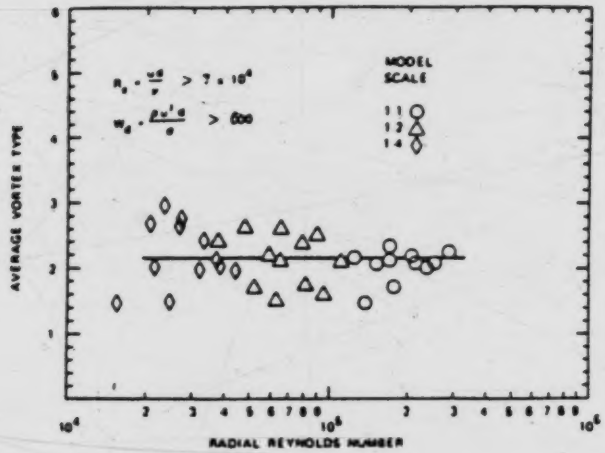

Average Vortex Types for Various Radial Reynolds Numbers, Uniform Approach Flow, Both Pipes Operating

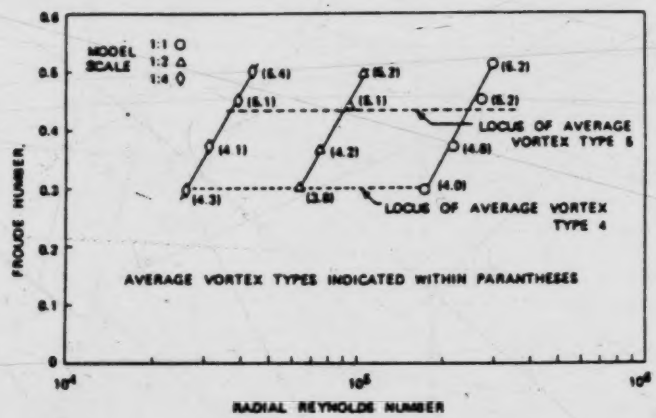

Average Vortex Types on Froude Number versus Radial Reynolds Number Plot, Data of Screen Blockage Tests

Figure 2. Variation of Vortex Type with Reynolds and Froude Numbers. (adapted from Hecker, 1984).

1.5.1 Evaluating Pump Sump Performance

The performance of a pump sump is most often evaluated qualitatively by the type of flow patterns that can be seen inside it. The size and strength of vorticies in the sump is often the criteria for the design of a successful facility. Vorticies are divided into several categories according to strength, and a limit as to the strongest allowable vortex governs sump design. An example of such a system of vortex designation is shown in figure 3. The persistance of a vortex, the percent of the time a vortex of a given strength exists, is another parameter used to identify vortex problems. Sweeny et al (1982) measured the persistance of a vortex class with a multi-button recorder, where an observer pushed a button corresponding to the vortex type present for the length of time that it was present.

Swirling flow inside the intake is often indicated by a straight vaned propeller located inside the intake pipe. Wijdieks (1984) gives a safe value for the swirl in the intake pipe using the measured rotation of such a propeller. He also measured velocity profiles in the intake and developed several statistical criteria for the required uniformity of the velocity profile. The presence or absence of vorticies and swirling flows is used to evaluate performance because these are the major sources of hydraulic problems.

Measured parameters can also be used to evaluate the performance of a sump. Daggett and Keulegan (1974) plotted

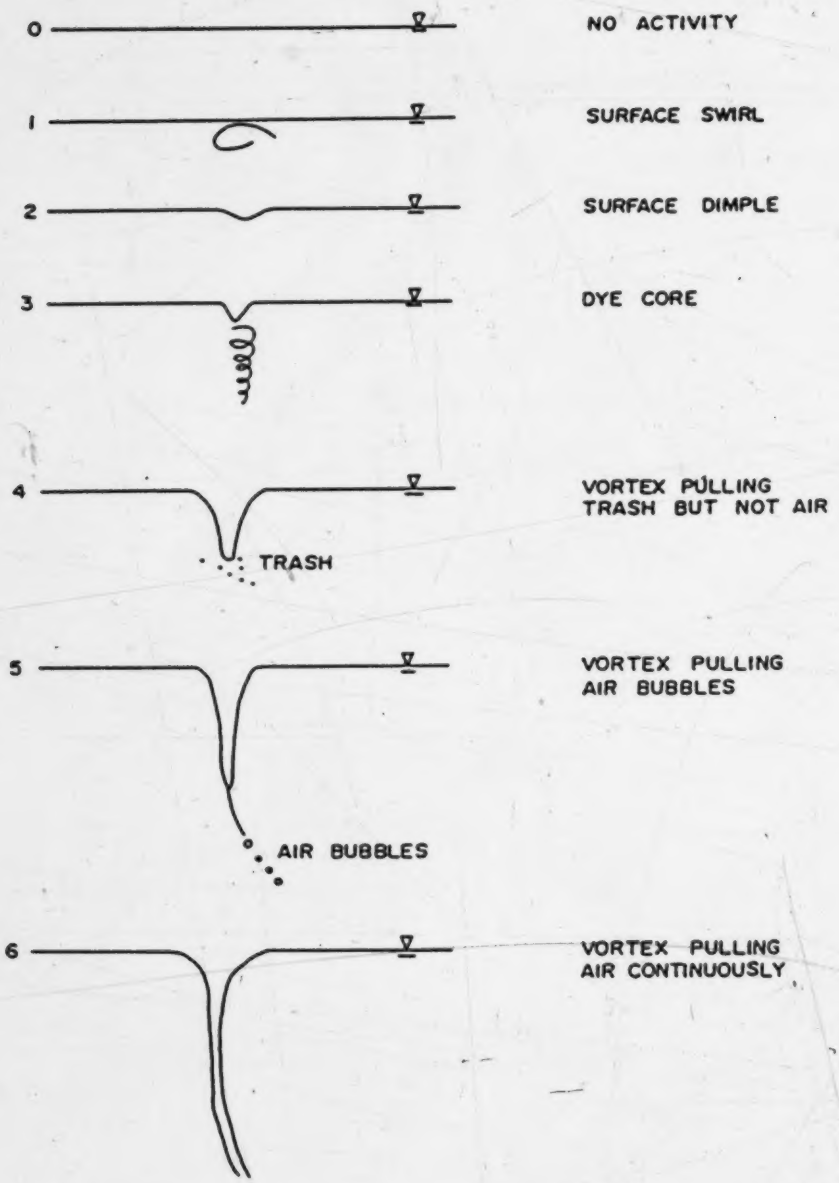

Figure 3. Vortex Classification System. (adapted from Kells et al, 1984)

the circulation number against the relative submergence and defined regions where the sump performed adequately. This method requires the measurement of the kinematic viscosity, the density, the circulation and the submergence. Measurement of the circulation can be done by measuring the tangential velocity at a specific distance from the air core.

The critical submergence is another parameter used to describe flow in sumps. This 'critical submergence' is the intake submergence at which air begins to be drawn into the intake. This parameter was used extensively to determine the presence of scale effects and to set the limits on the Reynolds and Weber numbers. Venkataratma *et al* (1981) found that this parameter depends on the velocity in the intake in a highly varied manner. Jain *et al* (1978) found that in cylindrical tanks with a central drain on the floor, the critical submergence varied with the Froude number alone in a highly predictable manner. Apparently, the turbulence and curved vortex filaments in pump sumps lead to more varied and unstable conditions.

The above procedures can be used to evaluate the performance of both models and prototypes. To design a sump that performs well hydraulicly, a model must be built since both evaluation procedures require physical measurements and/or observations. No standard design can be used since the shape of a sump is usually dictated by the site.

1.5.2 Minimum Sump Volumes

The minimum volume that a sump must contain depends on the maximum number of starts of the suction pump in a certain period. The maximum number of starts depends on the motor heat generated per start-up and the maximum allowable temperature of the motor running the pump. For a fixed speed pump, the following must be taken into consideration:

1. Required discharge rate.
2. Number of pumps operating from the same sump.
3. The capacity of each pump.
4. The operating level for each pump (NPSH).
5. Minimum time between start-ups.

The required volume of the sump for a fixed speed pump can be found from the simple formula derived by Prossser (1977).

$$T = 4V/Q$$

where, V = Sump volume.

T = Time between starts.

Q = the pumping rate.

For a frequency of 10 starts per hour for example, T= 6 min., the sump would have to be one and a half times the discharge rate Q (units of volume/ minute).

For a variable speed pump, the number of starts per hour becomes insignificant, and the minimum sump volume is governed by the control system that controls the speed of the pump.

1.5.3 Aspects of Good Sump Design

Prosser (1977) gives a list of general rules that should be followed in the design of pump sumps. This list is reproduced below with some minor modifications.

1. The flow approaching the pump intake, whether a horizontal or vertical bellmouth, should be uniform across the channel.
2. The kinetic energy associated with changes in level or crosssection should be dissipated well away from the final approach to the pumps.
3. Obstructions, such as supporting pillars, should be streamlined to prevent flow separation and swirl generation near the intake. This does not hold for baffles that are intended to increase turbulence to allow fast expansion of flow from pipe into sump.
4. Areas where stagnant water may occur should be filled in.
5. Average velocities should be kept low: about 0.6m/s for flow entering the sump, and 0.3m/s maximum for the approach flow to the bellmouth.
6. Trash racks should serve a double purpose as flow straightening devices whenever possible.

Figure 5 shows examples of good sump design, and figure 4

shows a typical bellmouth detail designed for good, non-separating, flow into intakes.

1.5.4 Aspects of Poor Sump Design

The object of a pump sump is to provide storage and good flow conditions to the pump. A summary of unwanted hydraulic conditions in sumps are listed below.

Jets - Jets cause swirl as they expand, and if the jet impinges on walls or support columns, large unsteady wakes form adding to the swirl in the sump.

Separated Flow - Regions of separated flow are sources of vorticies and unnecessary sump swirl.

High velocity Flows - These cause problems similar to jets.

Unsteady Flow - This is a cause of unsteady pump loading and vibration.

Surface Waves - Large surface waves are a sign that either the velocities are too high, or the flow is unsteady.

Free-Falling Fluid - This causes aeration that reduces pump efficiency.

These poor hydraulic conditions are the result of poor sump configurations. A general list of poor design practices is given below, and illustrated in figure 6.

1. Undersized penstocks, control gates or valves - These will cause jets and/or high velocity flows in the sump.
2. Sharp corners - These are areas of vortex generation.

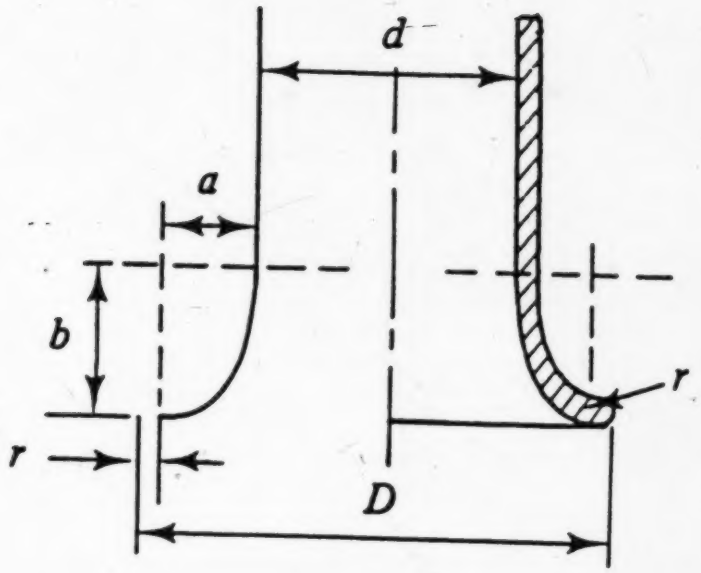

Typical bellmouth design
based on quarter ellipse
(major axis = b
minor axis = a)
Bellmouth diameter
$D = d + 2a + 2r$)

Figure 4. Typical Intake Bellmouth Detail. (adapted from Prosser, 1977)

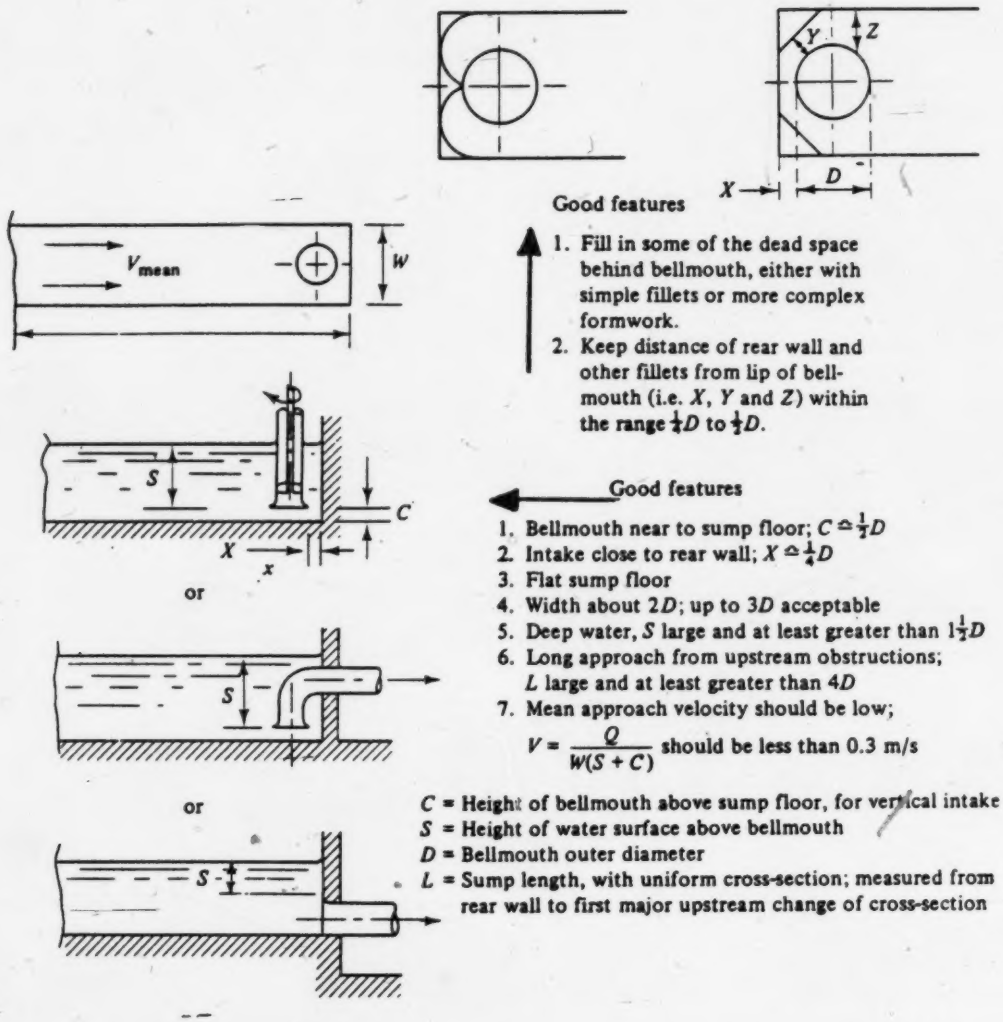
Y
Z
X
D
Good features
1. Fill in some of the dead space behind bellmouth, either with simple fillets or more complex formwork.
2. Keep distance of rear wall and other fillets from lip of bellmouth (i.e. X, Y and Z) within the range ¼D to ½D.
V mean
W
S
C
X
x
or
Good features
1. Bellmouth near to sump floor; C ≙ ½D
2. Intake close to rear wall; X ≙ ¼D
3. Flat sump floor
4. Width about 2D; up to 3D acceptable
5. Deep water, S large and at least greater than 1½D
6. Long approach from upstream obstructions; L large and at least greater than 4D
7. Mean approach velocity should be low; V = Q/W(S + C) should be less than 0.3 m/s
or
C = Height of bellmouth above sump floor, for vertical intake
S = Height of water surface above bellmouth
D = Bellmouth outer diameter
L = Sump length, with uniform cross-section; measured from rear wall to first major upstream change of cross-section

The main aspects of a good single cell sump

The clearance of the bellmouth from the floor should be in the range ¼D to ¾D. If C is less than ¼D, the flow area under the lip of the bell is less than the flow area into the bell and the resulting deceleration causes unsteady flow in the bellmouth. If C is greater than D there is a tendency for the upward component of flow into the bellmouth to become unstable and promote swirling flow. The proximity of the end and side walls to the bellmouth inhibits the production of swirling flow and vortex formation.

Figure 5. Good Sump Designs. (adapted from Prosser, 1977)

3. Rapidly diverging passages - This leads to flow separation and may cause surging in the sump.
4. Steep slopes - This may produce aeration through hydraulic jumps and may cause unsteady flow in the sump.
5. Weirs with no energy dissipating devices - This causes aeration and surging.
6. Blunt pillars, piers or guide vanes - Cause unnecessary amounts of swirl in the sump due to large wakes.
7. Asymmetric Designs - Although they can be made to work, they often increase swirl in the sump.
8. Insufficient submergence - This leads to intense vortex activity, and ingestion of air into the pump.

1.5.5 Sources of Vorticity

De Siervi et al (1982) have proposed two separate origins for the vorticity in pump sumps. The first source of the vorticity in sumps is the intensification of the ambient vorticity, generated far upstream. Three dimensional drift of vertical vortex filaments into the inlet results in a strong concentration of these filaments around the stagnation streamline near the inlet. This phenomena does not depend on the viscous properties of the fluid, and may actually be calculated for simple sumps with the potential flow equations.

The second source of vorticity is the variation of circulation around the length of the inlet cylinder that

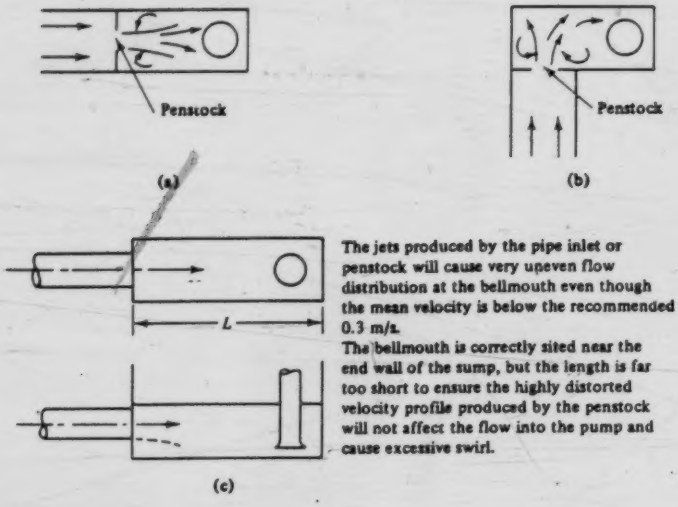

The jets produced by the pipe inlet or penstock will cause very uneven flow distribution at the bellmouth even though the mean velocity is below the recommended 0.3 m/s.
The bellmouth is correctly sited near the end wall of the sump, but the length is far too short to ensure the highly distorted velocity profile produced by the penstock will not affect the flow into the pump and cause excessive swirl.

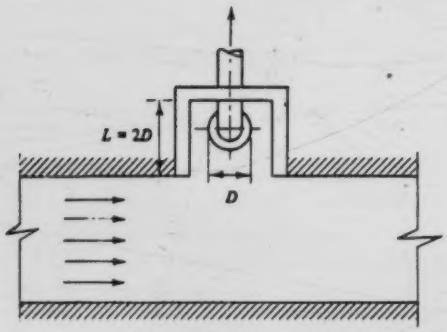

The short chamber in the side of a channel will cause violent swirl around the intake bellmouth unless L is greater than $8D$.

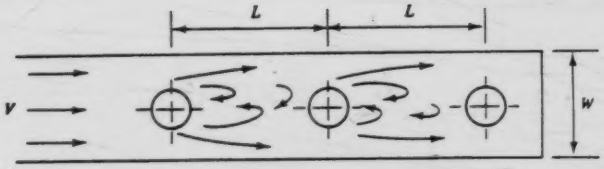

Not recommended (unless $L > 8D$ and $W > 3D$ and $V_M < 0.3$ m/s

The wakes from upstream intakes will have serious effects on the performance of succeeding intakes.

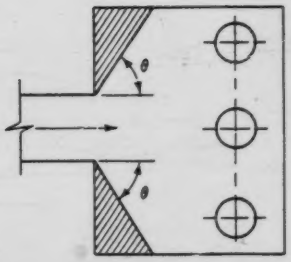

Not recommended
For $\theta > 20°$
($\theta = 60°$ as shown)

This shows an attempt to feed flow normally to the line of the pumps. Uniform approach flow cannot be achieved with the very wide angle of divergence from the inlet culvert to the sump.

Figure 6. Poor Sump Designs. (adapted from Prosser, 1977)

goes along with vortex shedding. Viscous effects are important here since the circulation distribution around the inlet depends on the separation of the boundary layers on the outer surface of the inlet. Calculation of this flow is much more complicated, and requires knowledge of the lines of separation and the pressure field on the cylinder.

At zero degrees of yaw, when the flow is directly into the mouth of the inlet, the inlet vortex is created by the intensification of the ambient vorticity. At ninety degrees of yaw, when the flow is at right angles to the inlet mouth, boundary layer phenomena create the inlet vortex.

1.5.6 Improving Poor Sump Designs

There are a number of methods available for improving the flow in pump sumps, or allowing the use of shorter sumps. If a sump is long enough, flow disturbances generated at the entrance are supressed before they reach the intake. A sump this long would not be economical. Shorter pump sumps may also have an adequate hydraulic performance, but require special flow modifiers. Floor beams, corner fillets, backwall splitters, sump dividing walls and anti-vortex beams have all been tried at one time or another.

1.5.6.1 Surface Vortex Elimination

Surface vorticies are generally the most severe problems encountered in sump design. The only really effective way to eliminate these vorticies is to keep the intake under enough water to prevent their

formation. Prosser (1977) recommends a minimum intake submergence of 1.5D for this purpose, where D is the bellmouth diameter. One device that is effective in supressing surface vorticies is the anti-votrex beam. This beam spans the entire width of the wet pit and intersects the water surface. This beam acts as a sluice gate and directs the flow along the floor of the sump.

The effects of the anti-vortex beam are not all beneficial, however. Floor and sidewall vorticies are often intensified, the probability of separation at the suction bell increases, and the prerotation of the flow in the intake pipe also increases in the presence of an anti-vortex beam.

1.5.6.2 Supression of Floor Vorticies

Floor vorticies are common to almost all sump installations and, according to Tullis (1979), are the most difficult to eliminate. The floor vortex is usually strong and stable with a constant direction of rotation and is concentrated near the centreline of the pump. Floor vorticies are a potential source of cavitation as well as a source of prerotation of flow in the intake pipes. They should be restricted in strength, if not completely eliminated.

One method of preventing floor vorticies is to place a cone under the suction bell. This method has its drawbacks however, as it often increases the

strength of wall vorticies. The floor vortex may also form anyway and attach to the tip of the cone.

Floor blocks placed under the suction bell are a more effective method of eliminating floor vorticies. These blocks increase the turbulence near the floor of the sump, and this turbulence breaks up the vortex. The major drawback of this method is that the increased turbulence is drawn into the pump and may cause vibration and cavitation.

Floor beams and turning vanes placed under the suction bell are the most effective preventer of floor vorticies. These devices can also be useful in eliminating vorticies emanating from the walls.

1.5.6.3 Supression of Wall Vorticies

Side wall vorticies can generally be eliminated by changing the distance between the walls and the intake pipe. Prosser (1977) recommends wall clearances of 0.5D between the sump and the wall, where D is suction bell diameter. Backwall splitters and increased wall roughness can also eliminate wall vorticies. Kells *et al* state that these backwall splitters should not extend above the water surface since they generate less intense vorticies when submerged.

The use of a confined approach to the suction bell that is similar to a draft tube is effective in eliminating surface wall and floor vorticies. This method is put forward by Tullis who cautions that it

has only been used on one project to date. This complicated design would also likely prove more costly than conventional designs and would still require a model test. Figure 7 shows a detail of this design.

1.5.6.4 Sump Dividing Walls

The use of sump dividing walls in multipump facilities is not recommended since these walls often generate swirl in the sump. If the flow from the entrance is not completely straight, the dividing walls split the flow at an angle, causing more problems than they correct. Kells *et al* (1985) found that dividing walls did not improve flow in their two pump sump, and in fact added to the vortexing problem. Figures 8 and 9 illustrate some of these flow improvement devices.

1.6 Conclusions

The Design of Pump sumps is a field about which little is known. Because of this lack of knowledge, even sumps that are minutely different from designs that work well must be designed using a hydraulic model. Pump sump models should be designed so that:

- The Froude numbers are the same in model and prototype.
- Intake pipes are larger than 2 inches, and the scale is larger than 1:20.
- The model Weber number (W) is larger than 120.
- The model Reynolds number is larger than 1×10^4.

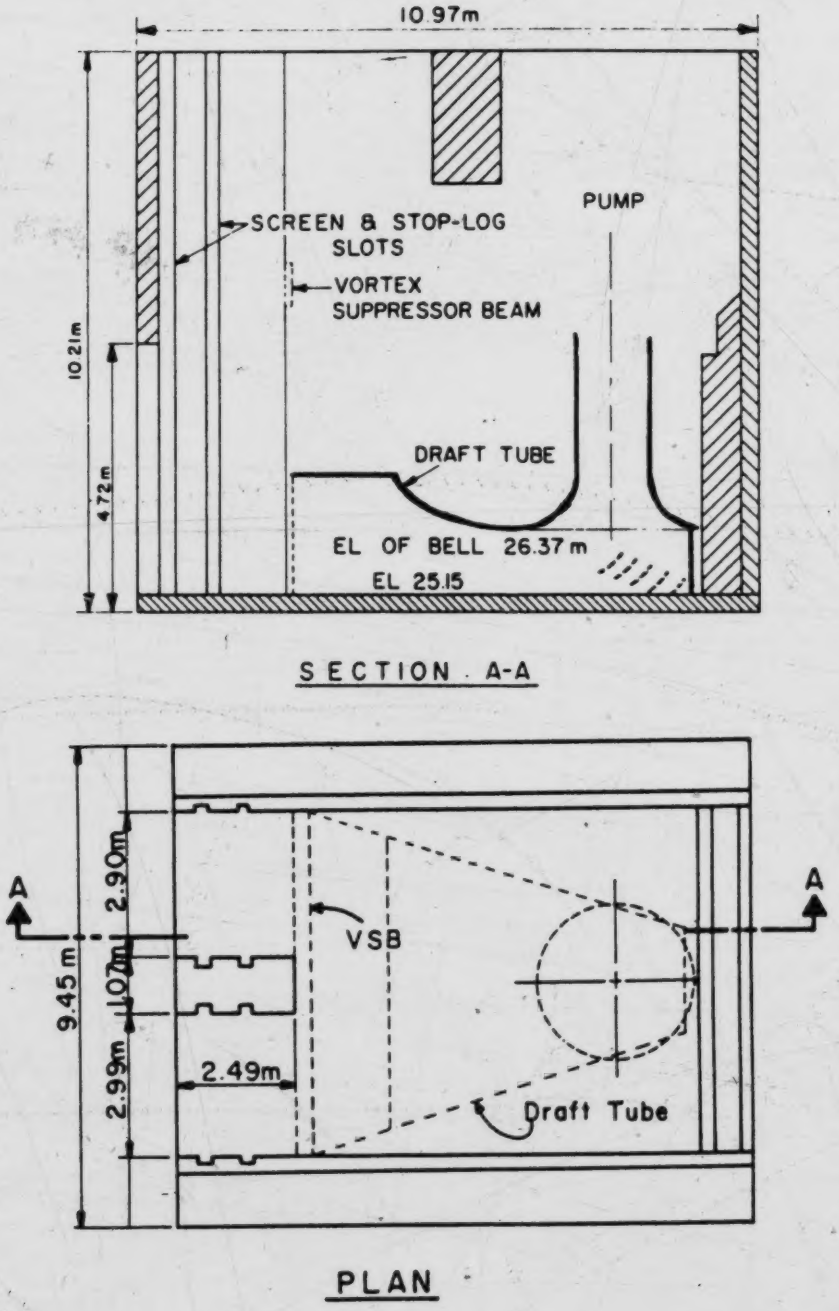

Figure 7. Draft Tube Sump Intake. (adapted from Tullis, 1979)

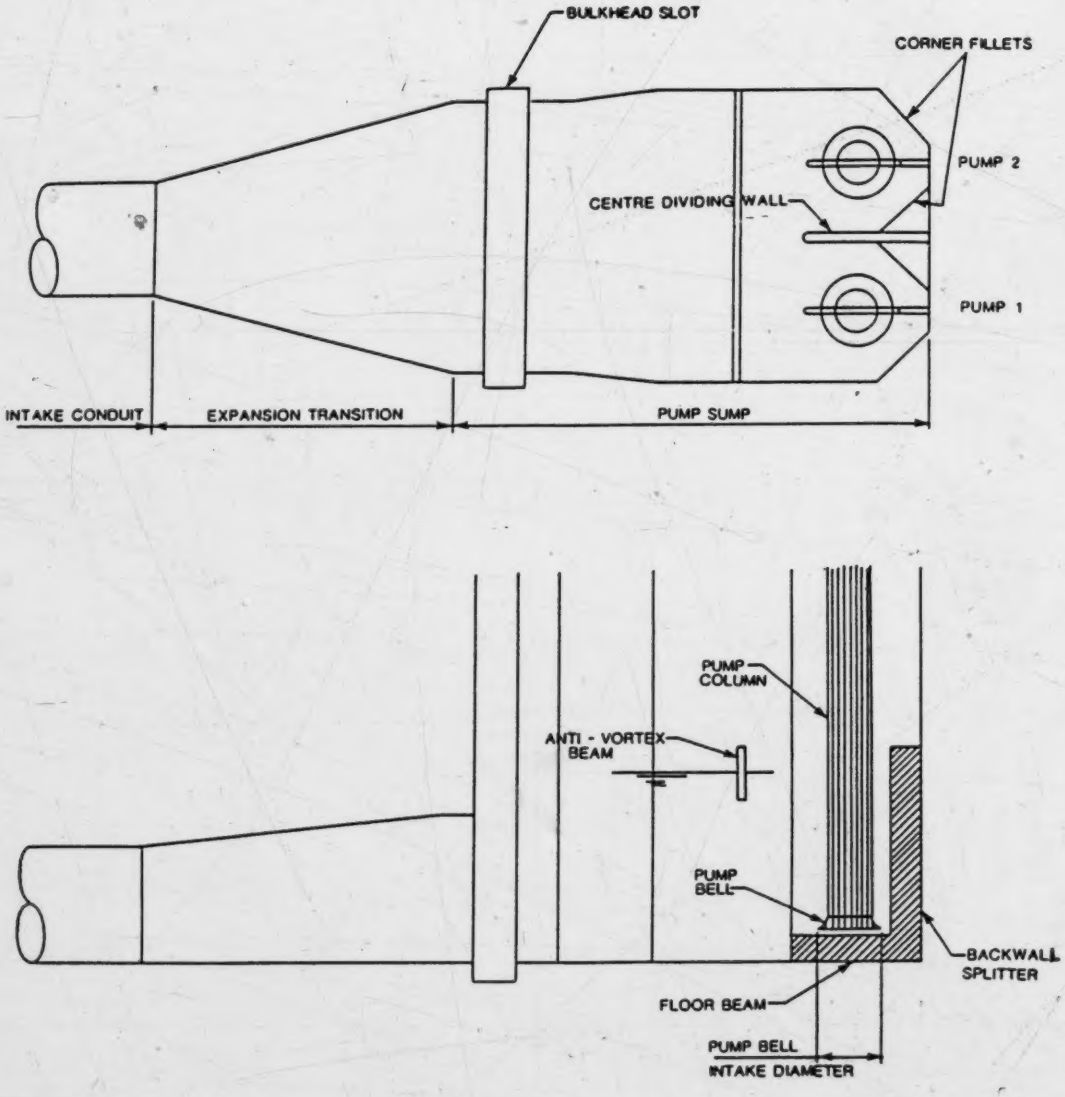

Figure 8. Devices that Improve the Hydraulic Performance of Sumps. (adapted from Kells et al, 1983)

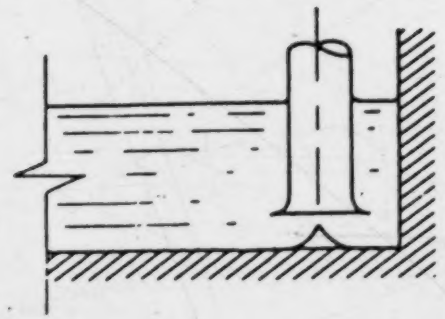

Cones

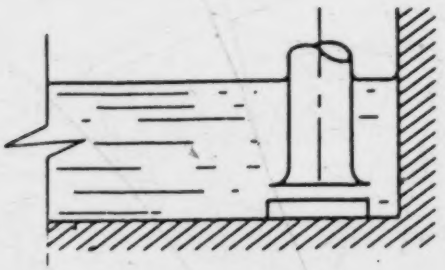

Short splitters
or cross

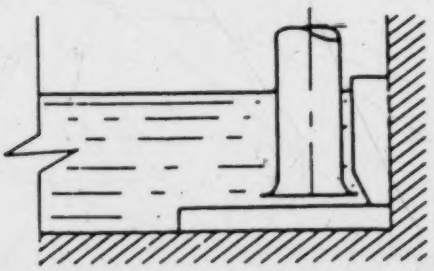

Long splitter;
splitter behind
pump casing

Figure 9. Flow Improvement Devices. (adapted from Prosser, 1977)

If a sump cannot be made long enough to damp out disturbances created at the entrance, flow modifying devices such as anti-vortex beams and floor beams may be used to improve the flow condtions.

2. PART TWO: EXPERIMENTAL STUDY

2.1 INTRODUCTION

Because of the lack of any detailed study of the flow structure in pump sumps, it was thought that a general study of such a flow structure would be of value. The study was made feasible by the availability of the Laser Doppler Anaemometer (LDA) in the Graduate Hydraulics laboratory of the University of Alberta, along with the donation of a sump model from Northwest Hydraulic Consultants. The sump had been used in a traditional model study for the Fourty Mile Coulee project in southern Alberta. This study is described by Kells *et al.* in the Transactions of the CSCE annual conference of 1985.

Due to time considerations and the limited availability of the LDA equipment, it was decided to study the flow structure of two sump designs. Both designs were based on the sump plan recommended for construction by Northwest Hydraulics Consultants. The first design had no flow improvement devices. The second plan included the recommended flow improvement devices. The sump was operated at the minimum recommended submergence and the maximum recommended discharge for both designs. It was felt that these operating conditions would provide realistic conditions and would be most likely to reveal troublesome flow characteristics.

2.2 Laser Doppler Anaemometry

Laser Doppler Anaemometry (LDA) is a new method of fluid velocity measurement that uses the Doppler shift in light beam frequency to measure the velocity of small inert particles suspended in the flow. The LDA system allows measurement of instantaneous velocities without requiring the presence of physical devices in the flow, devices that often change the flow patterns. Other advantages of the LDA system are the ability to measure turbulence and the small volumes in which the velocities are measured. The LDA method requires optical access to a clear fluid containing some suspended particles. The only disadvantage to the LDA system is that the depth of penetration into the flow is governed by the focal length of the lens.

2.2.1 Some Physics of LDA Flow Measurement

When two coherent light beams, such as those produced by a laser, cross, an interference pattern of maxima and minima fringes is set up. The LDA determines the velocity of a particle passing through the area of beam intersection by measuring the time that the particle takes to cross a known number of interference fringes. The accuracy of a measured velocity is ultimately determined by the number of fringes in the region of beam intersection.

The LDA system depends on the presence of particles of the right size and shape to reflect enough light to analyse. The particles should be neutrally bouyant and small enough

to closely follow the flow. The number of particles present greatly affects the rate at which data is taken. Seeding the flow with particles thus reduces the time required to make velocity measurements. The addition of too many particles however, will weaken the beams and increase the time required to take data.

2.2.2 LDA Equipment Used in Tests

Following is a description of the equipment that comprises the LDA setup available at the T. Blench Graduate Hydraulics Laboratory at the University of Alberta. The laser used in the experiment was a four watt Innova 90 Argon-Ion laser manufactured by Coherent. By means of a beamsplitter, the single laser beam is separated into three beams: a blue beam with a wavelength of 488 nanometres, a green beam with a wavelength of 514.5 nanometres, and a blue/green mixed beam. These three beams form two perpendicular planes such that velocities can be found in two directions. Both the green and blue beams are shifted by fourty megahertz with the acoustic-optic or Bragg cell.

The velocity data were measured on a planar grid using a two dimensional computer controlled traversing system. This system consists of a mirror that deflects the beams by ninety degrees and a 160mm focal length front lens through which the beams penetrate vertically into the flow. With the beams orientated vertically, the velocities on horizontal planes may be measured. The focal length of the front lens

limits the distance that the beam intersection point can move into the flow.

The light scattered off the particles is reflected back through the optics and collected by the two photomultiplier tubes. These tubes convert the the light signal into an electrical signal. This electrical signal is resolved into the two components of velocity by the two counter processors. After a check has been made to ensure that the measurement of the two orthogonal velocity components is coincidental to within 1000 microseconds, these velocities are transferred to the computer through the buffer. The optics system as well as the electronics were made by Disa Electronics, now Dantec Electronics. This LDA system is represented schematically in figure 10, and photographically in plates 1 and 2.

Twenty thousand instantaneous velocities were taken at each point in the two dimensional grid. The Masscomp computer performed a statistical analysis procedure on this data to find:

U - the mean longitudinal velocity.

V - the mean transverse velocity.

u'^2 - the mean longitudinal turbulence.

v'^2 - the mean transverse turbulence.

$u'v'$ - the covariance of the velocity fluctuations, or the shear stress.

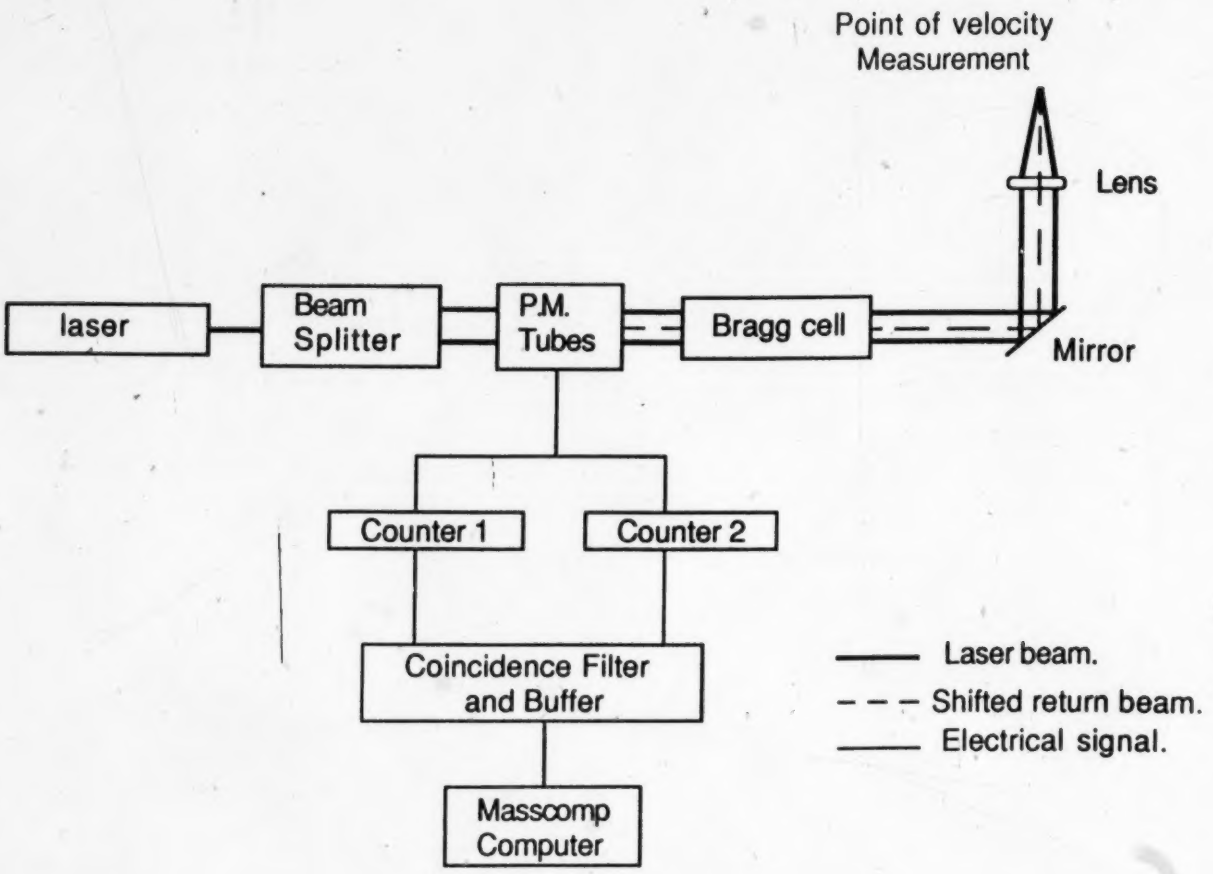

Figure 10. Schematic diagram of LDA data aquisition system.

Plate 1. Laser Doppler anaemometer set up under the sump showing traverse, laser source (lower left), and front lens (top).

Plate 2. View of laser beams penetrating the floor of the sump. The location where the velocity is read is at the intersection of the beams.

2.3 Experimental Arrangement

The overall arrangement of the sump and related equipment is illustrated in figure 11. The water is pulled up out of the sump through two intake bells by a pair of four inch pumps. These pumps push the water into a head tank from where it flows back into the sump through a ten inch pvc pipe. The discharge in the system is measured with two magnetic flow meters located just downstream of the pumps.

The model was constructed according to the Froude criteria and has a length scale of 1:8.44. For the two designs tested, the outside walls of both the entrance and the sump were identical. Figure 12 gives the dimensions of the unimproved sump, and figure 13 shows the improved sump with the dimensions of all changes. The sump itself was suspended two metres above the floor to allow the laser to operate beneath it.

The laser beams of the LDA penetrated the bottom of the sump through a clear plate installed for this purpose. With this set up the LDA was able to measure velocities in planes parallel to the floor only, vertical velocities could not be measured.

2.4 Experimental Procedure

For both designs the sump was operated at one discharge, 12.56 l/s, and at one submergence, LWL(2). These conditions represent the worst case permitted in the study by Northwest Hydraulic Consultants. It was thought that

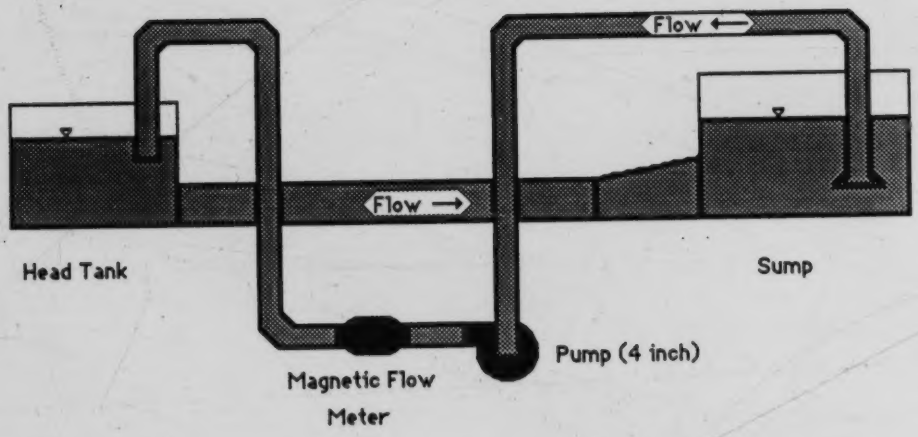

Figure 11. Overall view of the Sump set up.

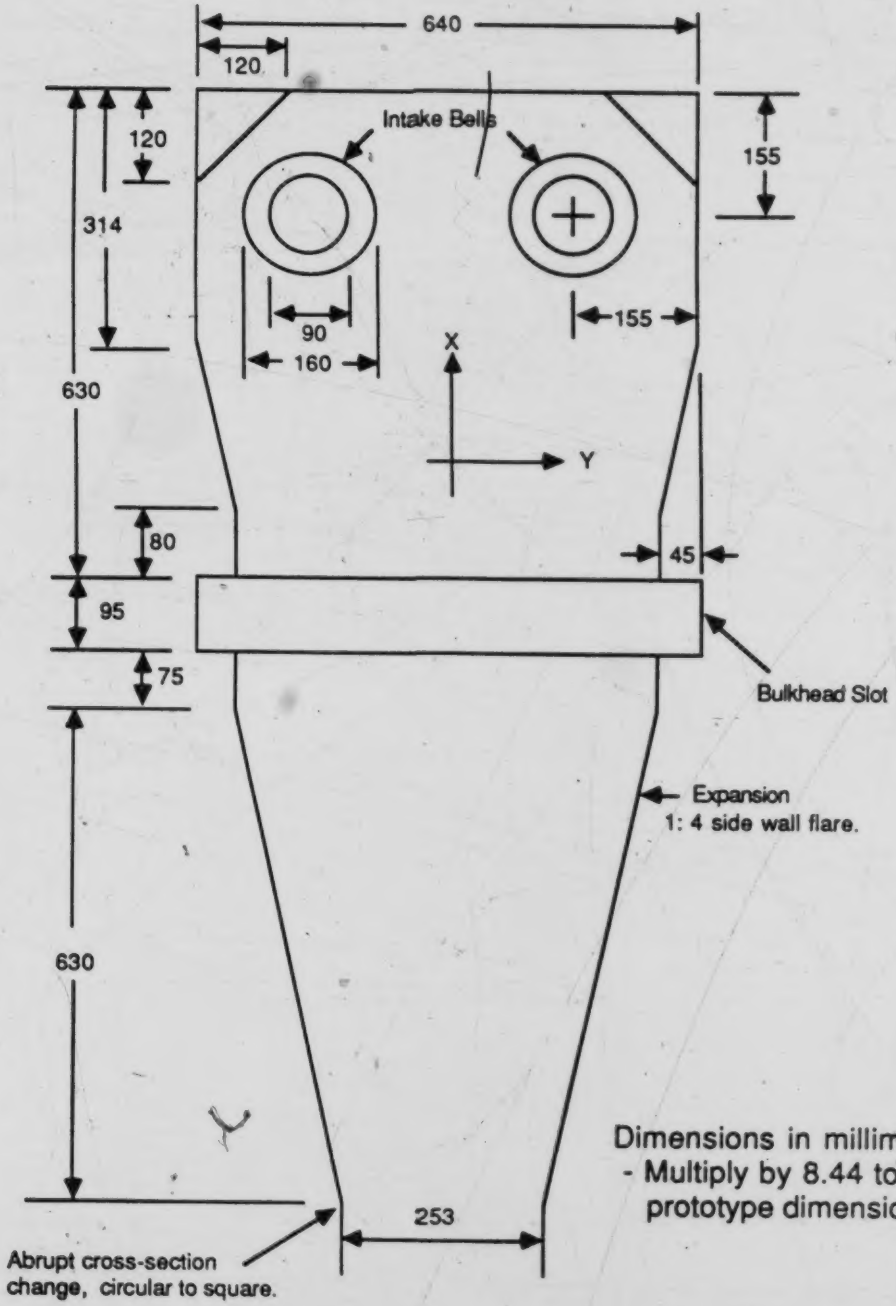

Figure 12. Plan view of the unimproved sump showing dimensions.

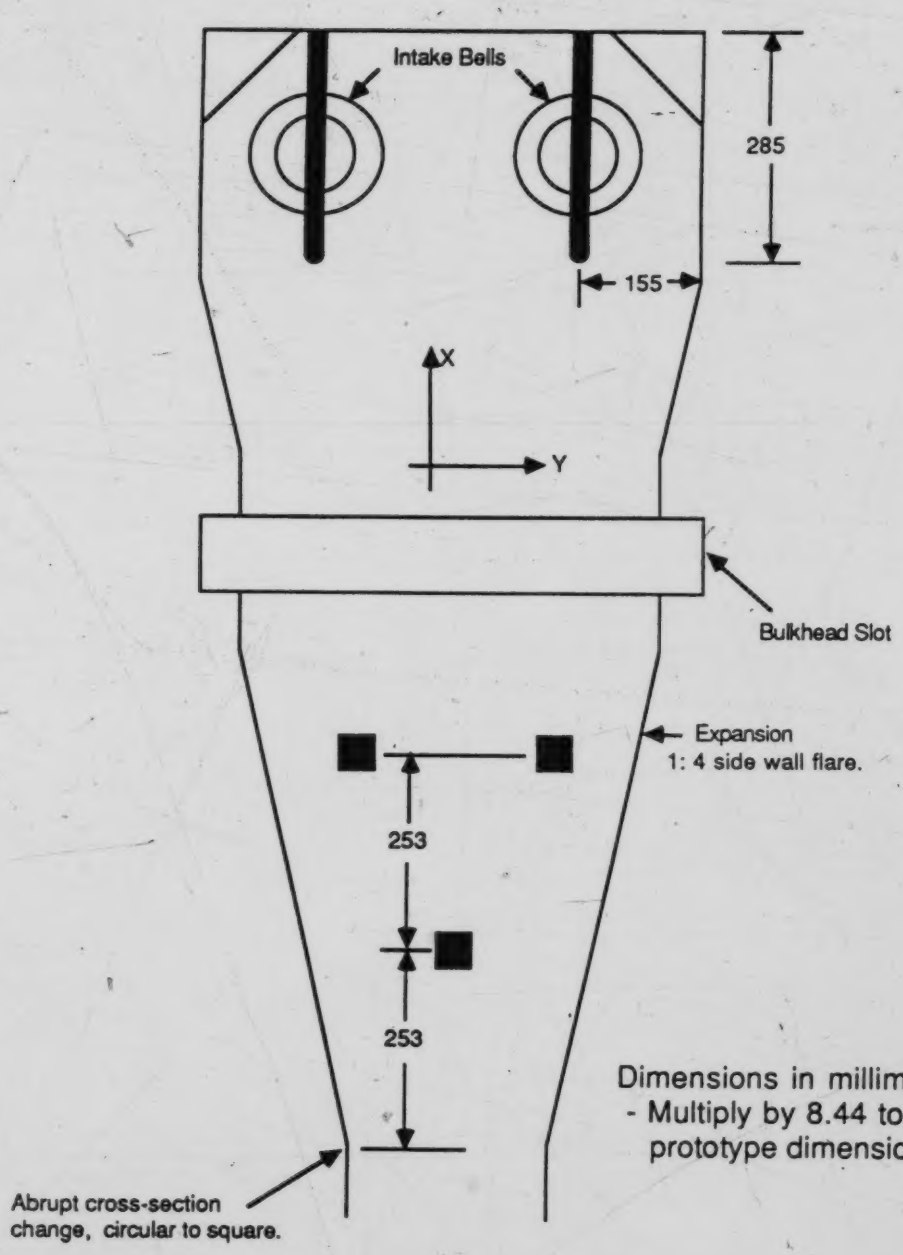

Figure 13. Plan view of improved sump showing dimensions of the improvements.

these extreme conditions would best illustrate the structure of flow in a pump sump. The submergence of the intakes is illustrated in the side view of the sump given in figure 14.

A dye test was conducted first in order to determine the general patterns of flow in the sump. Dye was injected with a needle at various locations in the sump to find the direction of flow. From these point tests, a rough map of the streamlines in the sump was constructed.

From the dye tests, important areas were identified for investigation with the LDA. For these areas, a two dimensional grid of points was programmed into the computer. The computer then moved the point of laser beam intersection to these locations and took a set of data. The laser took all the required data for one height before moving up to the next height as this required fewer adjustments to the voltage fed to the photomultiplier tubes.

2.4.1 Measuring Flow Velocities in the Sump

The laser Doppler anaemometer took twenty thousand readings at each specified point in the flow and averaged them to arrive at the horizontal velocities at that point. The time required to take one set of readings varied with the depth of beam penetration into the flow and the number of particles in the flow. A complete set of data might be taken near the bed in under one minute, but twelve centimetres into the flow a data set might take four to five minutes to complete.

Good data was taken where the flow was steady, but problems may exist with data taken in unsteady regions. In the unsteady areas, an eddy might last for half a minute or so, completely changing the direction of flow for that length of time. The magnitude of the velocities will not be representative in these regions since velocities in both directions will be included. These large scale eddies will also affect the values of turbulence and shear stress. The regions of unsteady flow include under the centreline of the bells, downstream of the intake bells, and the areas of return flow in the unimproved sump.

The LDA was able to take data in the horizontal directions, U along the length of the sump, and V across the sump as shown in the figures. Data was taken at levels very near the floor and at 30, 60, 90, and 120 millimetres above the lowest level. Data was taken at these levels for all areas except directly under the sump where other increments were used.

2.4.2 Percent of Flow in the Study Zone

The depth of flow that can be studied with the laser Doppler anaemometer is limited by the focal length of the front lens. For the equipment used in this study, the focal length was 160 mm. However, with the thickness of both the floor and lens, the range was limited to about 120 mm above the floor.

An estimate of the amount of flow passing through the areas where tests were conducted in the main sump was made by multiplying an average velocity on a certain cross section with the area of that section. The percentage of flow through the 120 mm test area ranged from 30 to 50 percent for sections three to one of the unimproved sump, and 40 to 60 percent for the same sections in the improved sump.

Approximately half of the flow moves through less than one third of the water depth, the area where the tests are conducted. Near the intakes all of the flow must pass through the area of measurement since the intake bells are located near the floor.

2.4.3 Checks on the LDA Velocities

Two independant checks were performed to ensure that the LDA was taking correct velocities. The first was an order of magnitude check using the average velocity in the return flow pipe. This average velocity can be calculated for the known discharge as,

$$V = 2Q/A = 0.70 \text{ m/s}$$

where,

V = the average velocity in the return flow pipe.

Q = the discharge of each pump.

A = the cross sectional area of the 10 inch diameter pipe.

If the LDA measured velocities are of the same order as this average value, then they are correct measurements. The actual values of the velocity in the main sump were slightly smaller, but the sump area is greater than that of the pipe requiring smaller velocities for the same discharge.

As a further check on the validity of the LDA readings, a propeller probe was used to measure the fluid velocities in the sump. The data from this probe are included in Appendix A. The measurements taken with the propeller correspond almost exactly to the LDA measured velocities.

2.4.4 Visualizing the Flow

The LDA equipment generates a large amount of data that must be rendered understandable. The data for this study is plotted as the variation of velocity with either a horizontal or vertical distance, a velocity profile. Several of these velocity profiles are drawn on one axis to show the variation of the velocity in the third direction. For example, in the main sump cross-sections the velocity at a given height is plotted against the distance across the sump, as in figure 17. To show the variation in the vertical direction, velocity profiles for different heights are plotted on the same axis. The use of three dimensional plots was considered, but the coarseness of the grid used would not allow the construction of a clear plot, and would make

the extraction of actual velocity values difficult. Local coordinates were used for each section or area where data was taken.

2.5 Vorticity Meter

One of the intakes was equipped with a straight-vaned propeller used to show rotation of the fluid in the intake pipes. The experience with the unimproved sump has led me to question the validity of any readings from such a device located near the mouth of the intake.

With the clear floor of the sump it was possible to closely observe the interaction of the vorticity meter and the floor vortex. When filament of the floor vortex was attached to the hub of the vorticity meter, the propeller would spin at a fast rate. However, the floor vortex would often attach to one of the vanes of the vorticity meter and stop it dead. The floor vortex could also extend past the vanes of the vorticity meter in which case the vorticity meter would also not move.

The rotation, or vorticity, of the flow entering the intake is concentrated along one line, the core of the floor vortex. Unless the hub of the vorticity meter coincides with this moving core, any data taken from it will be of little value.

As the fluid continues up the intake pipe, the centre of rotation will slowly align itself with the centre of the pipe due to the frictional effects of the walls. Vorticity

meters will only give true readings away from the entrance, where the centre of the fluid rotation coincides with the centre of the pipe. The vorticity meter was not used in this study.

2.6 Structure of Flow in the Unimproved Sump

The overall flow patterns were initially observed with a dye tracer, and the results are shown in figure 15. The dimensions of the unimproved design are shown in figure 13, and the locations of the cross-sections where the LDA data was taken are shown in figure 16. For this sump configuration the flow is very asymmetric. The jet emerging from the pipe clings to one wall in the short expansion area of the sump. This initial asymmetry contributes to a large circulation pattern in the sump. The jet from the expansion region moves along the wall to one intake, and around the backwall to the other intake. After the jet passes the second intake, its momentum is dissipated in large scale eddies, some of which are shed from the intake cylinders.

The pattern of flow shown in the figure is fairly steady, but the jet does sometimes move from one side of the sump to the other, inverting the flow pattern. The jet prefers to cling to the south wall of the sump, but can be switched to the north side wall by deflecting the jet with a small board. Severe floor vorticies were observed at the design flowrate and submergence, but no surface vorticies stronger than class three were in evidence.

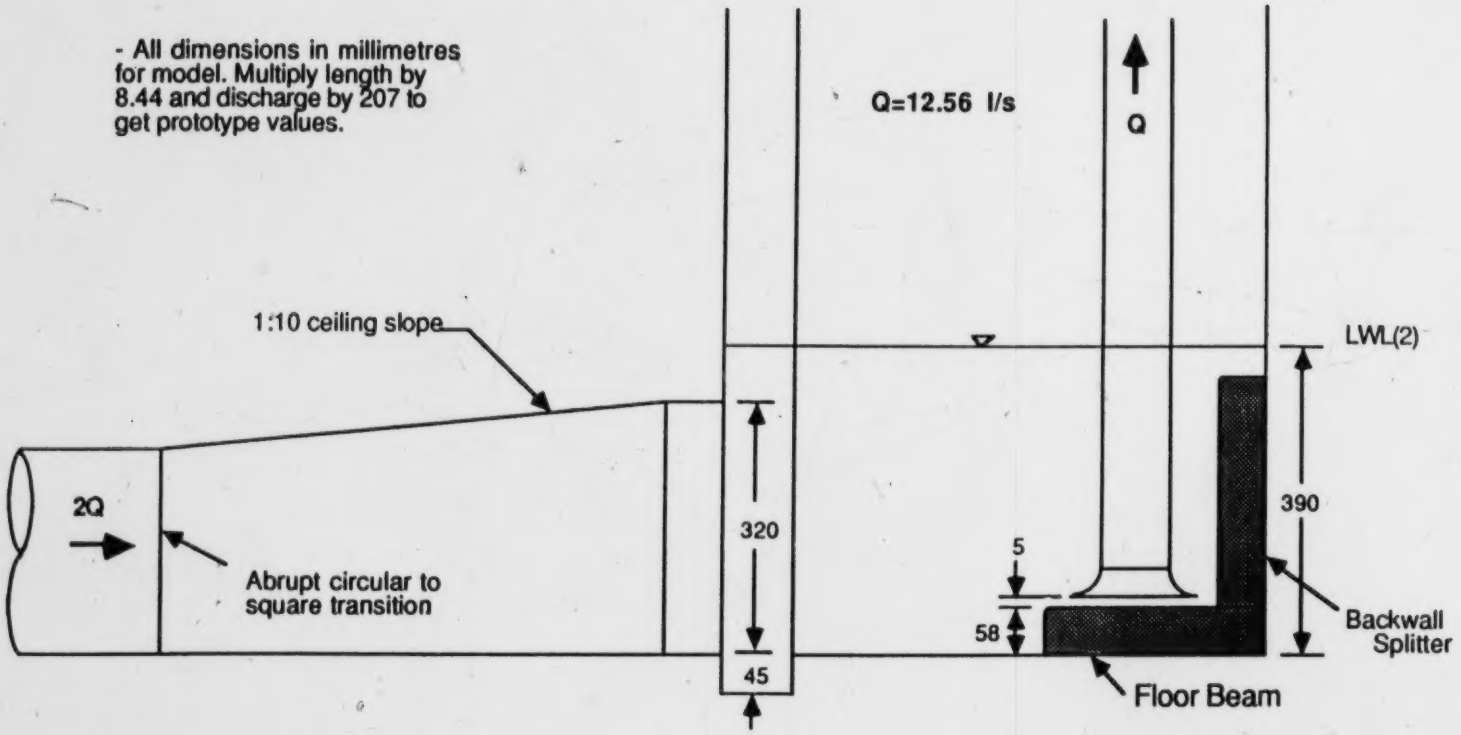

Figure 14. Side view of sump showing operating conditions.

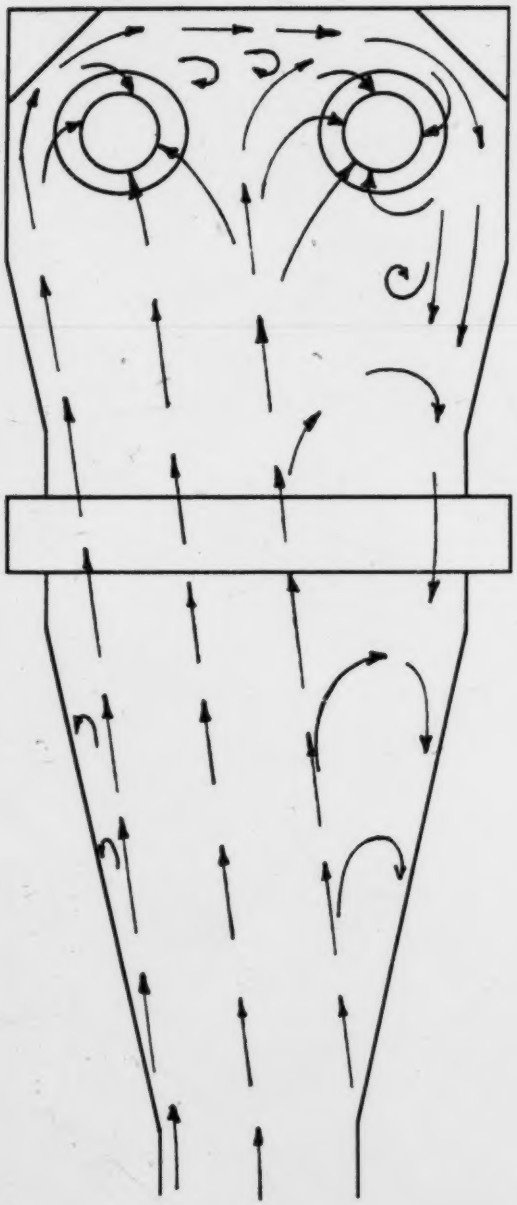

Figure 15. Patterns of flow in the unimproved sump.

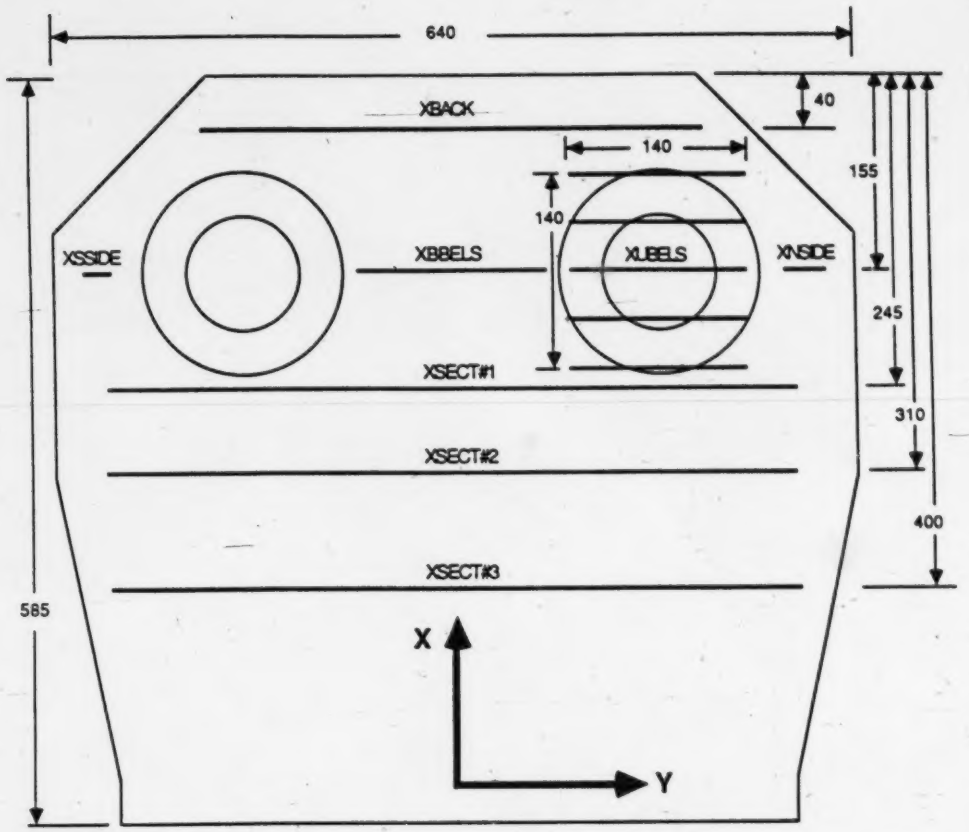

All Dimensions in millimetres.
To get prototype dimensions,
multiply by 8.44.

Figure 16. Plan view of the glass floor section of the sump indicating the locations of the cross-sections where data was taken. These cross-sections are centred in the sump or on the bell centre, except for the sections between the intake bells and the sump wall. These two sections are centred between the bell and the wall.

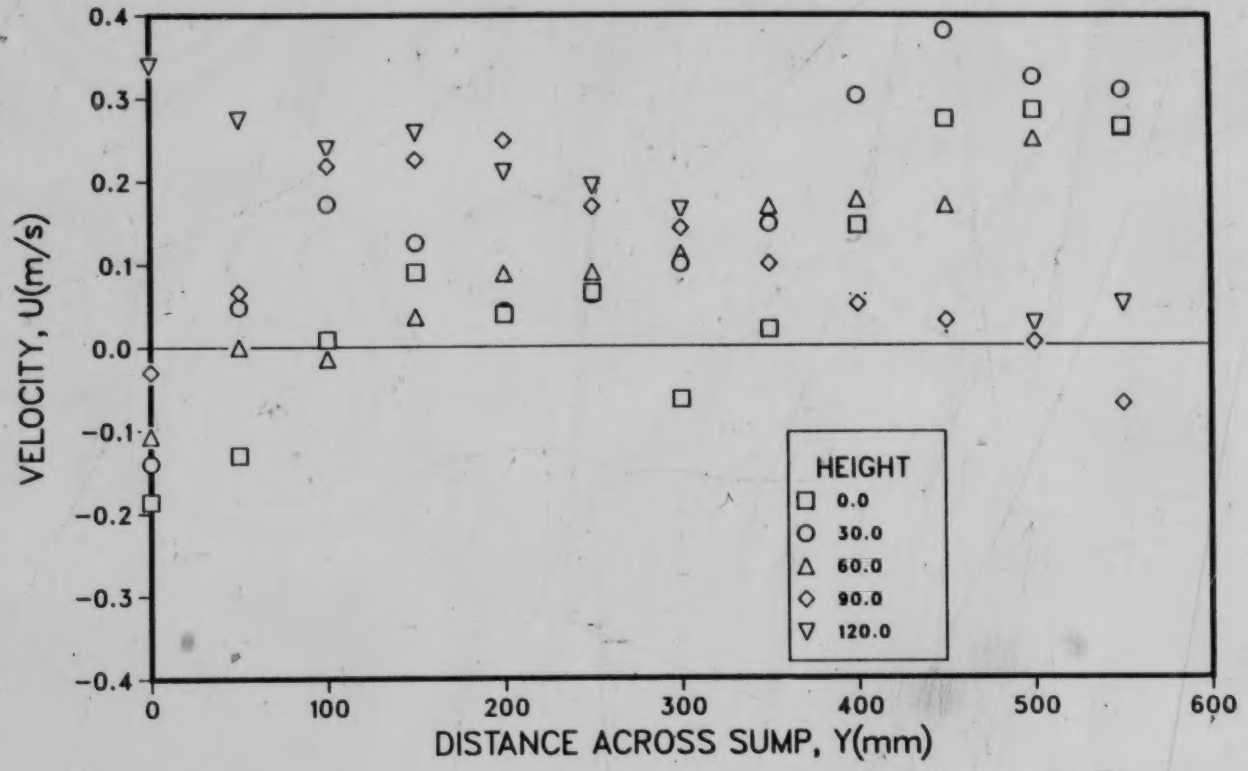

Figure 17. Longitudinal velocity profiles for the first section in the unimproved sump, xsect#1 in figure 16.

2.6.1 The Main Sump

The asymmetry of the flow in the sump can be seen in the velocity profiles. Figures 17 through 19 show the velocity profiles across the entire sump. The second and third cross sections show the jet from the pipe as an area of positive flow on one side of the sump, and the returning flow as an area of negative flow on the opposite side of the sump. Although this area of returning flow seems to be of a much more unsteady nature than the flow in the jet, the turbulence is no higher on this side of the sump. The strong forward flow of the jet as it passes beside the south intake pipe is shown in figure 20. The return flow of the jet is illustrated in a vertical velocity profile in figure 21.

Figure 19, on cross section 3 illustrates the unsteady nature of the jet. For this section, as the data was being taken, the jet moved from one side of the sump to the other. The data for heights very near the floor (ie. height = 0 on plots), at 30mm, and at 60mm were all taken with the jet clinging to one wall. As the LDA moved up to the next level, the jet switched to the opposite wall. This shows up as an inverted velocity profile for levels 90mm and 120mm above the floor.

Cross section number one, figure 17, is a complex mixture of velocity profiles. This section may also have been subject to an inversion as described in the above paragraph. The nearness of the intake bells can be seen to influence the velocity profiles of the heights 0mm and 30mm

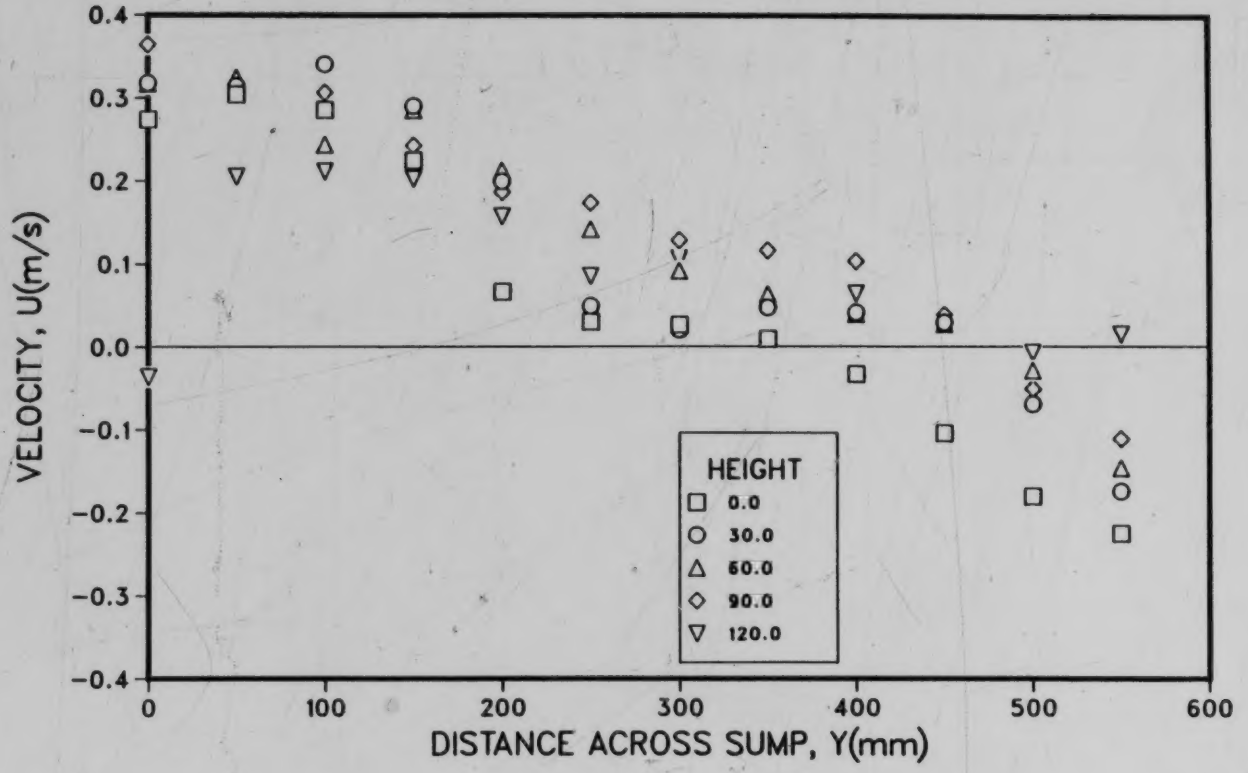

Figure 18. Longitudinal velocity profiles for the second section in the unimproved sump, xsect#2 in figure 16.

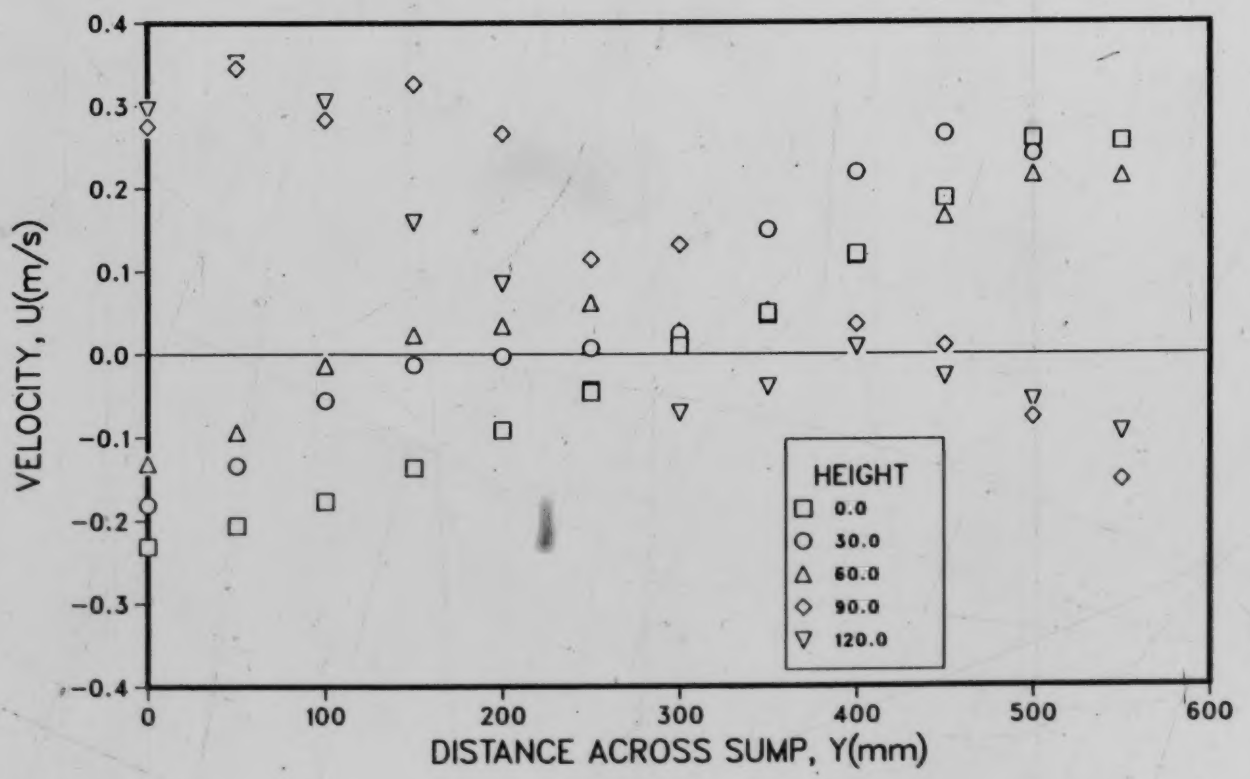

Figure 19. Longitudinal velocity profiles for the third section in the unimproved sump, xsect#3 in figure 16.

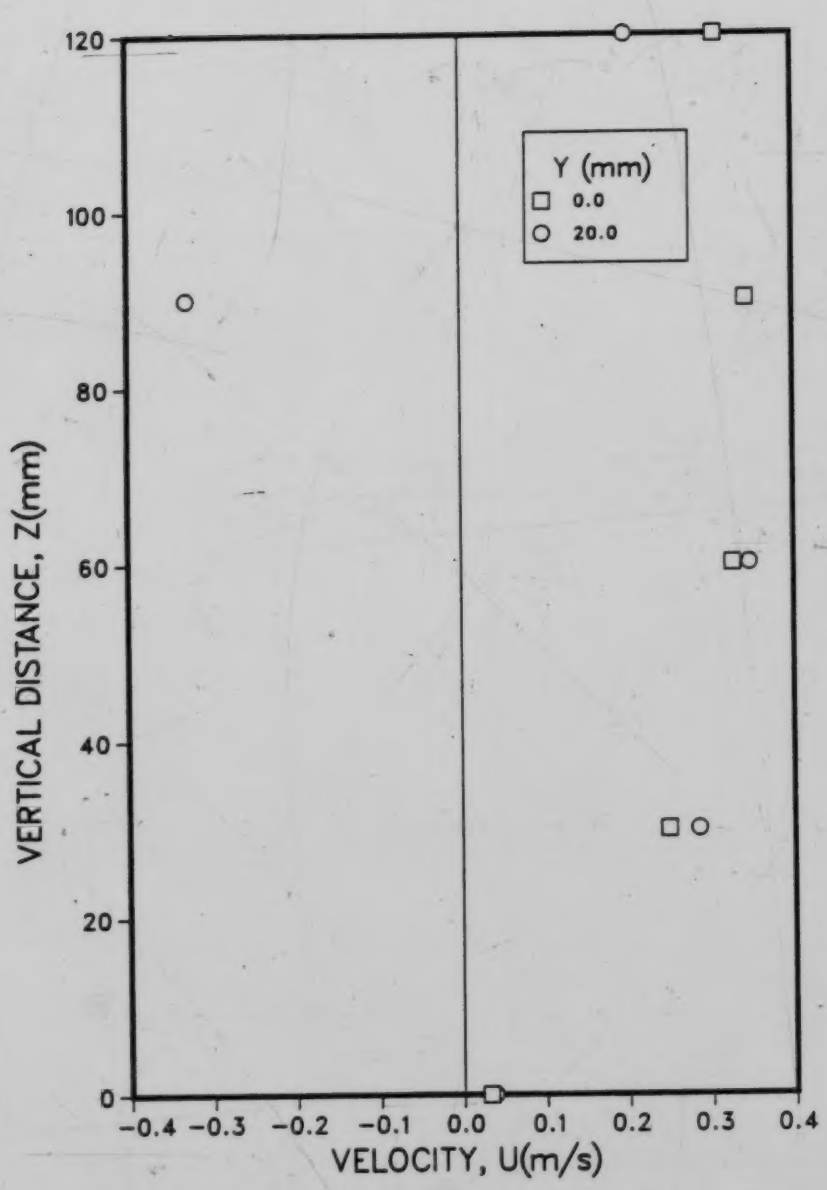

Figure 20. Longitudinal velocity profiles for the area on the south side of the south intake in the unimproved sump, xsside in figure 16.

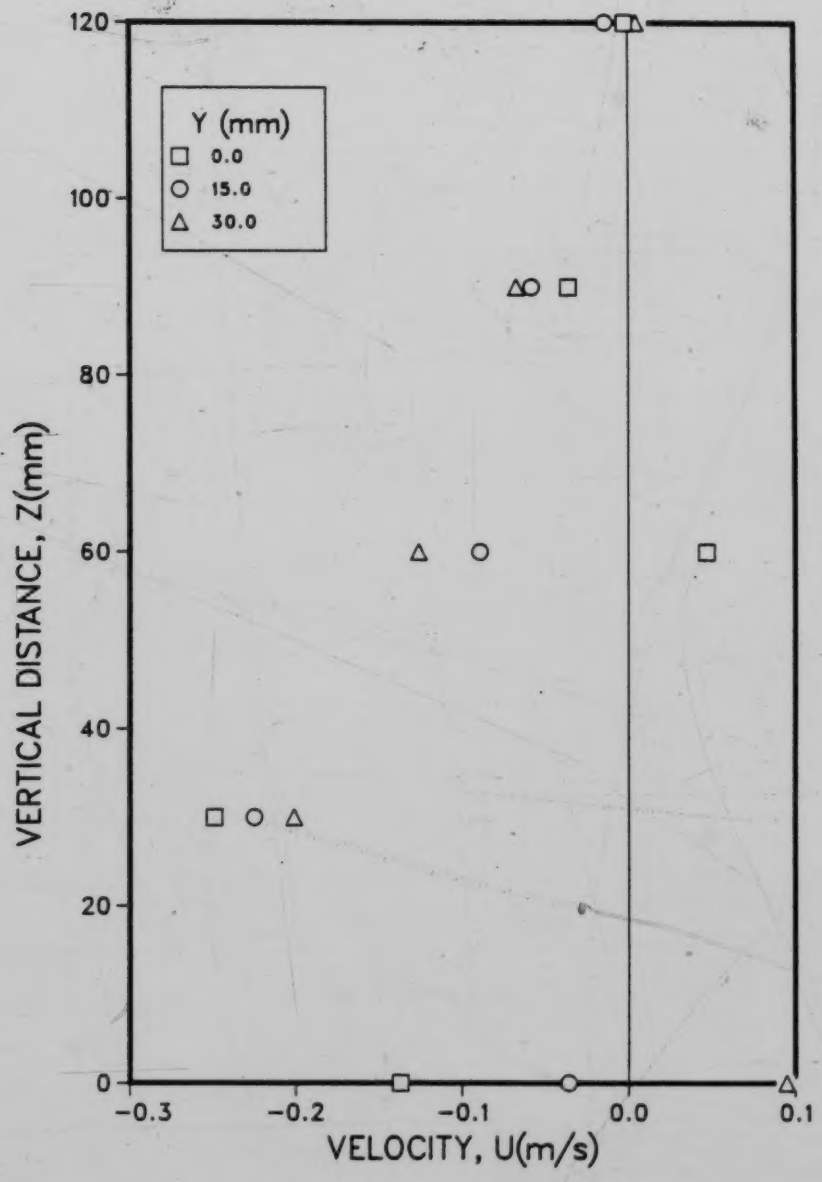

Figure 21. Longitudinal velocity profiles for the area on the north side of the north intake in the unimproved sump, xnside in figure 16.

above the floor. For these two velocity profiles there are two definite humps in the velocity profile at x = 100mm and x = 450mm, areas where the fluid comes under the direct influence of the 'sinks' that are the intake bells.

The cross section between the bells, figure 22, has a positive flow in the upper regions and a negative flow in the lower areas. This flow distribution indicates the tendency for vorticies joining the bells to form. The upper flows move to the backwall, descend and return along the floor forming a circulation pattern around a horizontal axis connecting the two bells. At higher flows, or smaller submergences, this pattern became so intense that a cavitation core vortex filament appeared. An example of this phenomena appears in plate 3.

In the velocity profile of the back wall, shown in figure 23, the influence of the intake bells can again be seen. In the regions very near the floor, two distinct humps in the negative direction are evident in the areas where the bells are located. The turbulence profile for this area, figure 28, is fairly constant across the back wall of the sump. There is a slight tendency for the turbulence to increase with height. This tendency is likely due to a greater abundance of large scale eddies further from the damping effects of the walls. Turbulence is produced near the wall due to the action of the boundary layer, but this is small in comparison to the turbulence that already exists. Figures 24 through 28 show the turbulence profiles

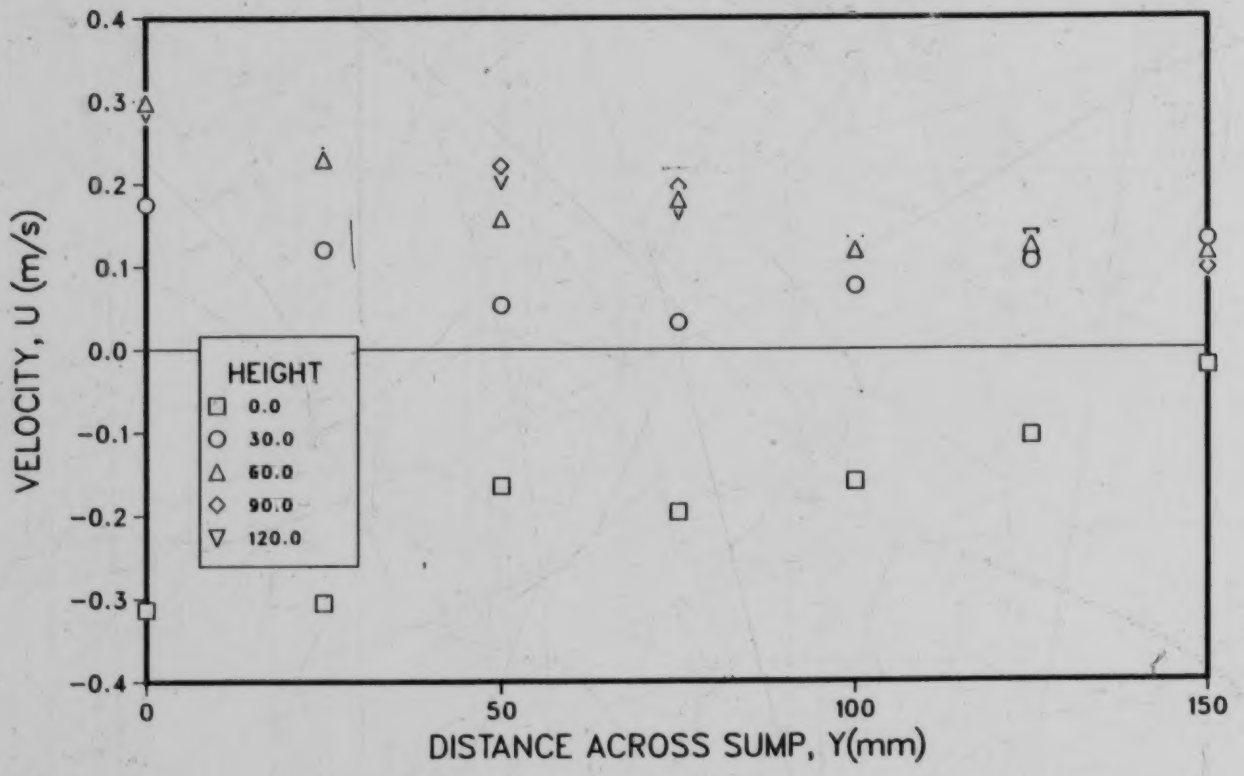

Figure 22. Longitudinal velocity profiles for the section between the bells of the improved sump, xbbels in figure 16.

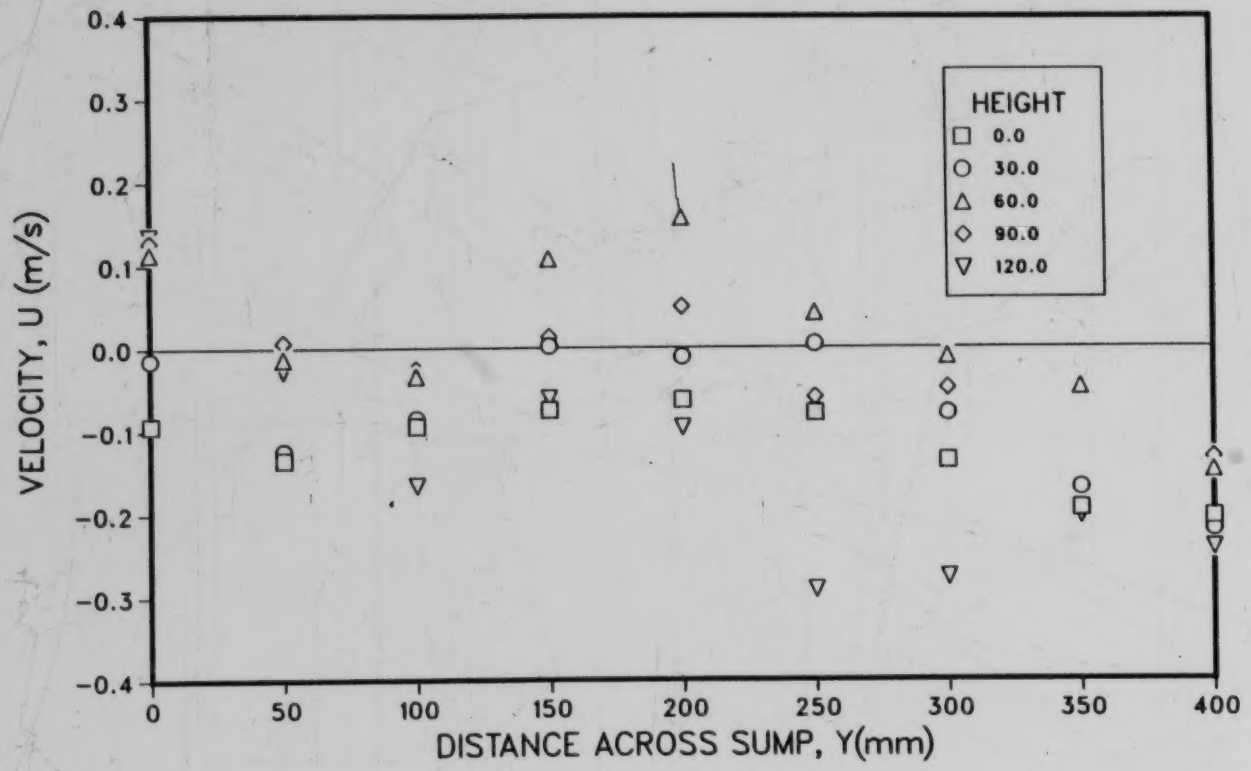

Figure 23. Longitudinal velocity profiles for the section near the back wall of the unimproved sump, xback in figure 16.

for the sections in the main sump.

2.6.2 Structure of Flow Under the Intake Bell

Figures 29 through 33 show the variation of the U component of the velocity. At sections one, two and five the flow is directed quite uniformly towards the centre of the intake bell. Sections three and four contain areas of positive and negtive flow on opposite sides of the intake. These profiles illustrate the intense floor vorticies seen constantly below the intake bells in the unimproved sump. An example of these vorticies is shown in plate four. The velocity profile of the third cross section is typical of what would be expected across a vortex. High velocities of opposing sign exist on opposite sides of the vortex centre, with an area of lower velocities near the centre. The area of low velocities near the centre is much larger than it would be for an ideal vortex. Some of the lower velocities in the centre area may be low due to the averaging of high velocities with opposing sign.

For the third and fourth sections, the areas where the floor vortex was active, the turbulence was very much higher than for the other sections. The turbulence is highest in the centre, the area of smallest velocity. High turbulence is to be expected in these areas since this is where the vortex core will pass most frequently. The vortex was very intense as evidenced by the cavitation core that was usually present. As the vortex core passes the point where the

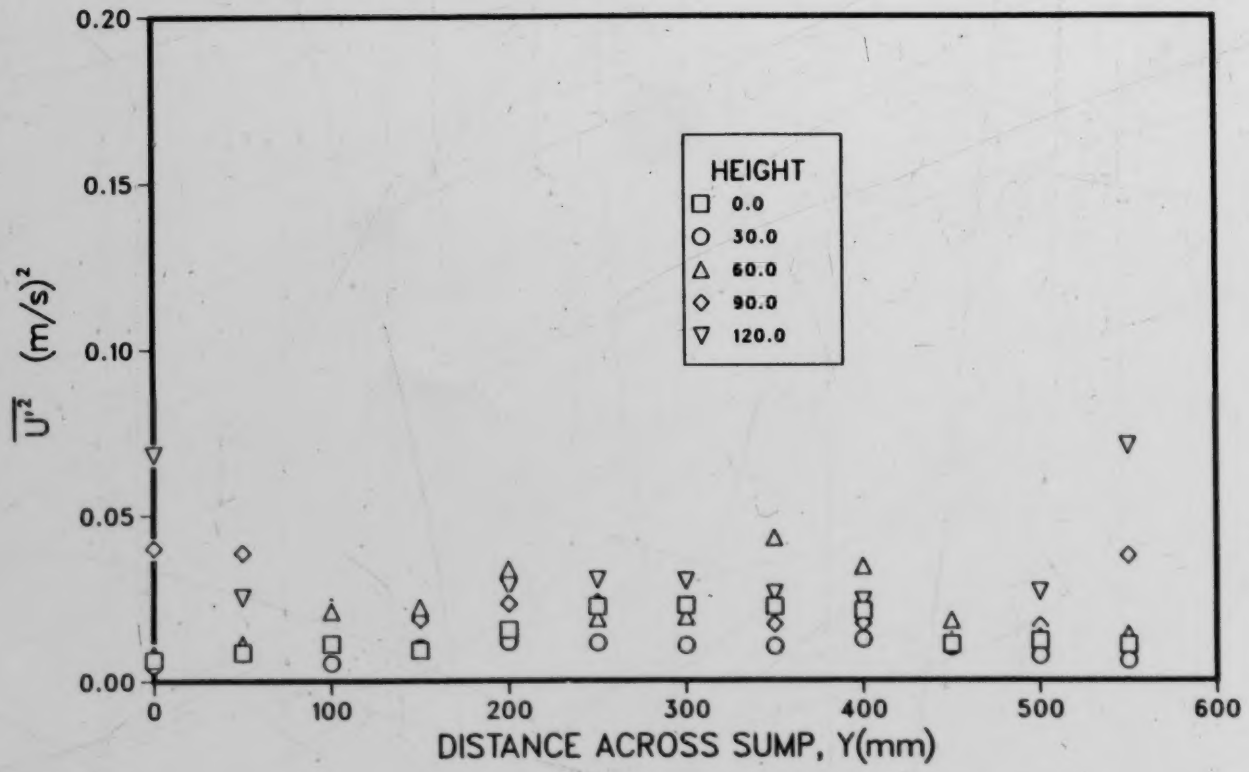

Figure 24. Longitudinal turbulent velocity fluctuations for the first section in unimproved sump, xsect#1 in figure 16.

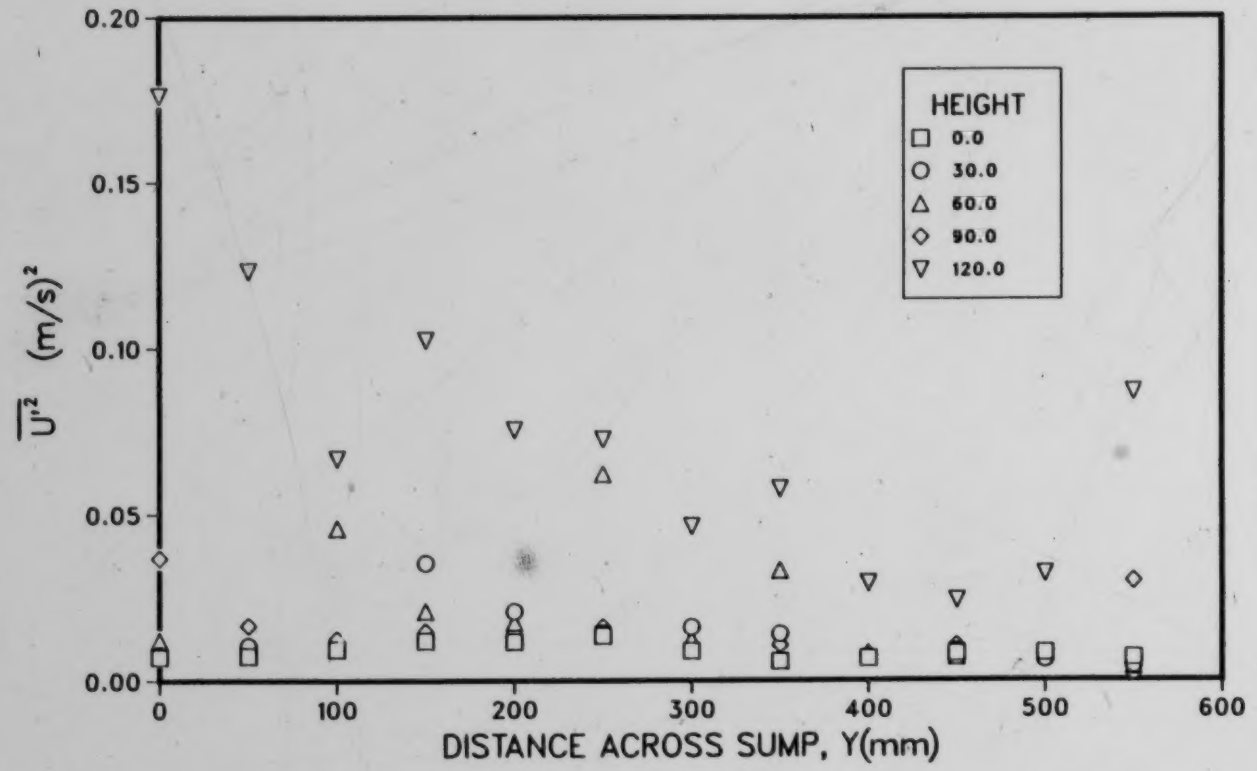

Figure 25. Longitudinal turbulent velocity fluctuations for the second section in unimproved sump, xsect#2 in figure 16.

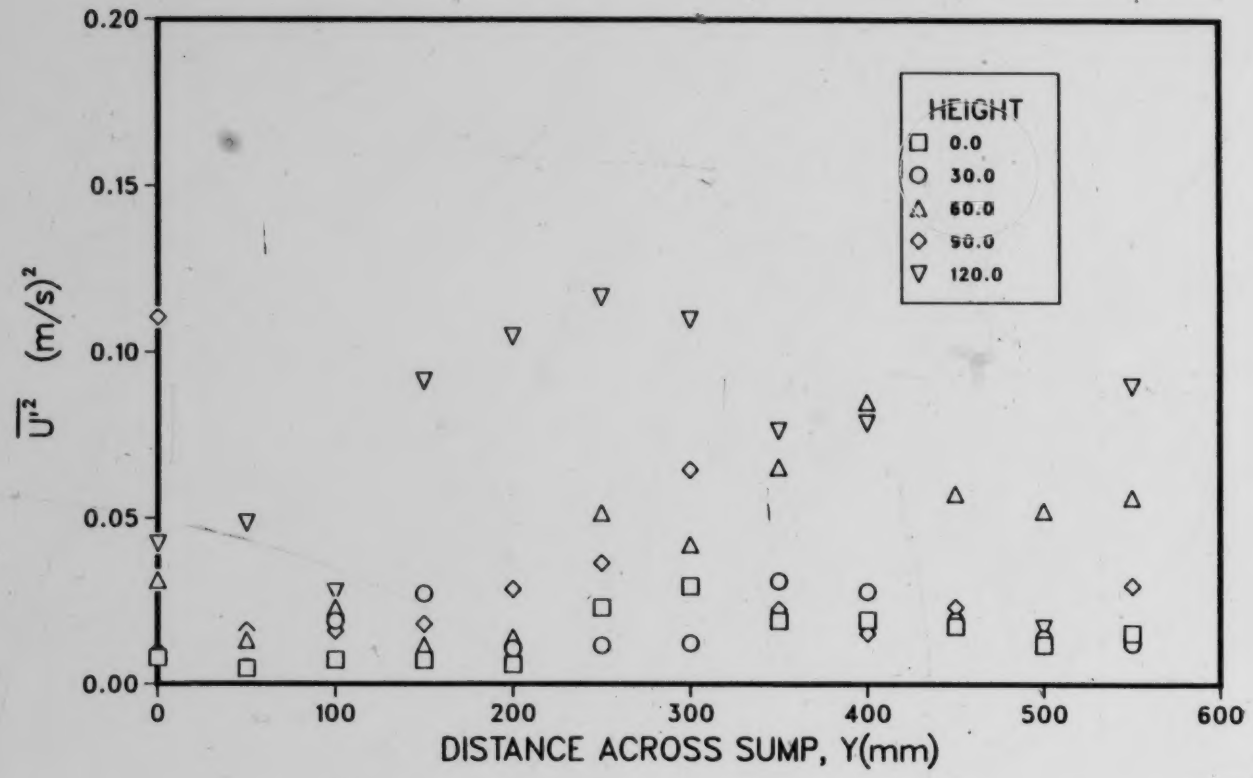

Figure 26. Longitudinal turbulent velocity fluctuations for the third section in unimproved sump, xsect#3 in figure 16.

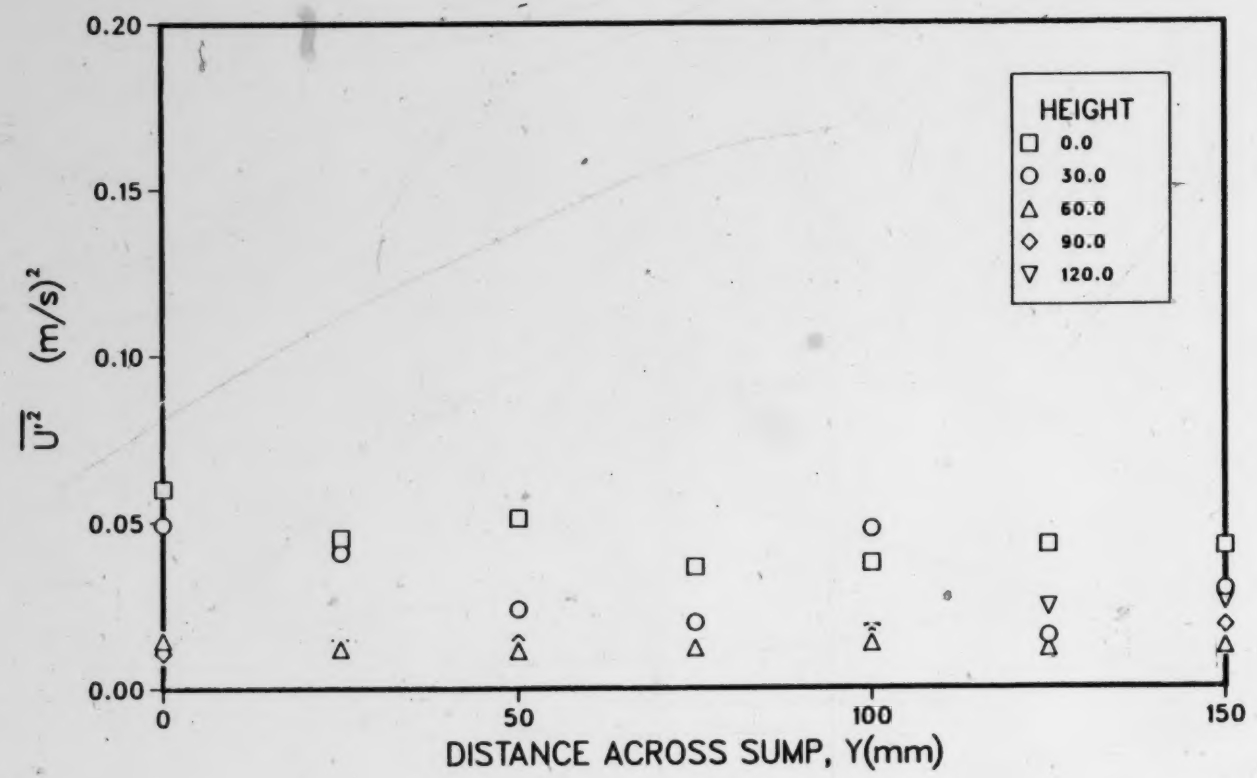

Figure 27. Longitudinal turbulent velocity fluctuations for the section between the bells of the unimproved sump, xbbels in figure 16.

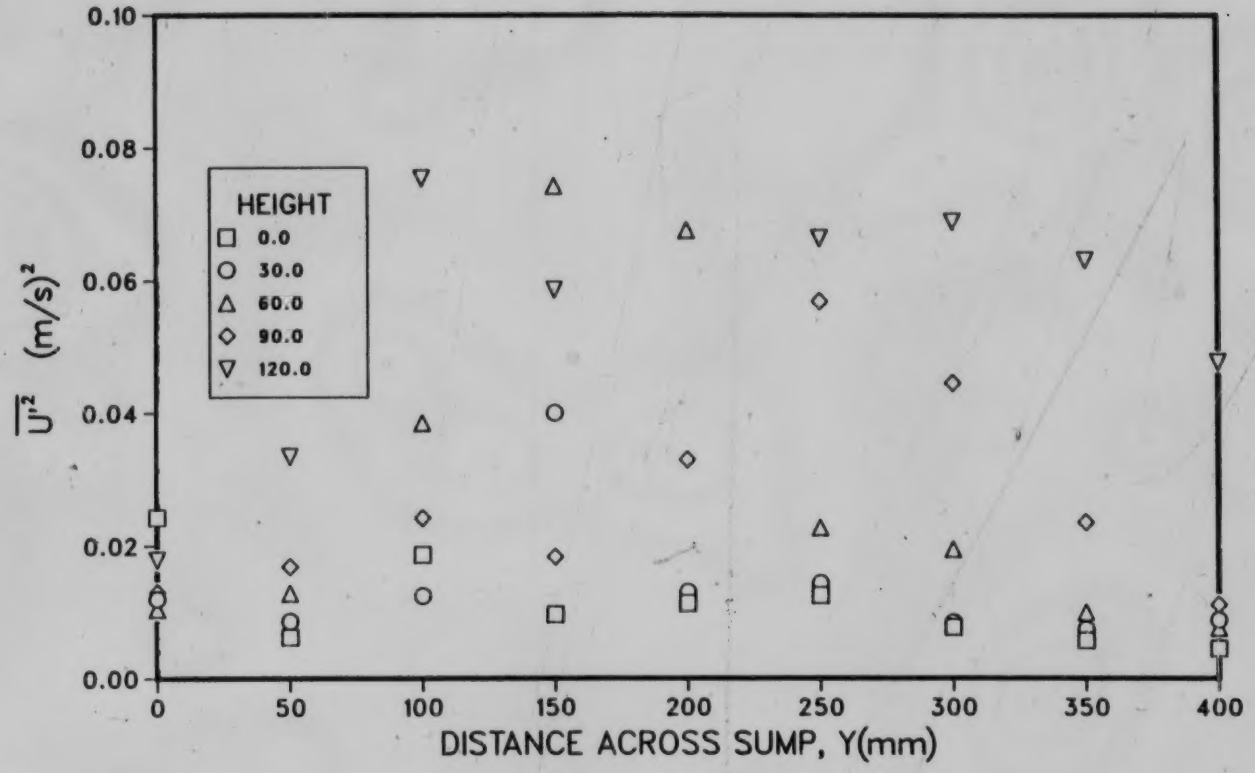

Figure 28. Longitudinal turbulent velocity fluctuations for the section near the back wall of the unimproved sump, xback in figure 16.

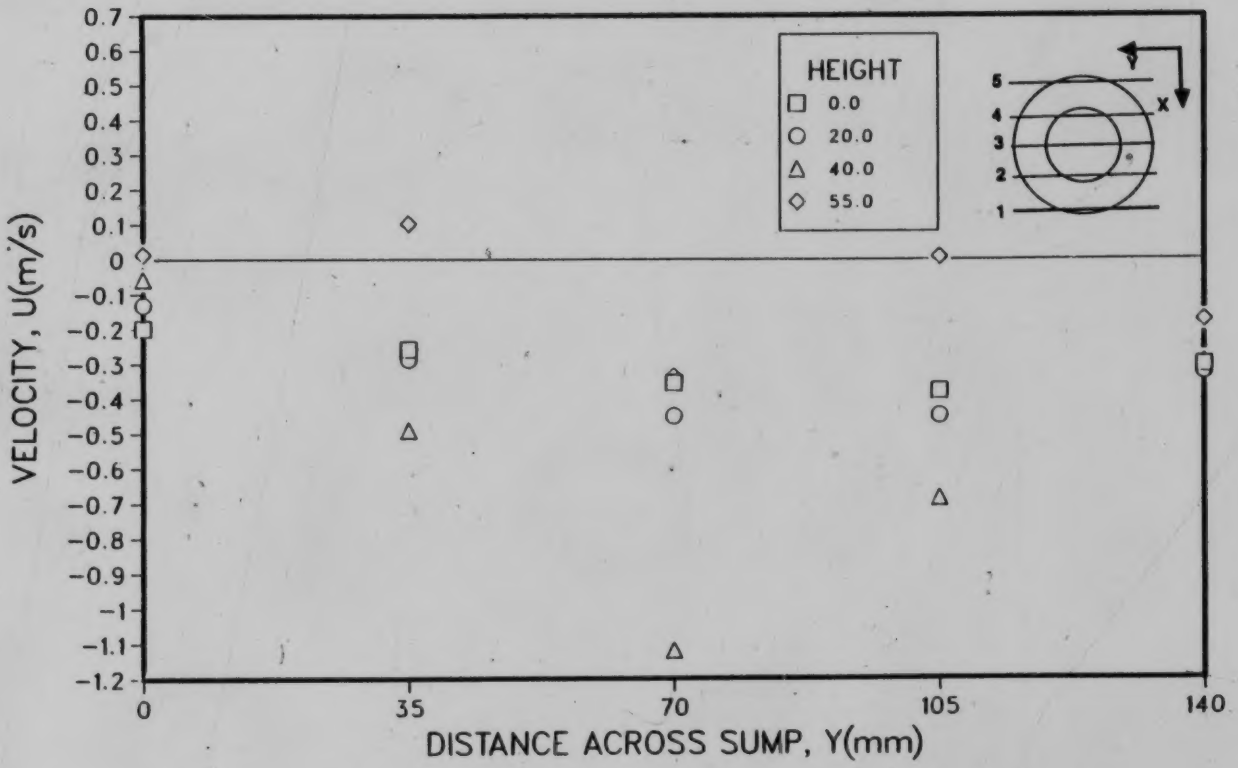

Figure 29. Longitudinal velocity profiles for the area under the north bell, section 1 in the area xubels of figure 16. Location shown in small inset figure.

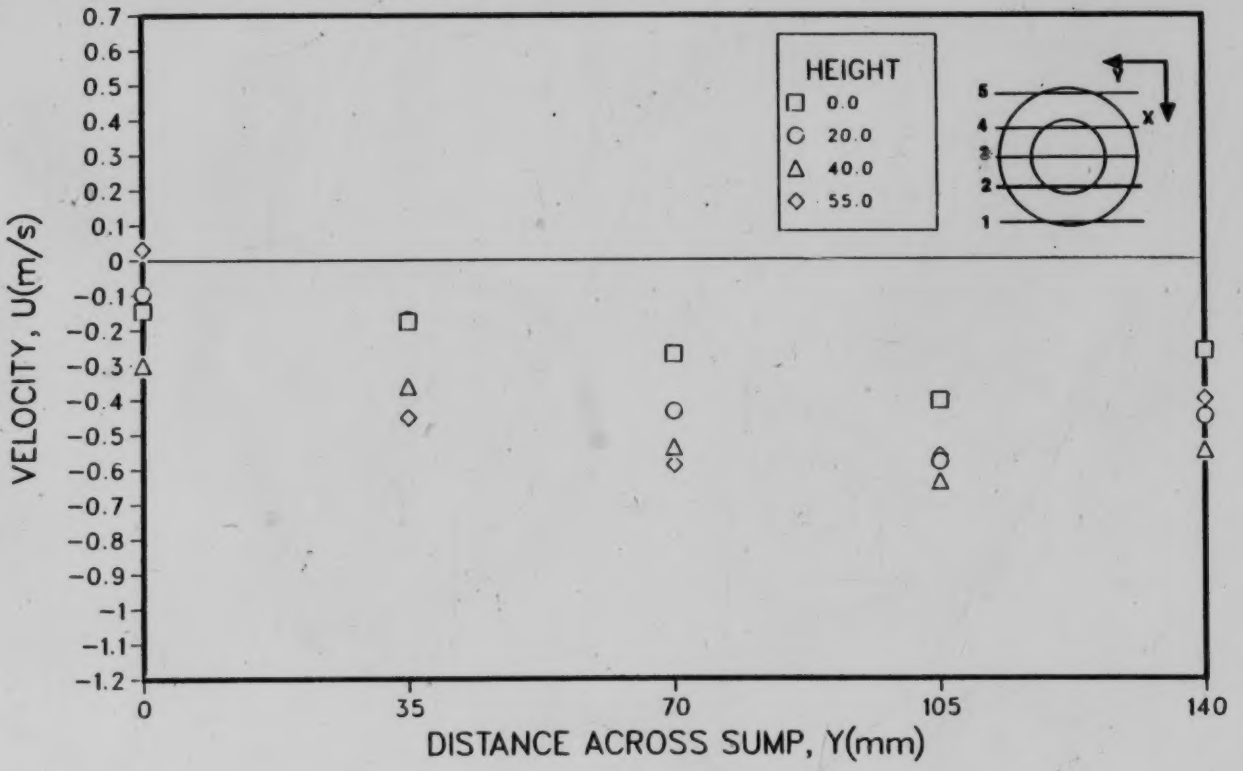

Figure 30. Longitudinal velocity profiles for the area under the north bell, section 2 in the area xubels of figure 16. Location shown in small inset figure.

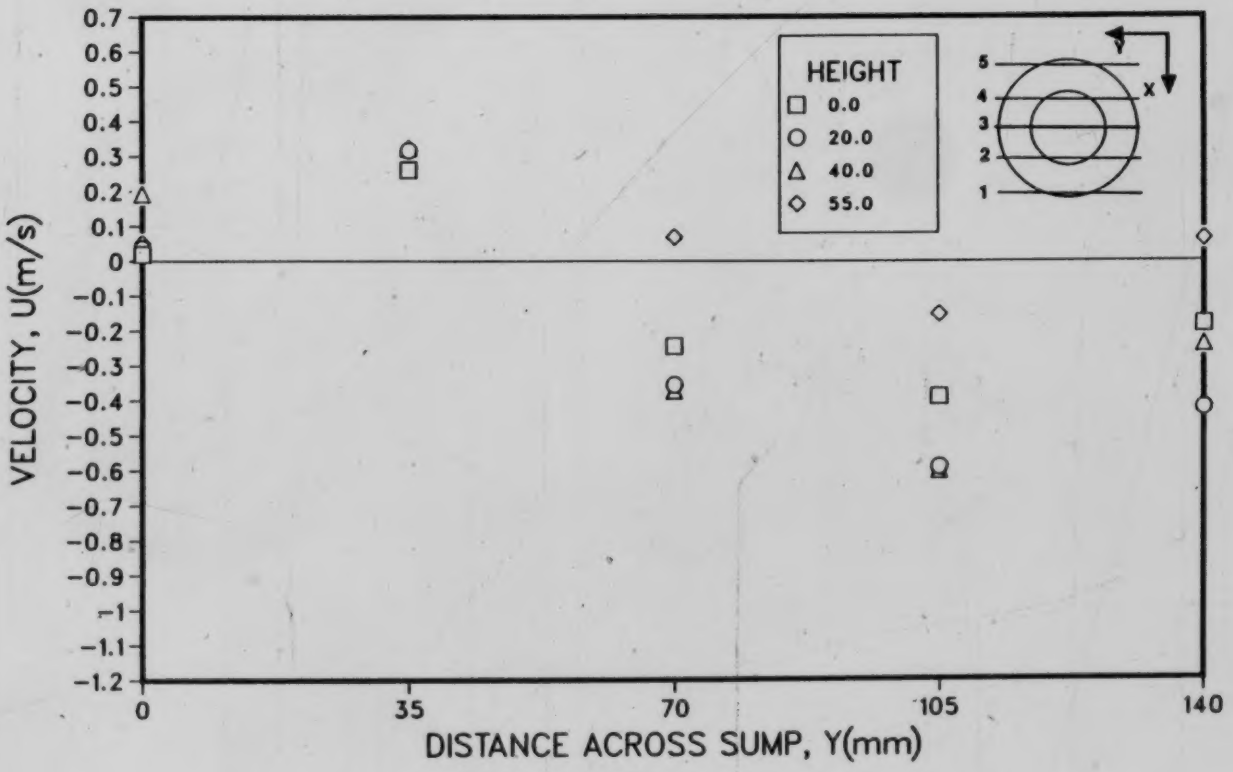

Figure 31. Longitudinal velocity profiles for the area under the north bell, section 3 in the area xubels of figure 16. Location shown in small inset figure.

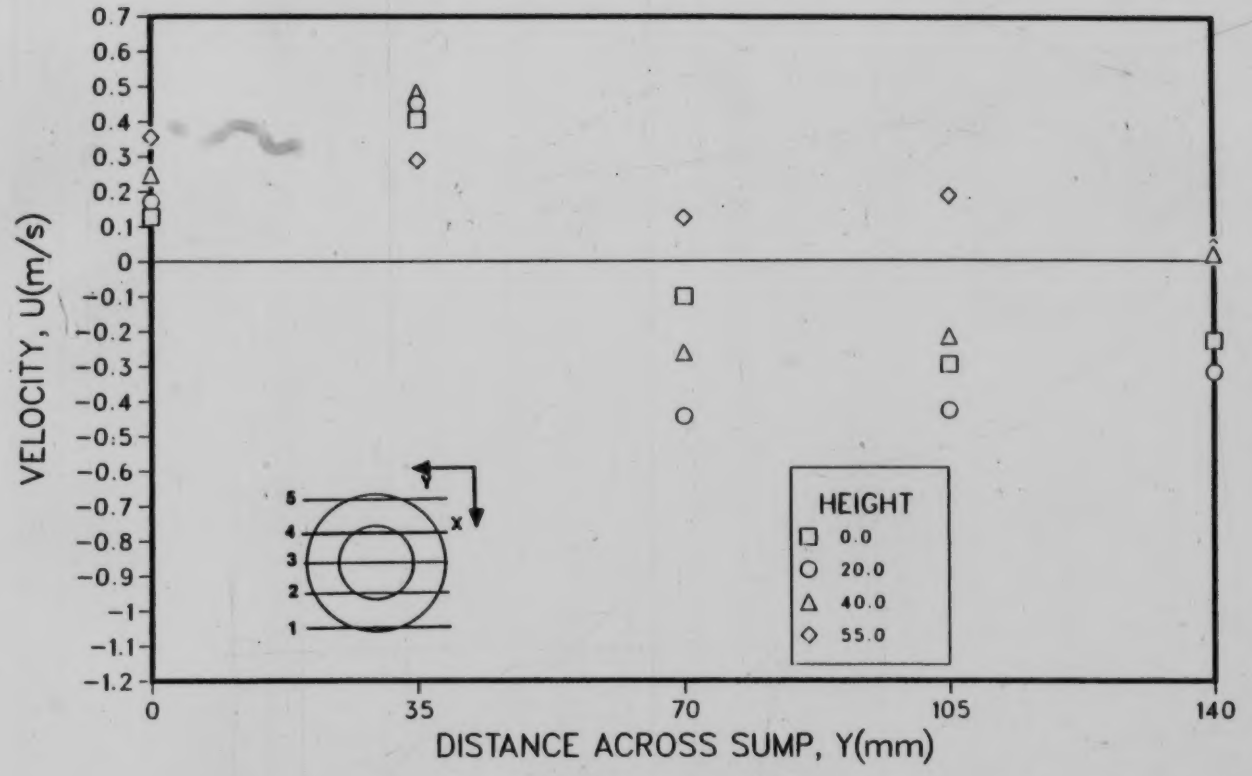

Figure 32. Longitudinal velocity profiles for the area under the north bell, section 4 in the area xubels of figure 16. Location shown in small inset figure.

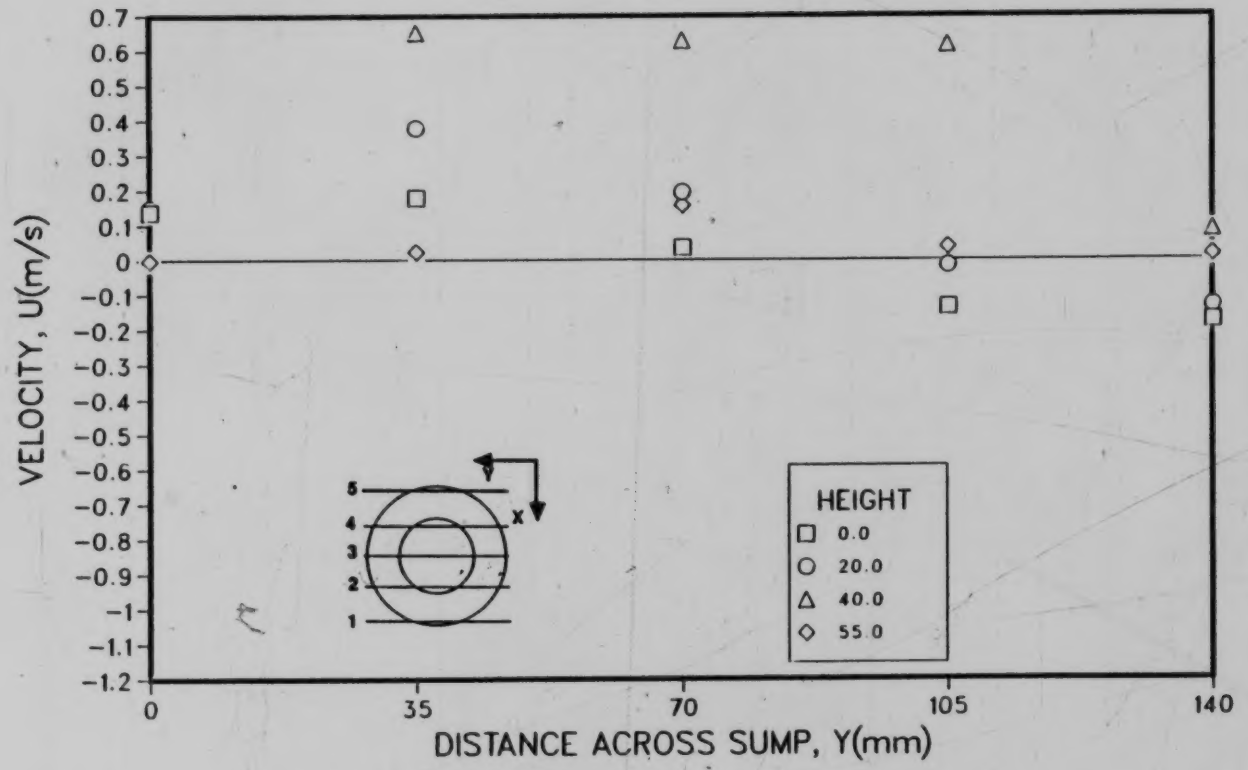

Figure 33. Longitudinal velocity profiles for the area under the north bell, section 5 in the area xubels of figure 16. Location shown in small inset figure.

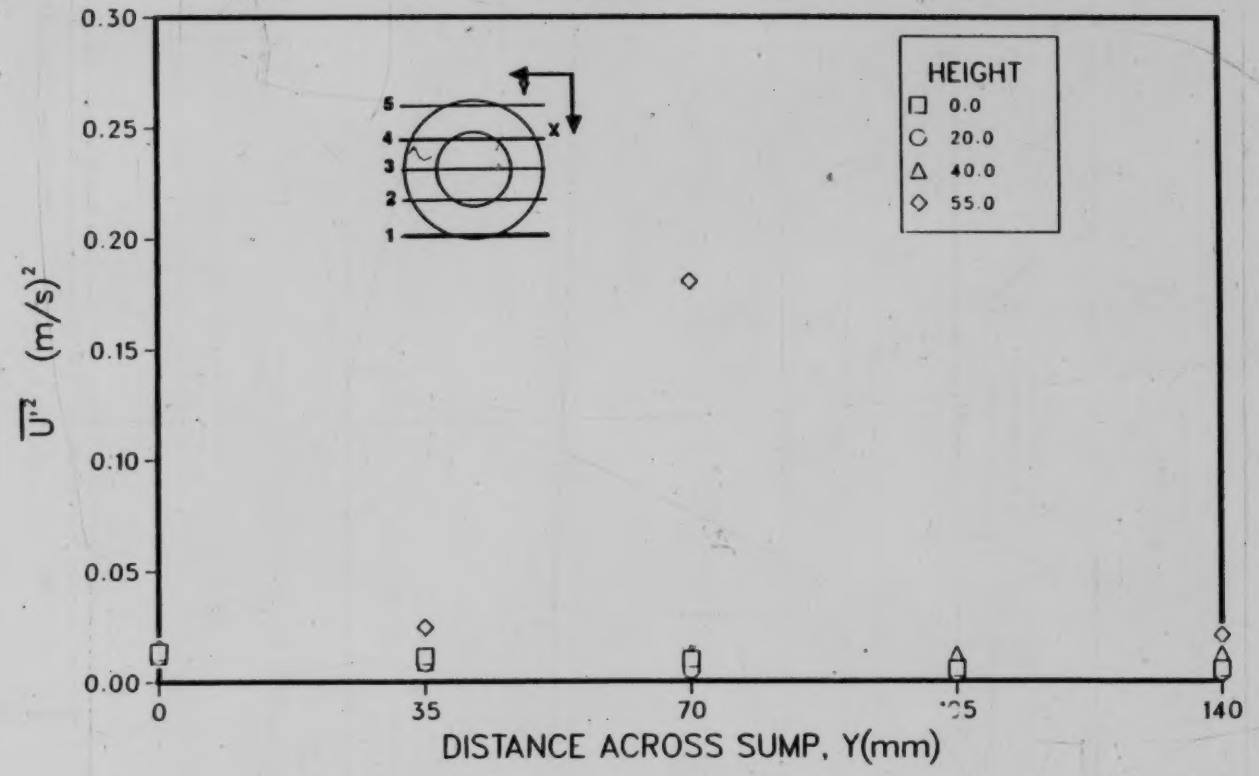

Figure 34. Longitudinal turbulent velocity fluctuations for the area under the north bell, section 1 in the area xubels of figure 16. Location shown in small inset figure.

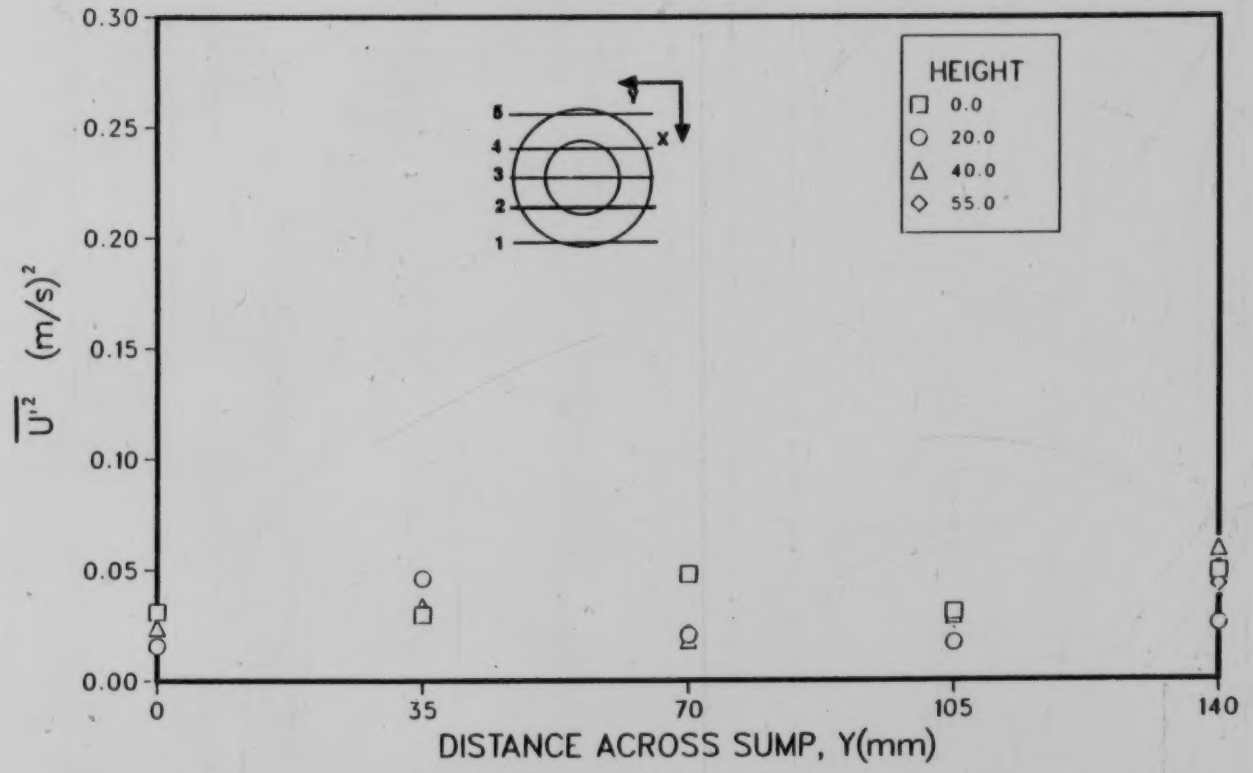

Figure 35. Longitudinal turbulent velocity fluctuations for the area under the north bell, section 2 in the area xubels of figure 16. Location shown in small inset figure.

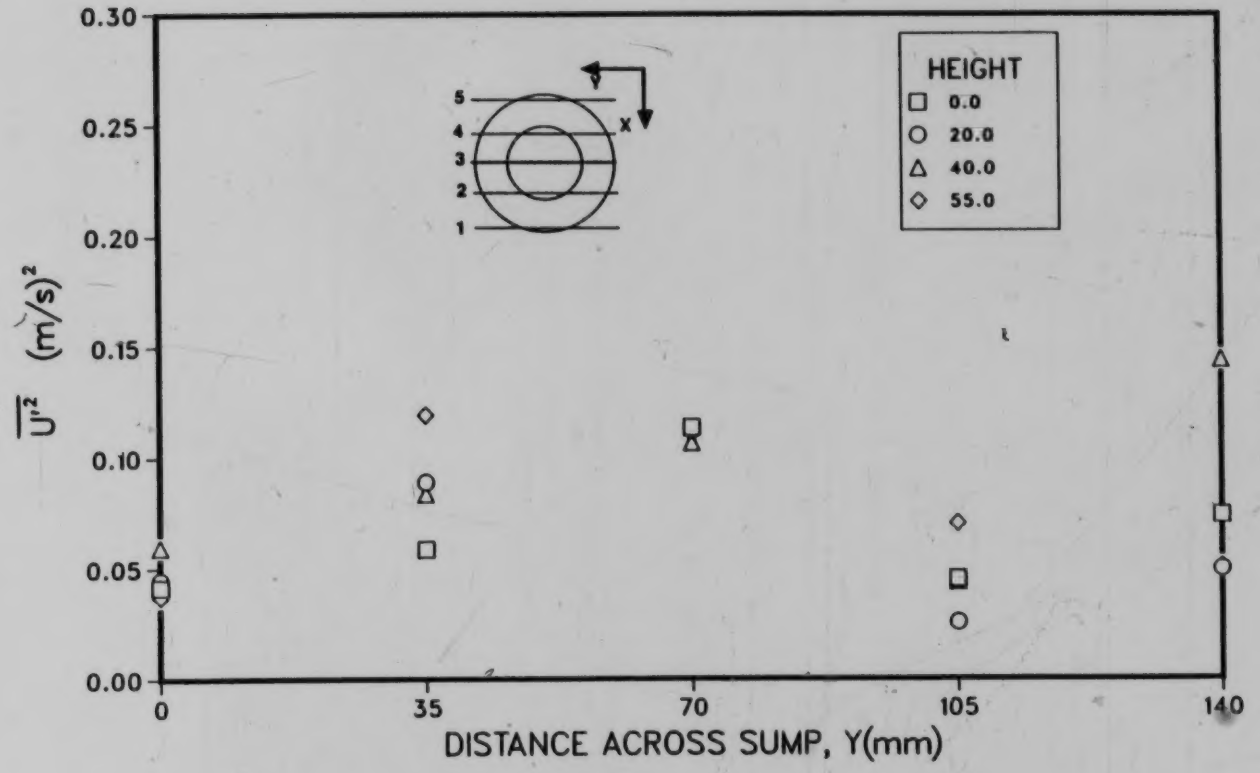

Figure 36. Longitudinal turbulent velocity fluctuations for the area under the north bell, section 3 in the area xubels of figure 16. Location shown in small inset figure.

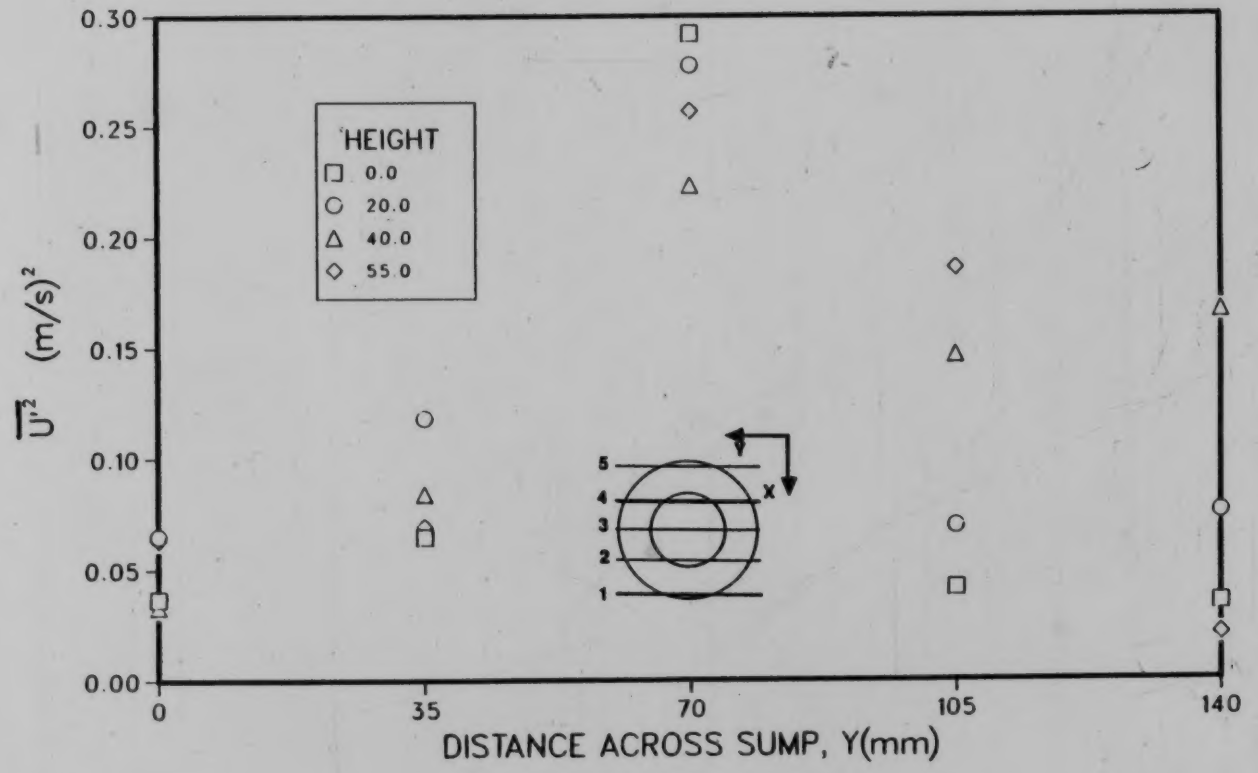

Figure 37. Longitudinal turbulent velocity fluctuations for the area under the north bell, section 4 in the area xubels of figure 16. Location shown in small inset figure.

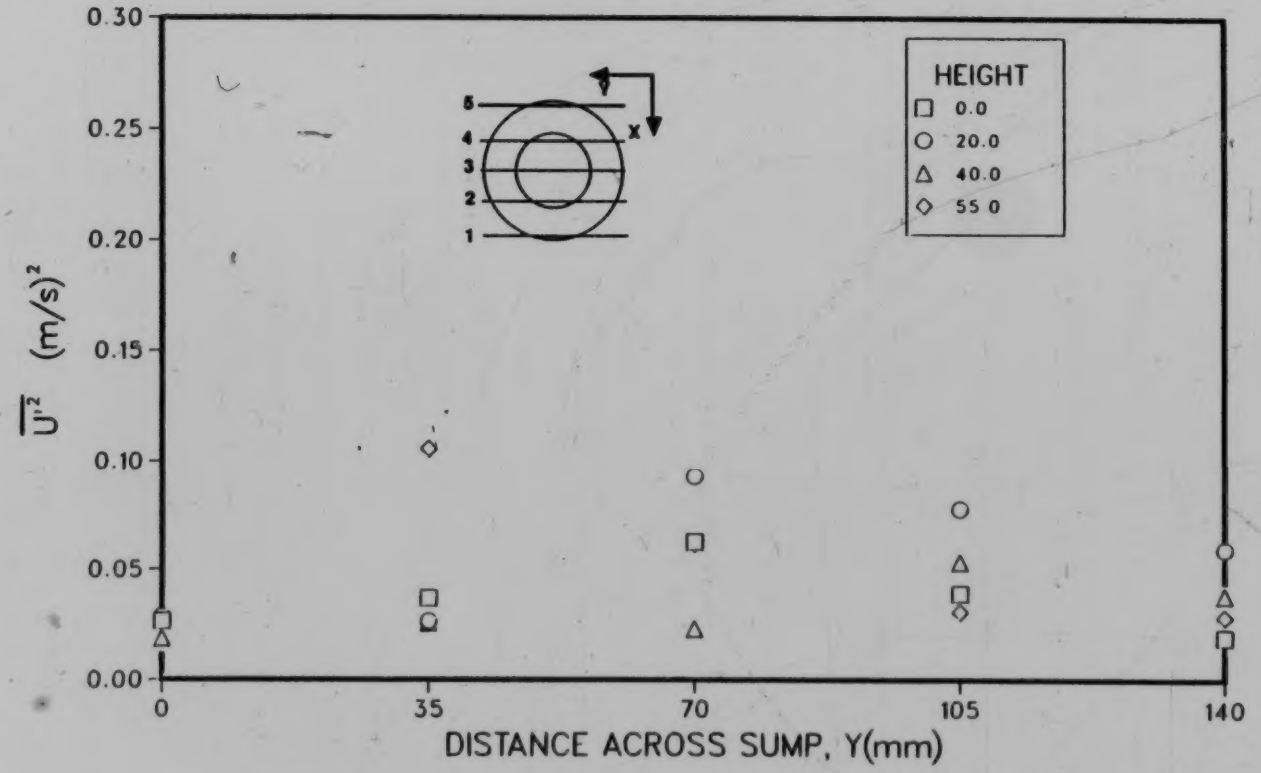

Figure 38. Longitudinal turbulent velocity fluctuations for the area under the north bell, section 5 in the area xubels of figure 16. Location shown in small inset figure.

velocity is measured, the velocity will change dramatically from positive to negative, or negative to positive depending on the direction of rotation. Figures 34 through 38 show the turbulence profiles for this area.

The transverse velocity profiles, figures 39 through 43, show the same features of the flow as did those in the longitudinal direction. The velocity profiles at y values of 0, 35, 105, and 140 millimetres show a steady flow towards the intake bell. No new trends can be found from these velocity profiles. The transverse velocity profile for y = 70mm, figure 41, again illustrates the vortexing motion under the bells. The velocities near the back wall are negative and those farther away are positive showing the tendency for the fluid in this area to circulate. This tendency does not show up as clearly here as it had in the U velocity profiles. The velocities for the centre of this profile are the highest, which is opposite to the U velocity trends. This could only be due to the vortex core staying on one side of the data collection point for the majority of the time. Plates 5 and 6 illustrate more vortexing problems.

2.6.3 Inside the Intake Pipes

Figures 44 and 45 show the vertical variation of both the transverse (V) and longitudinal (U) velocities at a distance of one quarter of the pipe diameter inside the intake pipe. This area of the sump contains the results of all the nonuniformities of the flow in the main sump. The

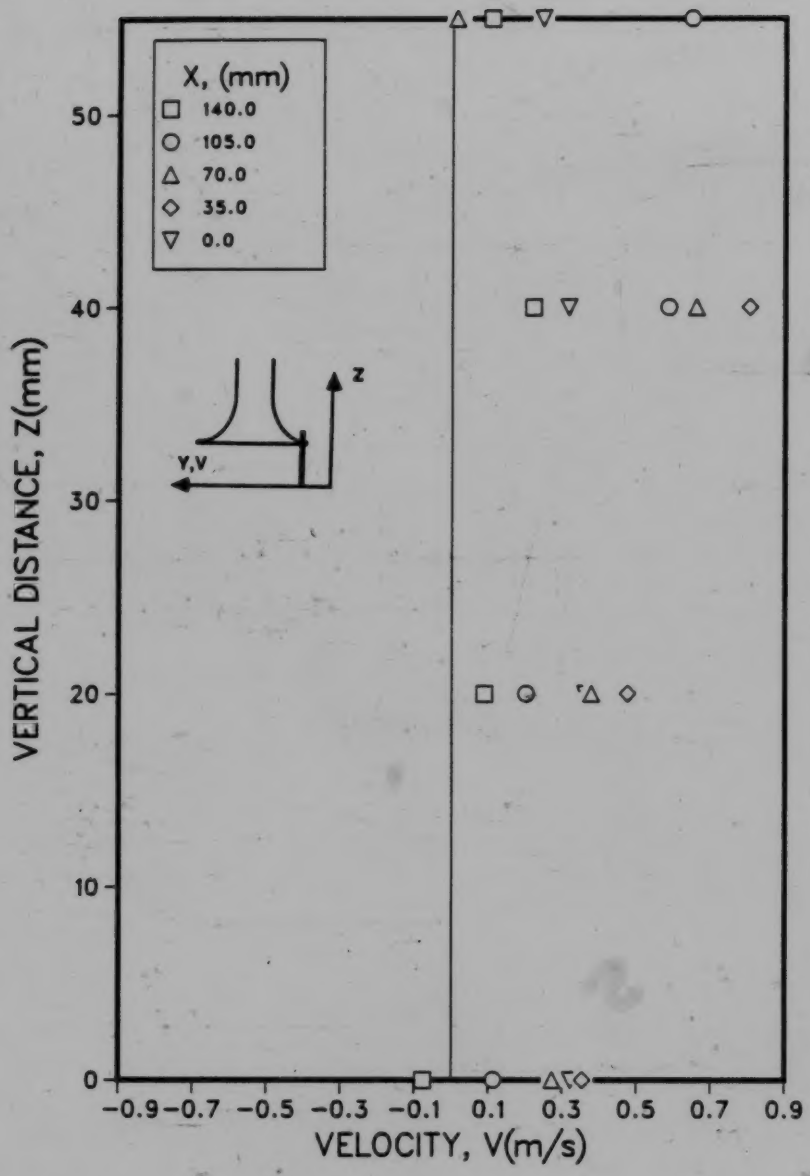

Figure 39. Vertical profiles of the transverse velocity under the north bell of the unimproved sump, profiles at y = 0 in the area xubels. Location shown in small inset figure.

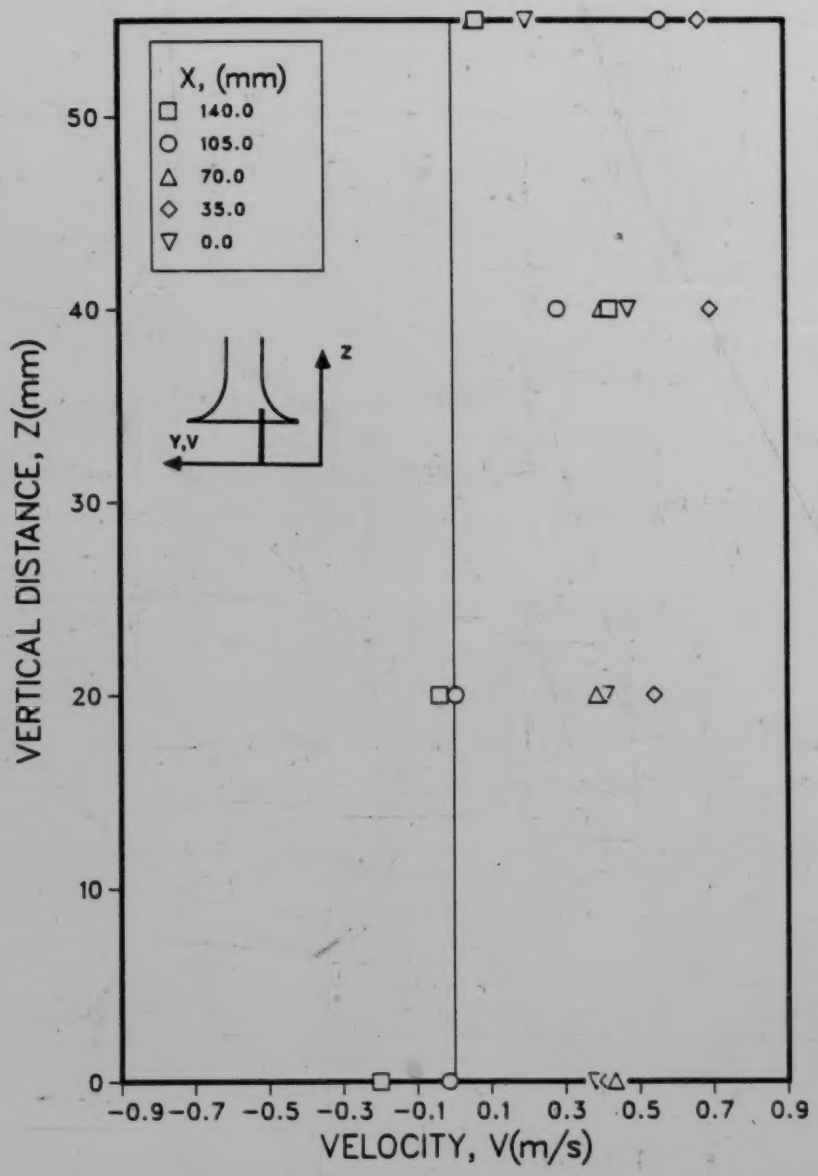

Figure 40. Vertical profiles of the transverse velocity under the north bell of the unimproved sump, profiles at y = 35 in the area xubels. Location shown in small inset figure.

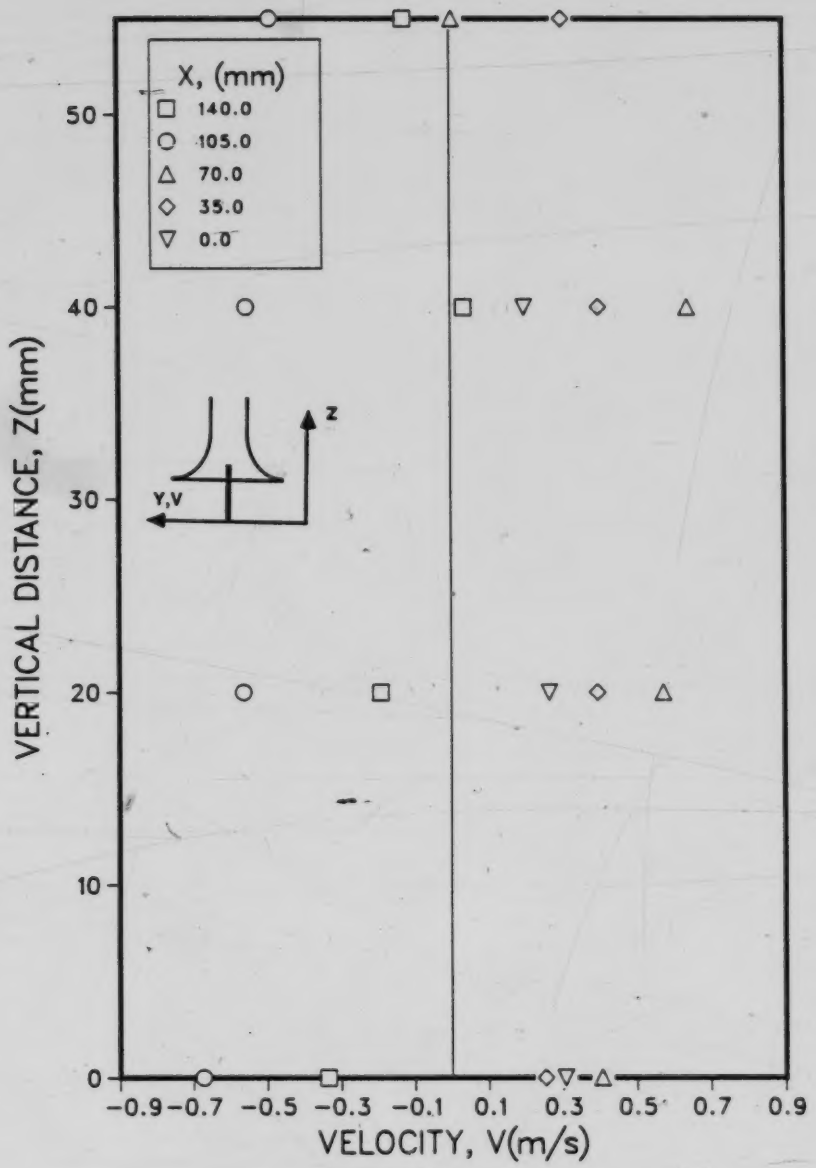

Figure 41. Vertical profiles of the transverse velocity under the north bell of the unimproved sump, profiles at y = 70 in the area xubels. Location shown in small inset figure.

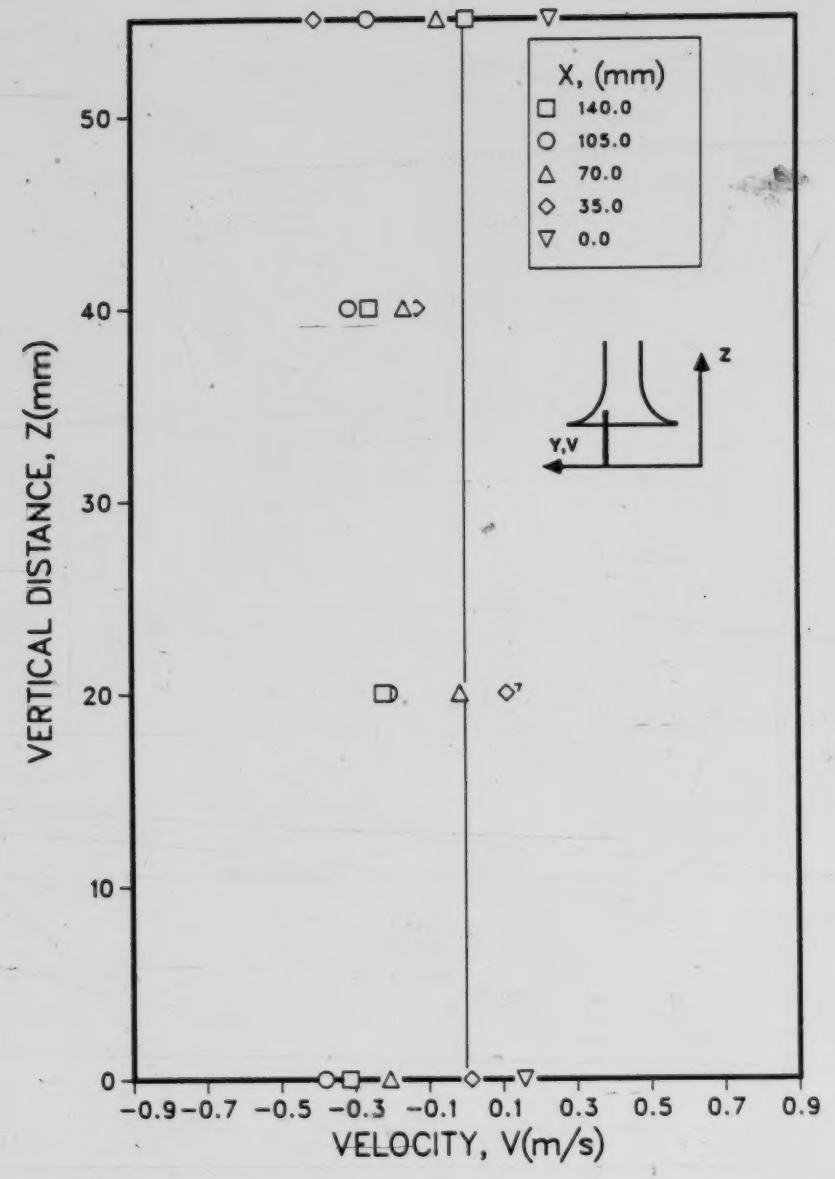

Figure 42. Vertical profiles of the transverse velocity under the north bell of the unimproved sump, profiles at y = 105 in the area xubels. Location shown in small inset figure.

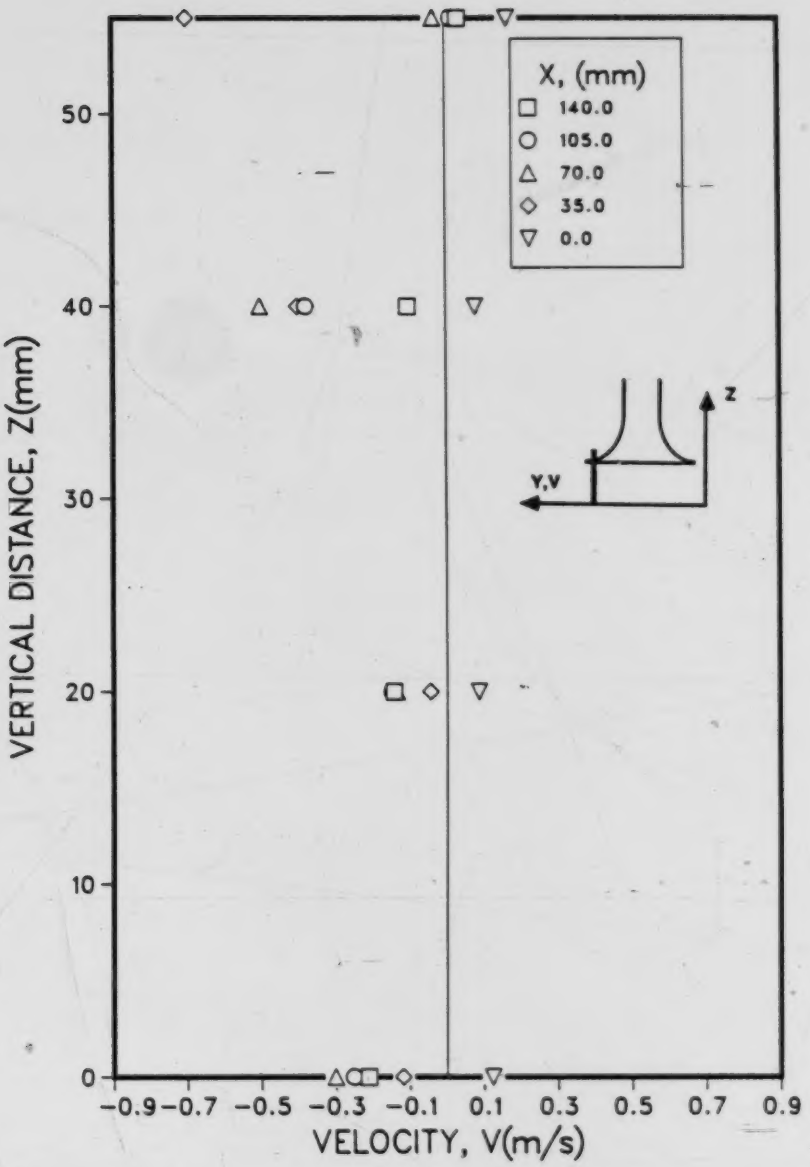

Figure 43. Vertical profiles of the transverse velocity under the north bell of the unimproved sump, profiles at y = 140 in the area xubels. Location shown in small inset figure.

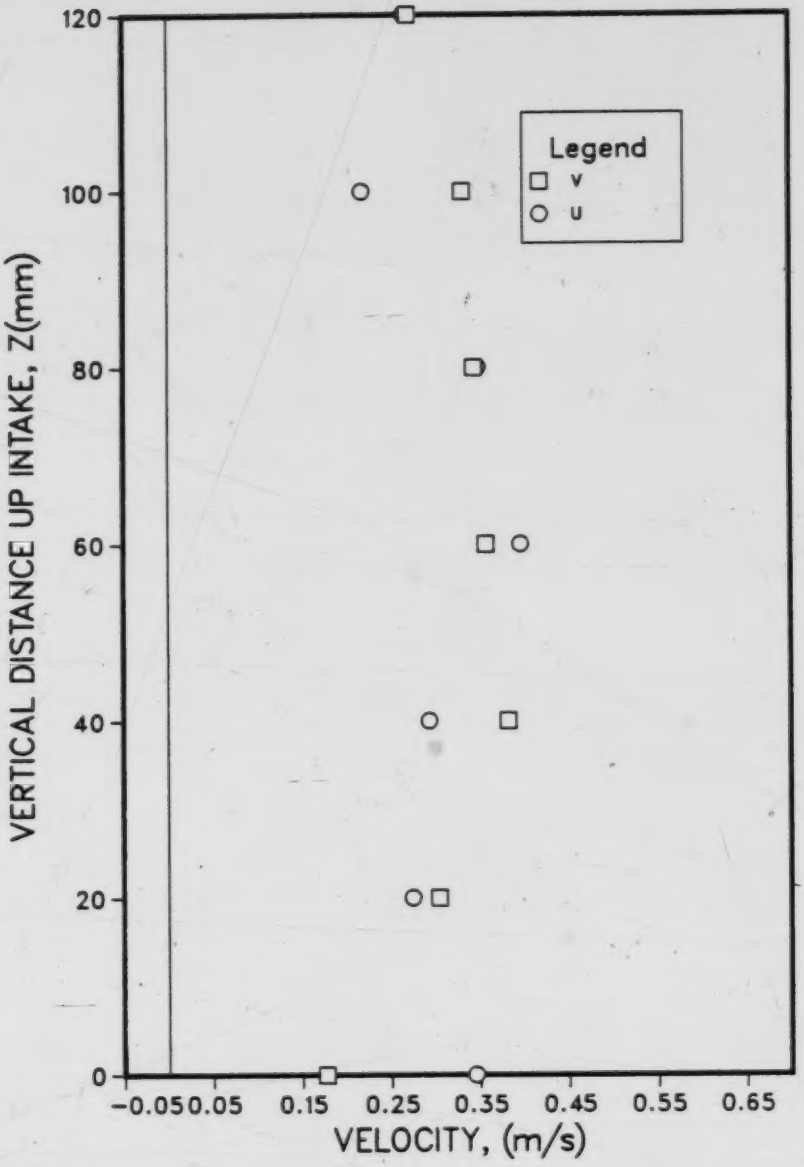

Figure 44. Vertical velocity profiles taken at one quarter of the pipe diameter from the inside wall of the south intake pipe.

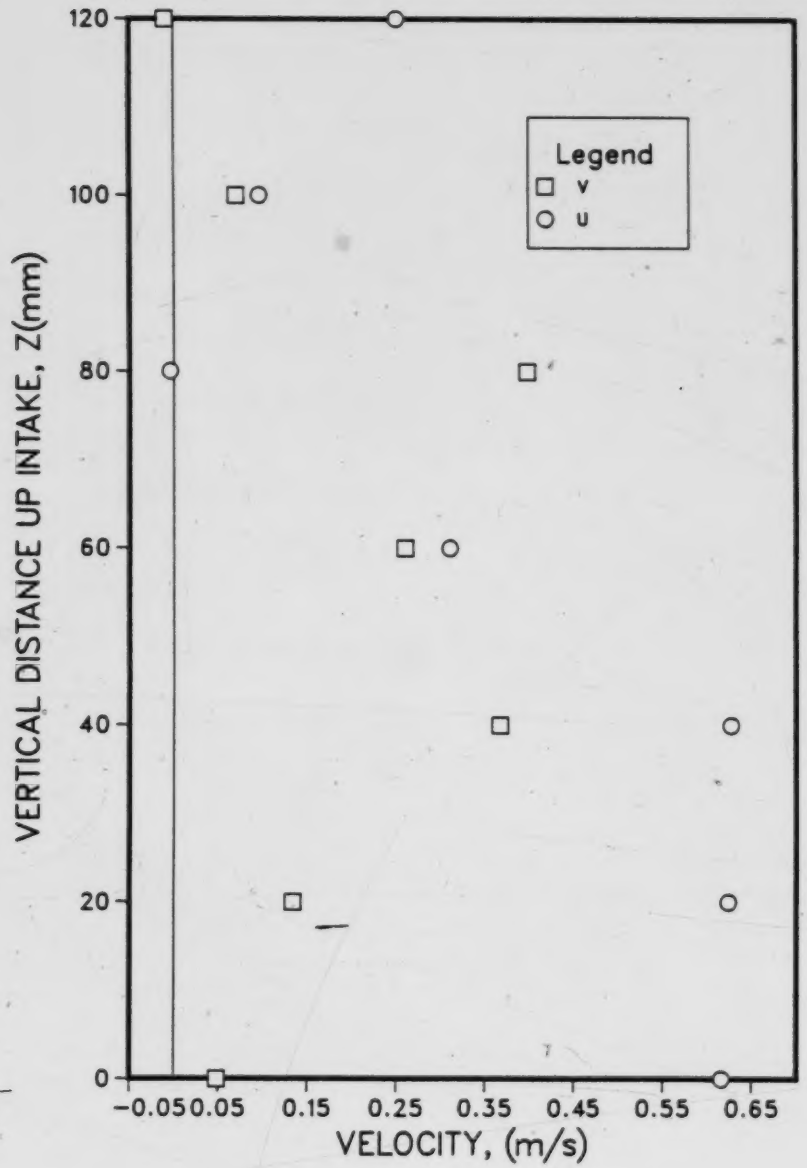

Figure 45. Vertical velocity profiles taken at one quarter of the pipe diameter from the inside wall of the north intake pipe.

velocities on the horizontal plane in the intake are half again as high as they are in the main sump. These significant velocities occur right up to the farthest reaches of the LDA equipment, and show that there is a very significant secondary flow in the intake pipes. The secondary flow is approximately twenty percent of the average flow in the vertical direction.

The flow up the intake cylinders has both upward and transverse components, a helical flow pattern. This helical flow will dramatically change the angle of attack on the pump impeller blades, which are designed for axial flow, and will seriously degrade the pump's efficiency. The swirling motion seems to damp out with height, but pumps will have to be a long distance away from the intakes to be unaffected.

2.7 Structure of Flow in the Improved Sump

For the second sump design studied, the improved sump, the general flow patterns were again observed with a dye tracer. The results of the dye study is a map of the flow patterns shown in figure 46. The flow patterns in this sump are made more symmetric by the baffle system in the expansion area. The jet emerges from the intake pipe and is broken up by the triangular baffle arrangement. The baffles ensure that the flow expands to fill the entire width of the sump, eliminating the large scale circulation pattern that exists when no baffles are present. The floor vorticies and the circulation behind the bells were corrected by the floor

Plate 3. Cavitation core of the bell to bell vortex is visible as a white line of air bubbles. Note that for plates 3, 5 and 6 the flows have been increased by 2.4 l/s, and the submergence decreased by 6 cm to allow photographs of the flow problems to be taken.

Plate 4. Strong cavitation core is visible in the floor vortex below the intake bell. This picture taken at design flows in the unimproved sump.

Plate 5. Surface dimple in severe flows illustrates how vorticies are created by being shed from the intake cylinders.

Plate 6. Wall to bell vortex is revealed by its cavitation core, the white line connecting the bell to the wall. View is from below the sump.

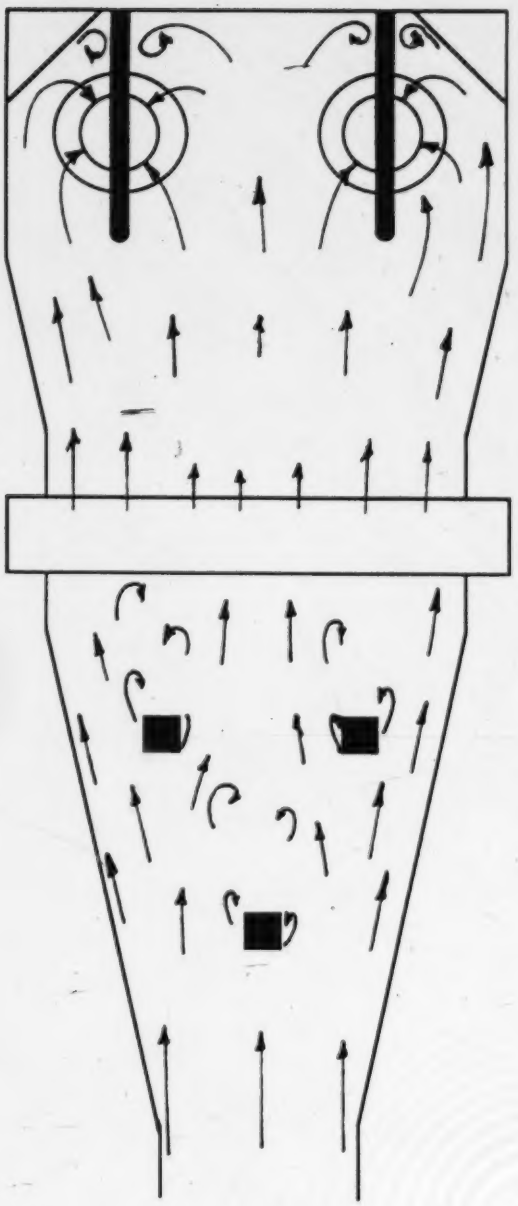

Figure 46. Patterns of flow in the improved sump. Results of the dye test.

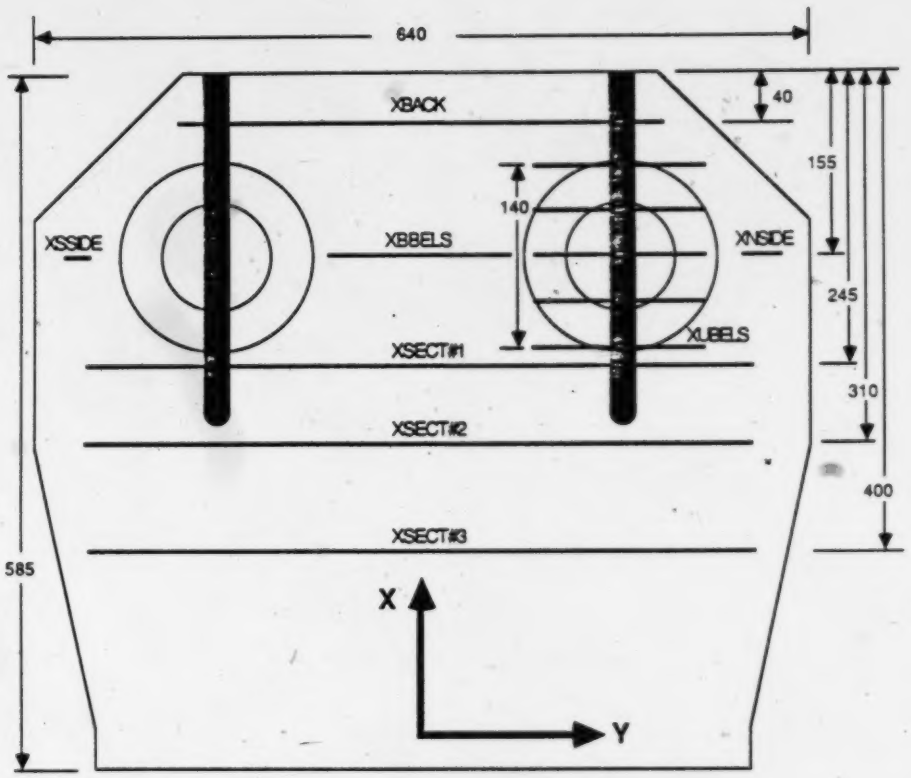

Figure 47. Plan view of the glass floor section of the improved sump indicating the locations of the cross-sections where data was taken. These cross-sections are centred in the sump or on the bell centre, except for the sections between the intake bells and the sump wall. Those two sections are centred between the bell and the wall.

beams and back wall splitters respectively. A pair of class 3 vorticies appeared along both sides of the back wall splitters.

The flow pattern in the improved sump is steady and has no unsteady overall circulation patterns or unsteady areas in the wake of the intake cylinders as exists in the unimproved sump. The fluid approaches the sump with a symmetrical variation in velocity across the sump, although the wake of the baffles is still very evident right up to the intakes. Figure 47 shows the cross sections where data was taken.

2.7.1 The Main Sump

The flow patterns for the improved sump design are very much more symmetrical than in the unimproved sump, but the velocity profile across the sump is not uniform. The velocity profiles of cross sections one, two and three show significant jets along both walls of the sump. These jets have about twice the longitudinal velocities of the centre sump area as can be seen in figures 48 through 50. The triangular baffle arrangement promotes this non-uniformity in velocity profile by blocking the centre of the expansion area while allowing an unobstructed passage to the sump along both walls. All three cross-sections covering the whole width of the sump have very similar velocity profiles with the speed of the jets along the wall increasing as the flow approaches the intakes. Figures 51 and 52 give the

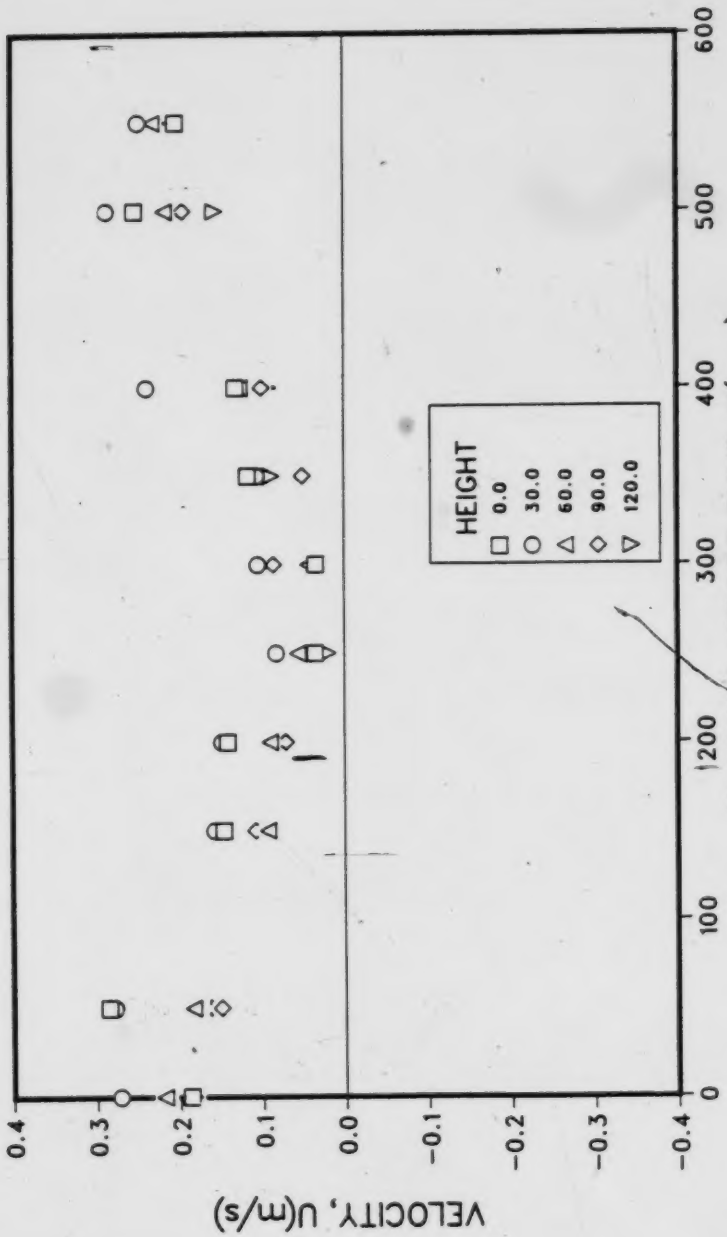

Figure 48. Longitudinal velocity profiles for the first section in the improved sump, xsect#1 in figure 47.

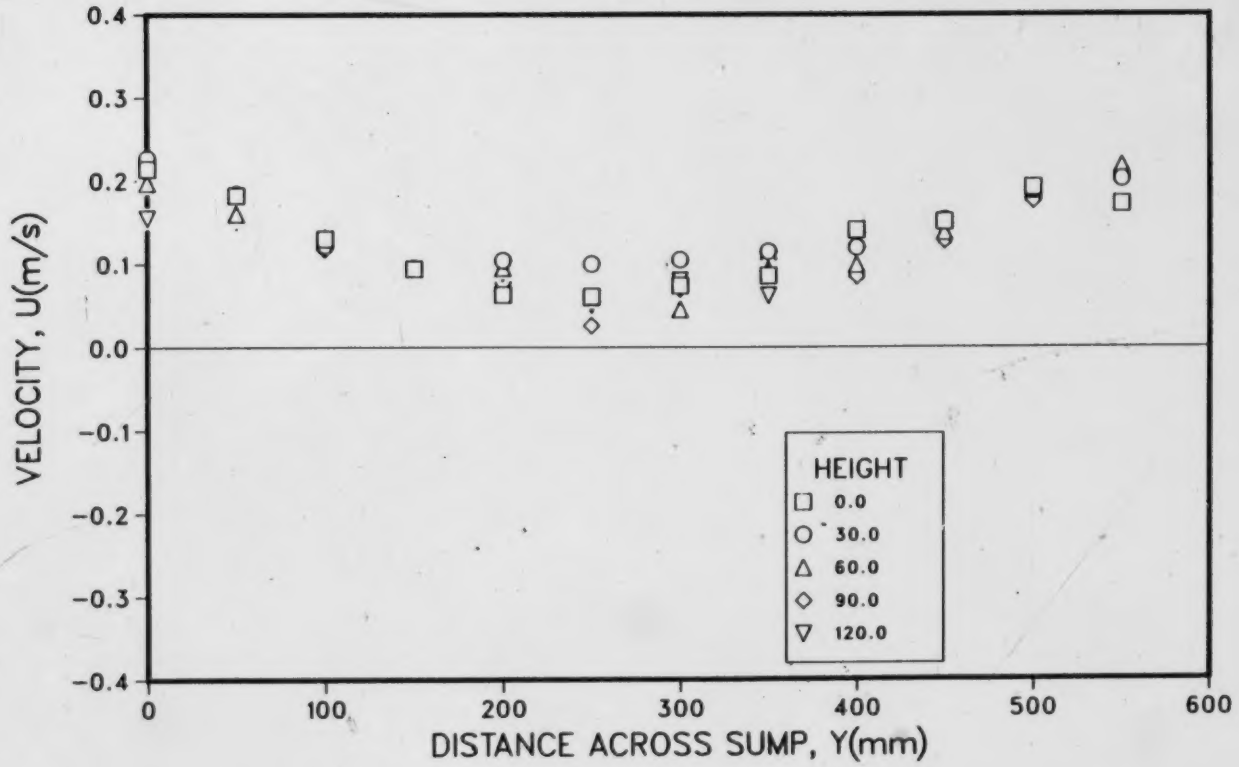

Figure 49. Longitudinal velocity profiles for the second section in the improved sump, xsect#2 in figure 47.

vertical velocity profiles beside the intake bells.

The baffled expansion helps significantly to reduce the velocities in the sump. Maximum velocities in the unimproved sump are as large as 0.4 m/s, but in the improved sump the maximum velocities are kept below 0.3 m/s. The average velocity in the sump must be the same since the discharge in the system is the same for both sumps. The velocities at the height of 30 mm are the largest of all heights for the velocity profile of cross section one, showing that this height is most affected by the intake bells. This trend was also seen in the velocity profiles of the unimproved sump.

The turbulence in cross sections one through three is reduced significantly over the unimproved sump. Although some higher values still exist in the faster regions of the flow, on the average the longitudinal turbulent fluctuations are reduced by half or more. Turbulence profiles for the main sump are given in figures 55 through 59.

Velocities between the intake bells, shown in figure 53, are very much smaller than in the main sump. The average velocity here is 0.05 m/s and is approximately uniform. The same variation in velocity profile with height exists as in the unimproved sump. The velocity varies from a larger positive value at the 120 mm height to a negative value of almost the same magnitude near the floor. This trend shows the tendency for a vortex with a horizontal axis, a roller, to form between the bells. The water flows towards the backwall in the higher reaches and is pulled down by the

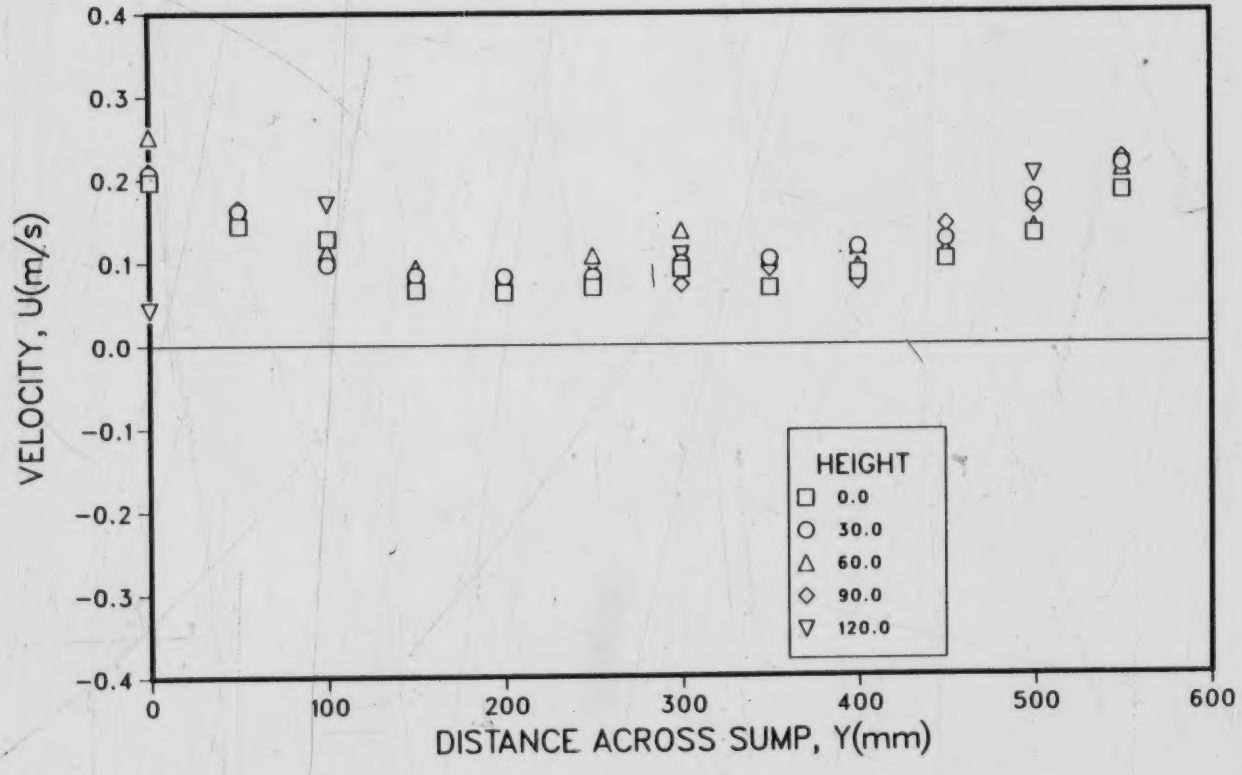

Figure 50. Longitudinal velocity profiles for the third section in the improved sump, xsect#3 in figure 47.

intake bells. Some of the flow enters the bells at this point, and the rest moves back into the main sump along the floor. The vertical gradient in velocity is very much smaller in the improved sump, and the roller motion appears, visually, to be weaker. The turbulence in the area between the bells is very much smaller than in the corresponding area of the unimproved sump, and is also less than in the rest of the sump.

The velocities in the section near the back wall of the improved sump, figure 54, exhibit much the same trends as were observed in the unimproved sump. There is again a definite pull towards the bells at the points near them, but the velocity profiles of different heights are very much more closely banded in the improved sump. There is some gradient of velocity in the vertical direction, showing the same trend towards a horizontal axis rotation as in the section between the bells. The turbulence in this area of the improved sump is almost an order of magnitude less than in the unimproved sump, indicating a much stabler and steadier flow.

2.7.2 Structure of Flow Under the Bell

The data taken under the bell in the improved sump was taken at the same locations as in the unimproved sump. Along the centre of the intake bells in the x direction no data could be taken because this area is taken up by the floor beam. Figures 60 through 64 show the variation in

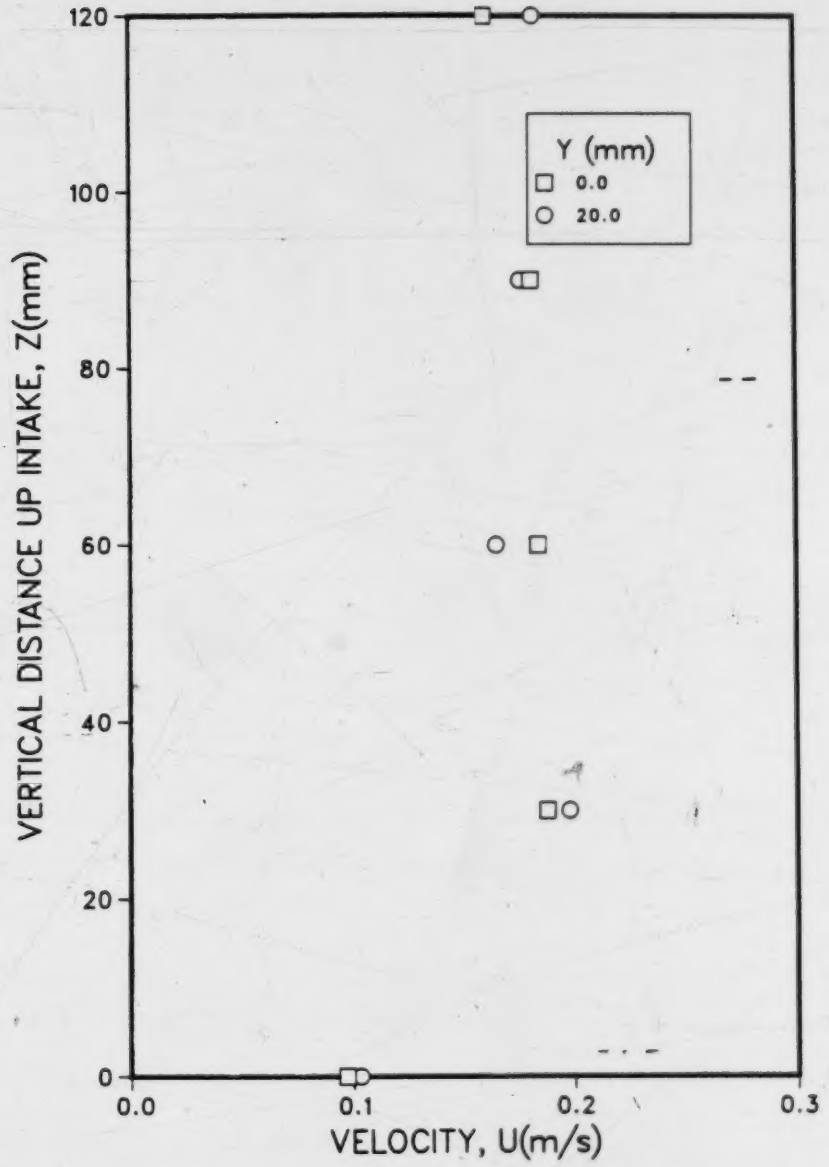

Figure 51. Longitudinal velocity profiles for the area on the south side of the south intake in the improved sump, xsside in figure 47.

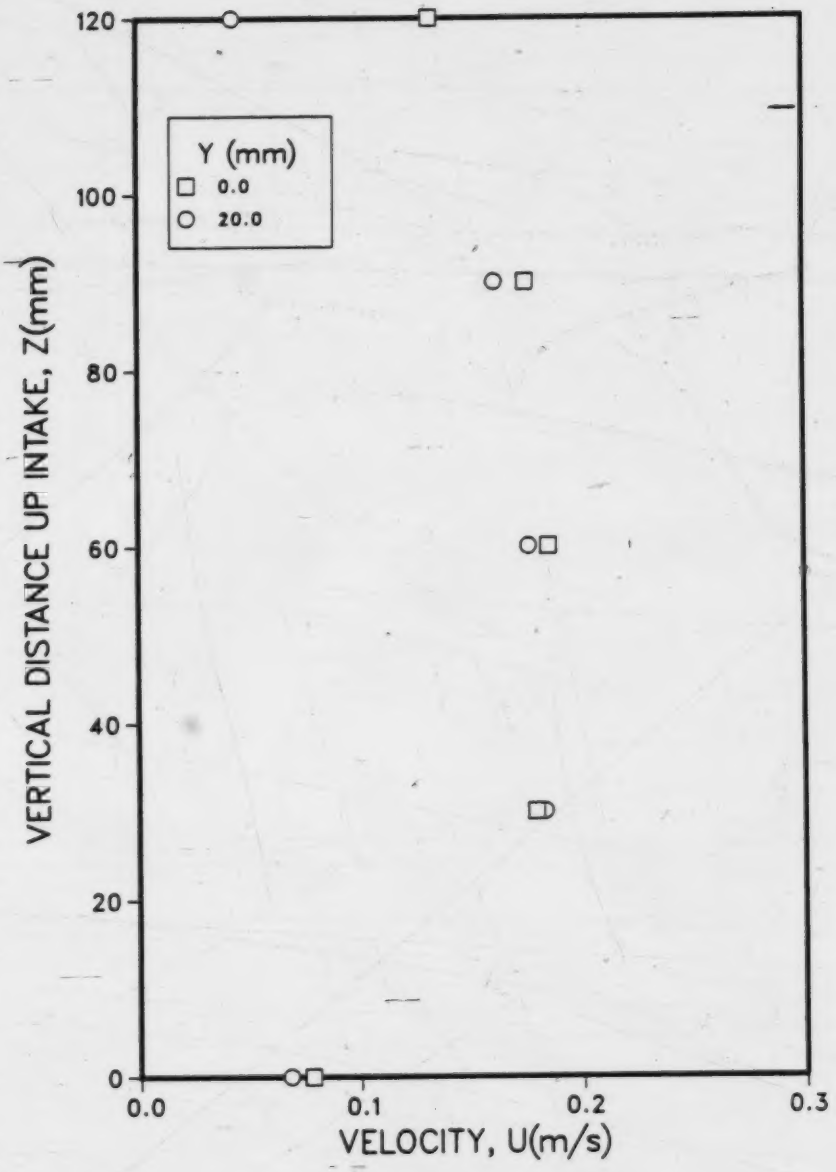

Figure 52. Longitudinal velocity profiles for the area on the north side of the north intake in the unimproved sump, xnside in figure 47.

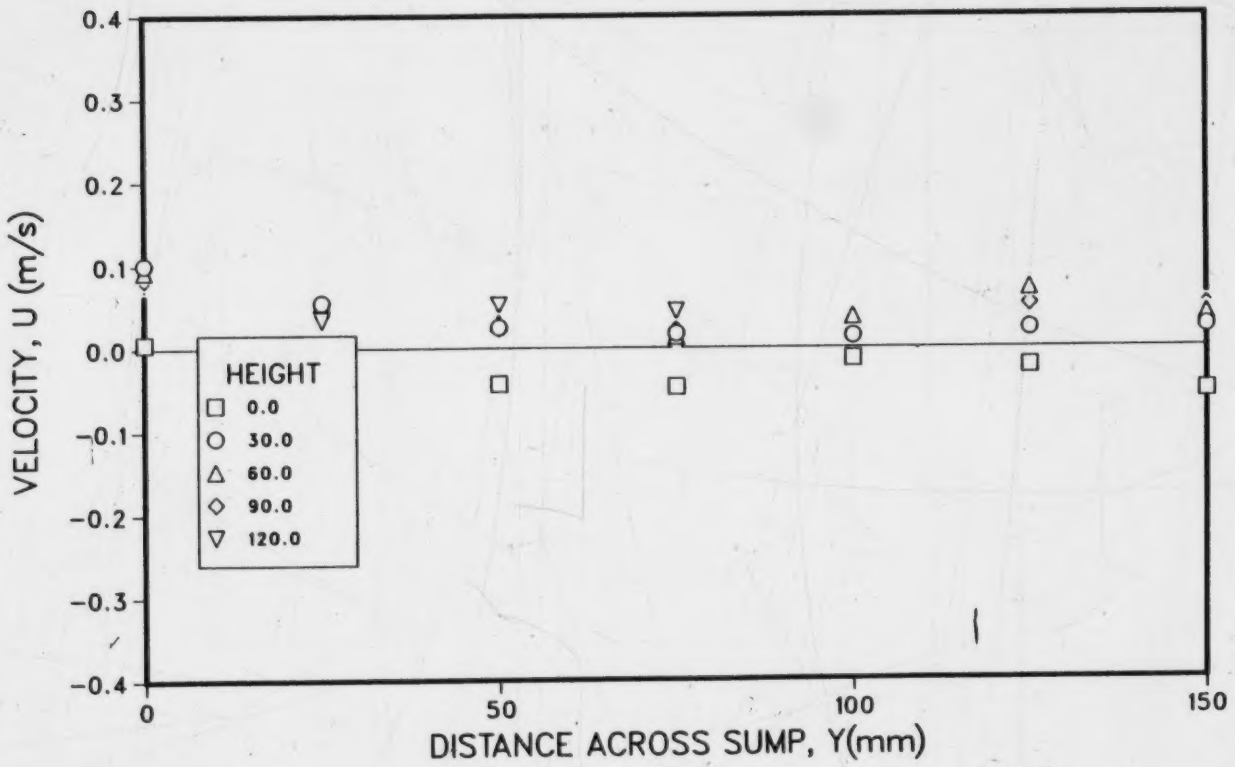

Figure 53. Longitudinal velocity profiles for the section between the bells of the improved sump, xbbels in figure 47.

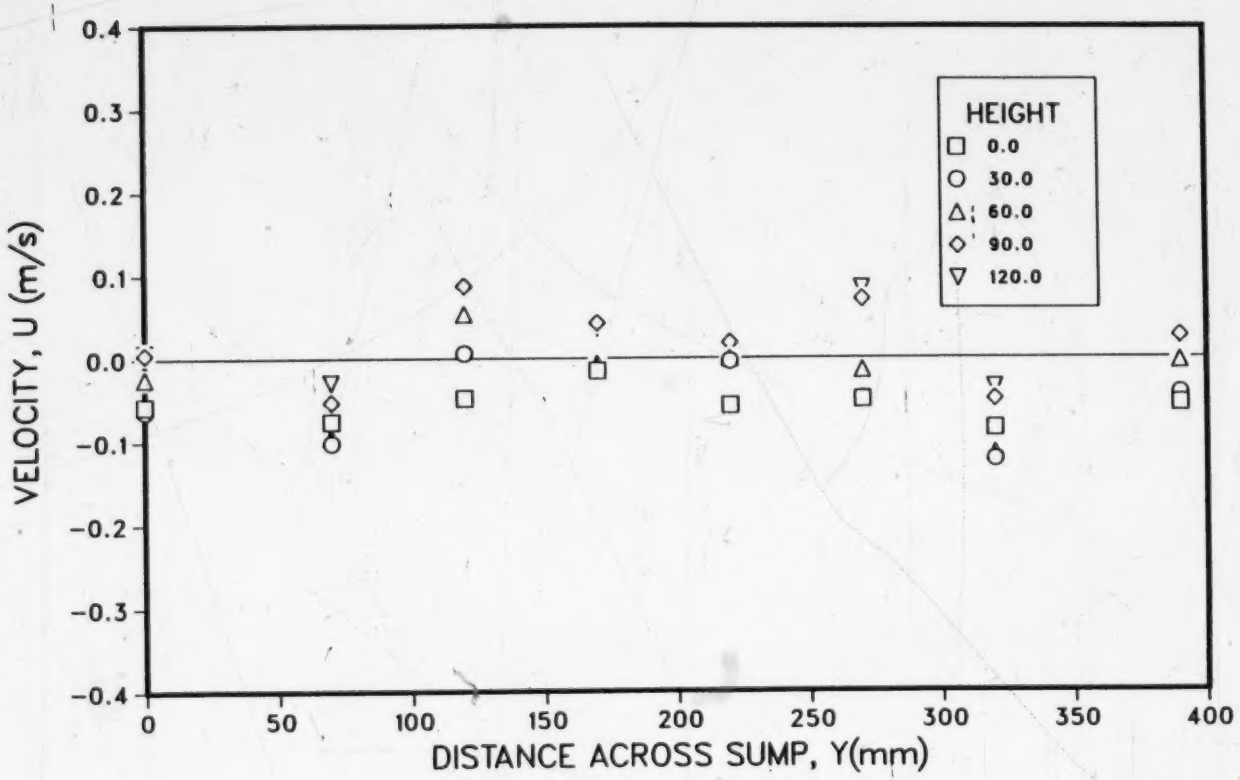

Figure 54. Longitudinal velocity profiles for the section near the back wall of the improved sump, xback in figure 47.

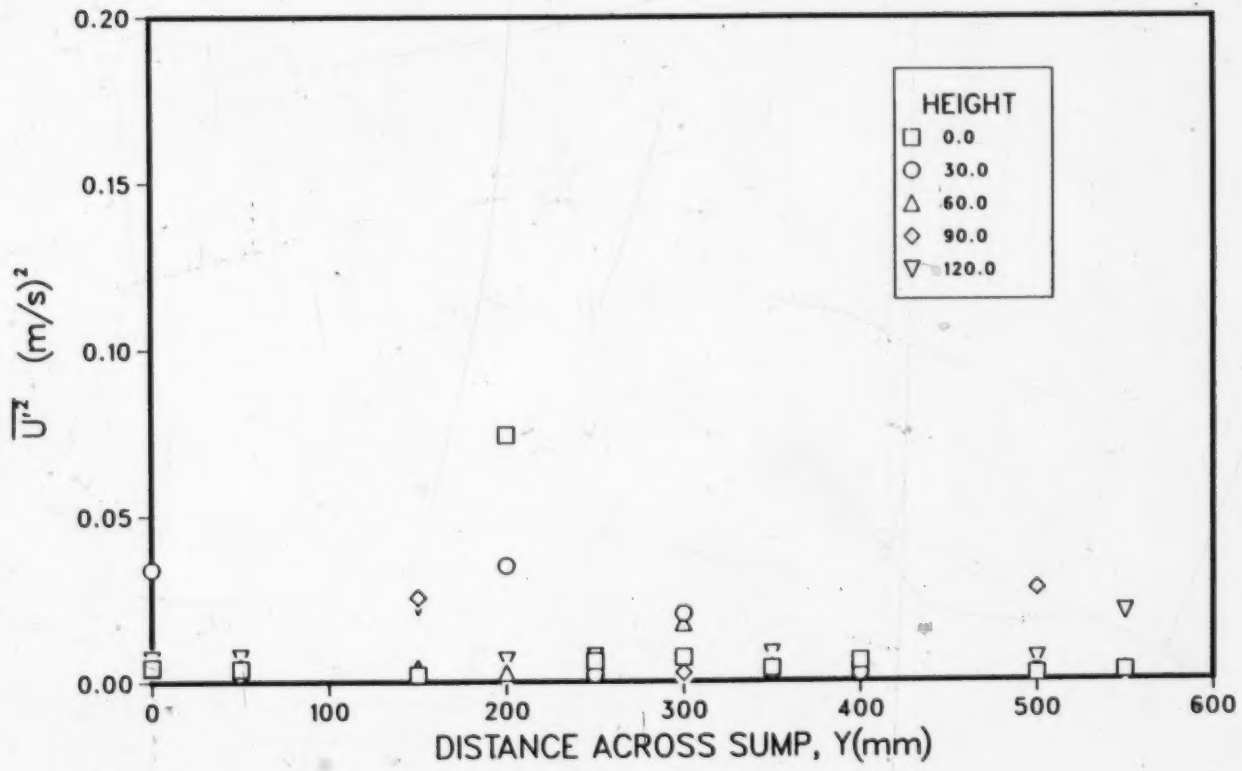

Figure 55. Longitudinal turbulent velocity fluctuations for the first section in improved sump, xsect#1 in figure 47.

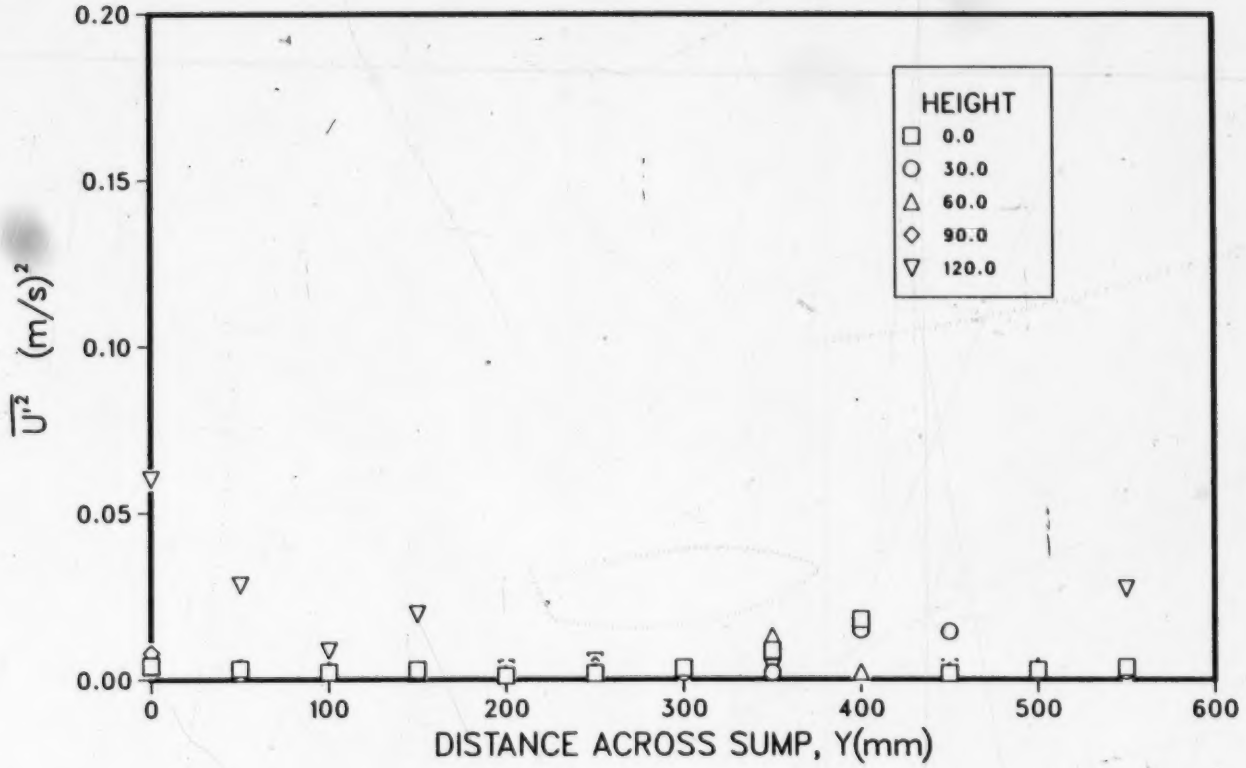

Figure 56. Longitudinal turbulent velocity fluctuations for the second section in improved sump, xsect#2 in figure 47.

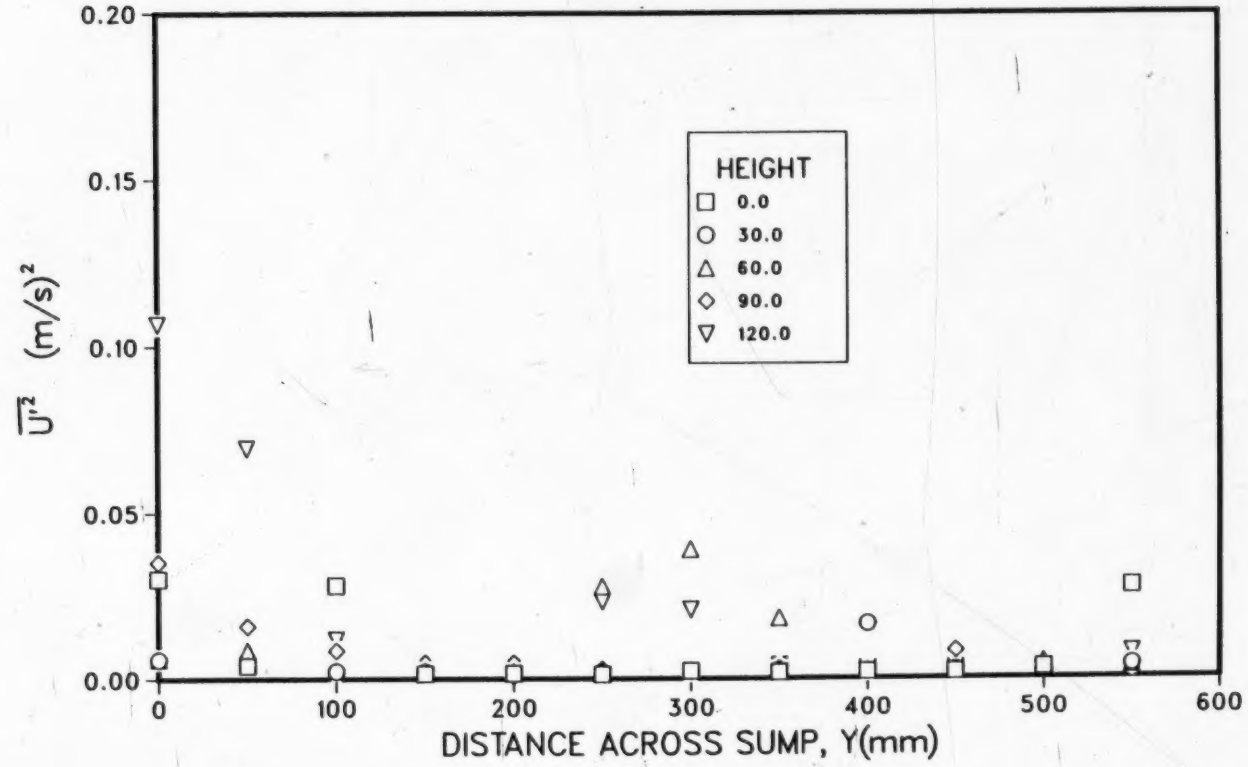

Figure 57. Longitudinal turbulent velocity fluctuations for the third section in improved sump, xsect#3 in figure 47.

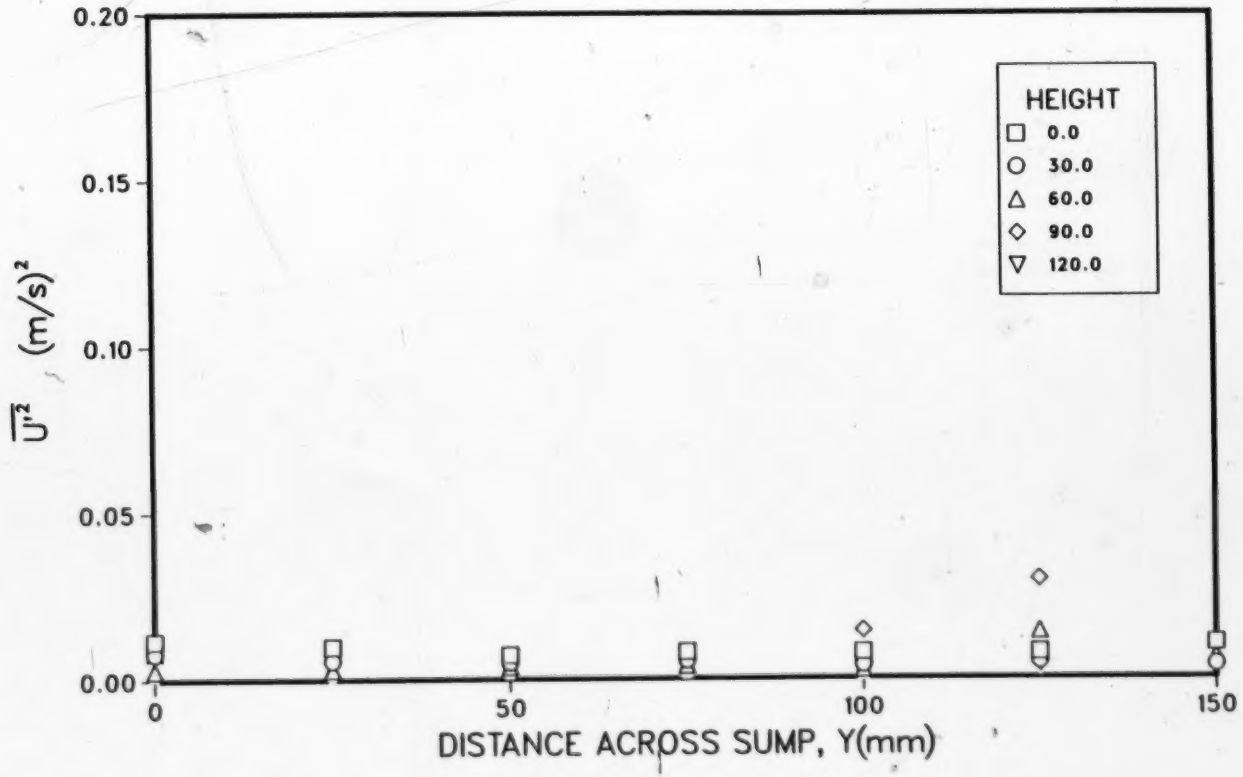

Figure 58. Longitudinal turbulent velocity fluctuations for the section between the bells of the improved sump, xbbels in figure 47.

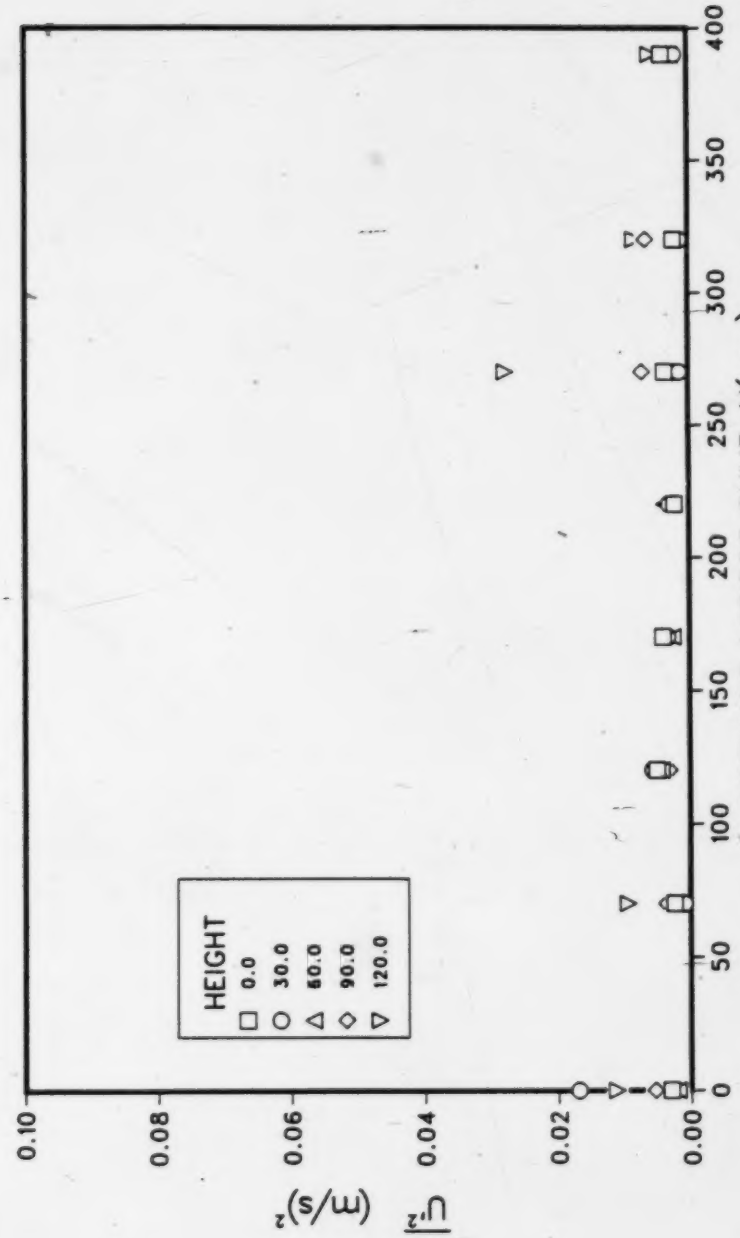

Figure 59. Longitudinal turbulent velocity fluctuations for the section near the back wall of the improved sump, xback in figure 47.

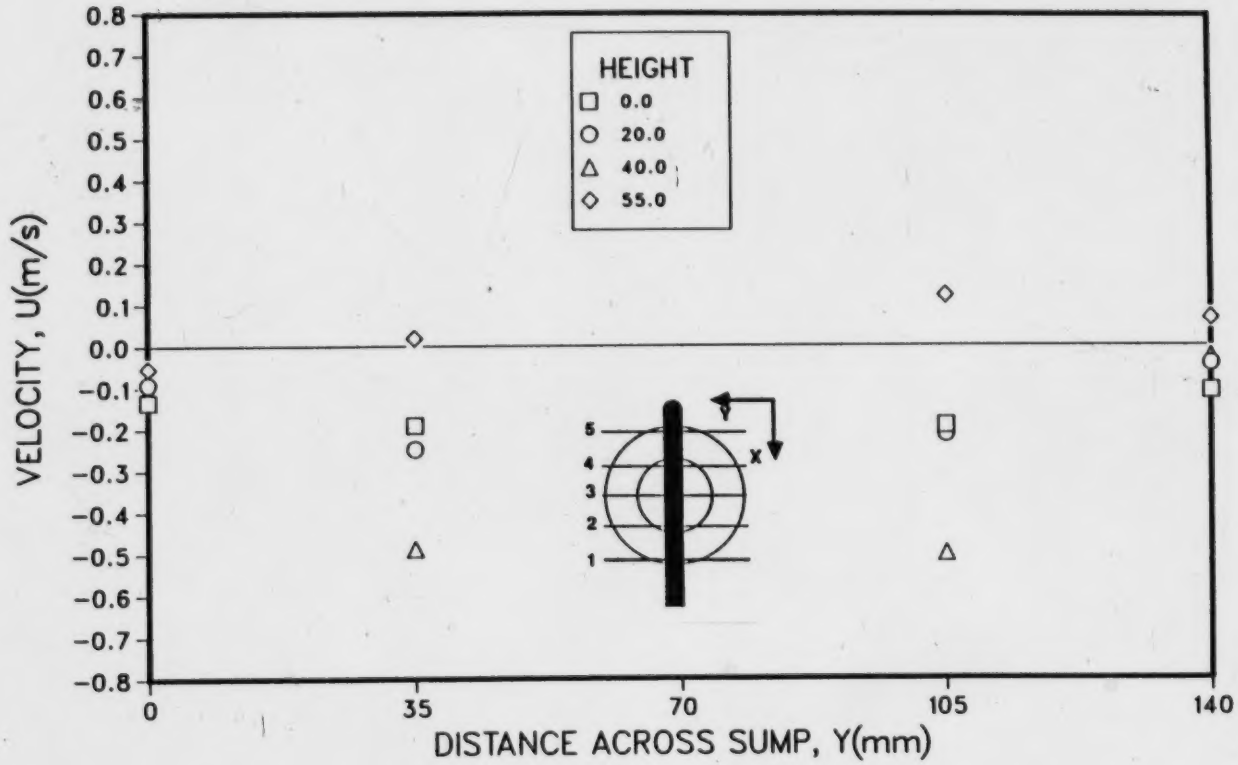

Figure 60. Longitudinal velocity profiles for the area under the north bell, section 1 in the area xubels of figure 47. Location shown in small inset figure.

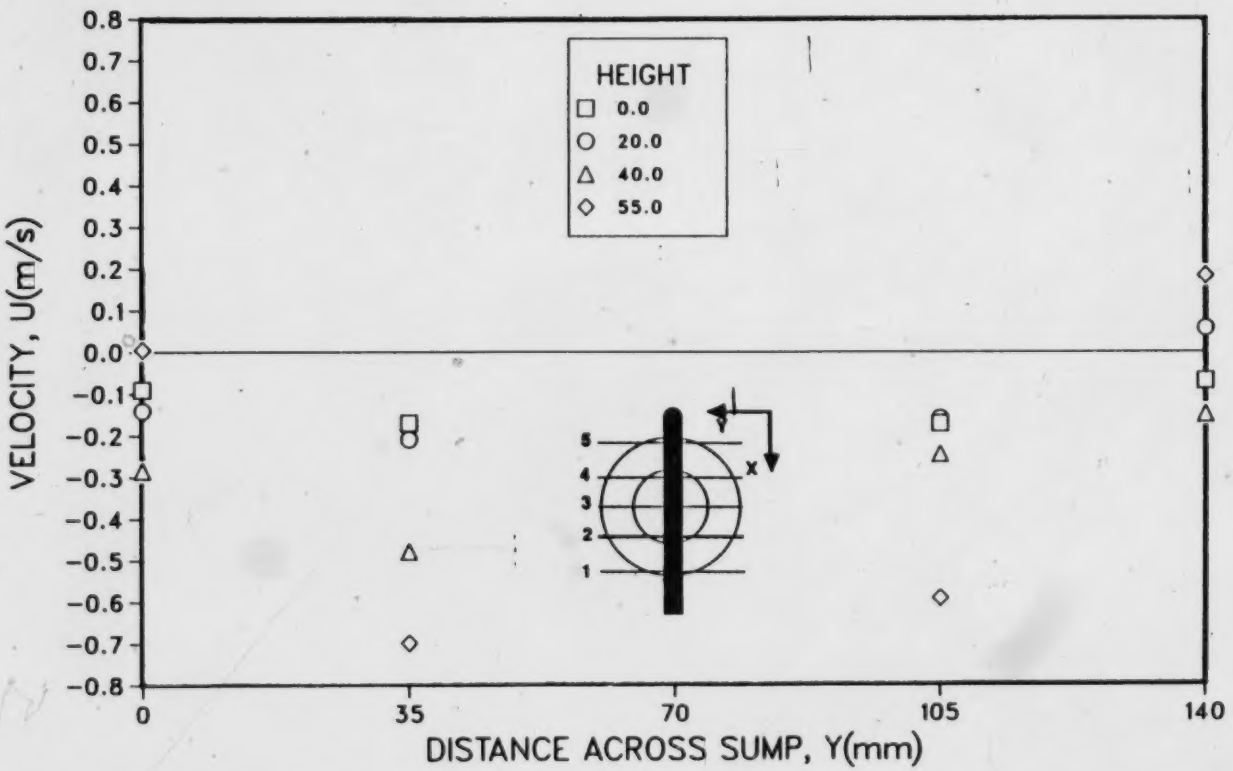

Figure 61. Longitudinal velocity profiles for the area under the north bell, section 2 in the area xubels of figure 47. Location shown in small inset figure.

longitudinal velocity, figures 70 through 73 the variation in transverse velocity, and figure 65 through 69 show the variations in the longitudinal turbulent fluctions.

The first thing to note about the longitudinal velocity profiles in the improved sump is their remarkable uniformity. The velocities on one side of the floor beam are almost a mirror image of those on the other side in all but the centre profile. The speed of the fluid is also of approximately the same average value in cross-sections two, four and five and is only slightly smaller in section one.

The transverse velocity profiles of the improved sump are very instructive. The profiles for the south side of the floor beam, at y = 0mm and y = 35mm, show that the maximum velocity occurs at the centre of the bell. The maximum velocities should occur here if there is a uniform radial flow into the intake. The velocities near the ends of the bell, x = 0mm and x = 140mm, should be more in the longitudinal or x direction, while in the centre, x = 70mm, all the velocity should be in the transverse or y direction.

The velocity profiles on the north side of the floor beam show the same trends as those on the south side. In the velocity profile for x = 140mm the velocities for corresponding distances from the centre (ie. x = 0mm, x = 140mm and x = 35mm, x = 105mm) are grouped, an ideal representation of what purely radial flow would show. The velocity profiles for y = 105mm are slightly less organized, but show the same trend.

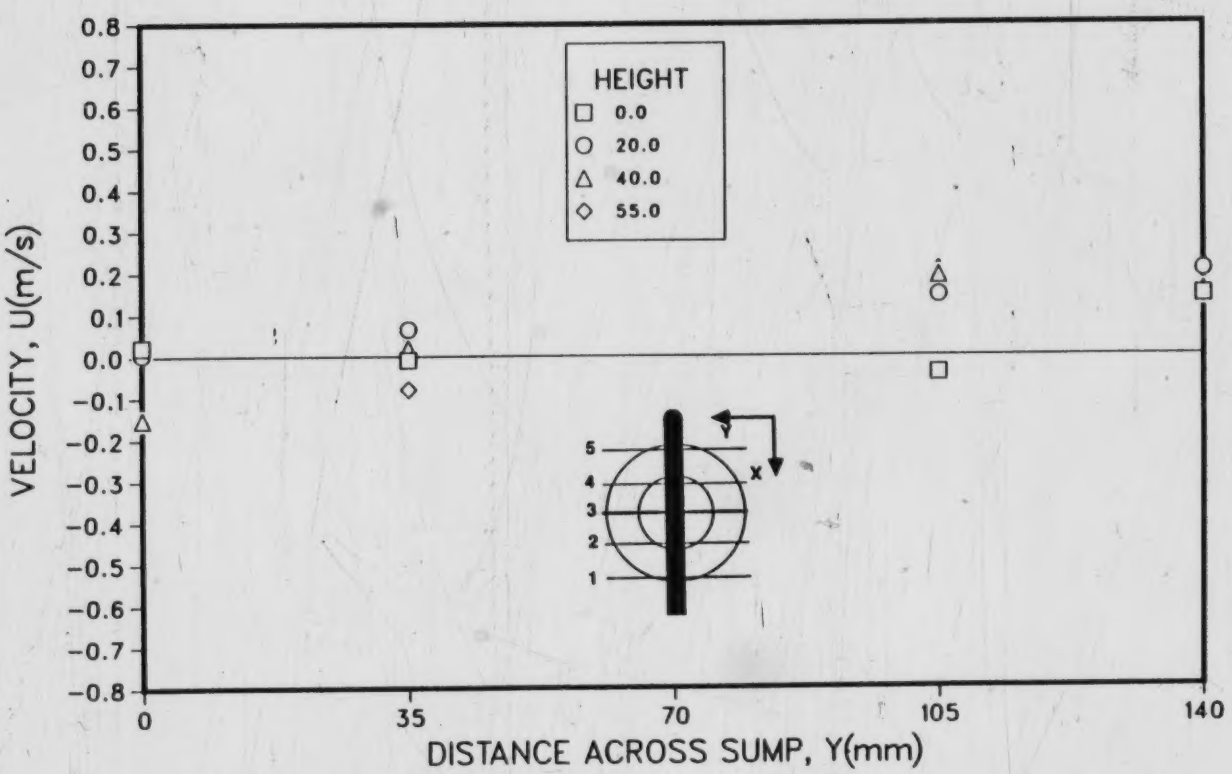

Figure 62. Longitudinal velocity profiles for the area under the north bell, section 3 in the area xubels of figure 47. Location shown in small inset figure.

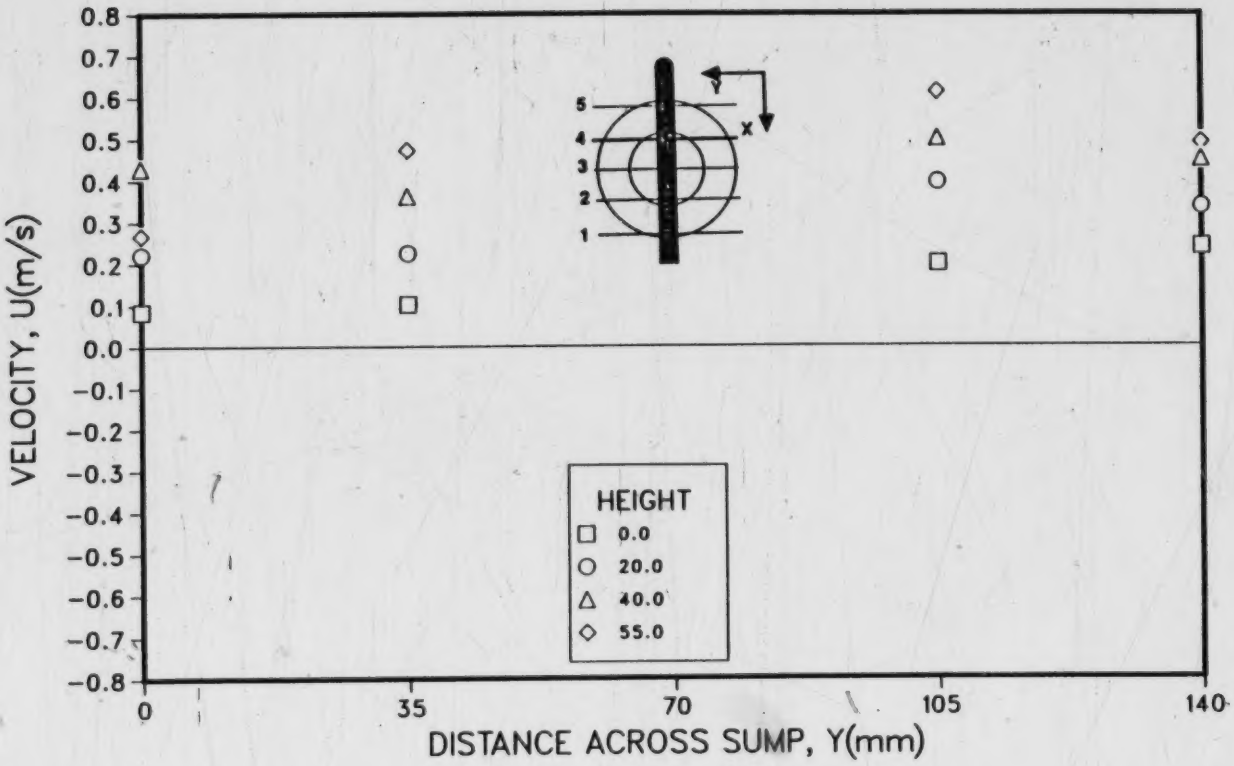

Figure 63. Longitudinal velocity profiles for the area under the north bell, section 4 in the area xubels of figure 47. Location shown in small inset figure.

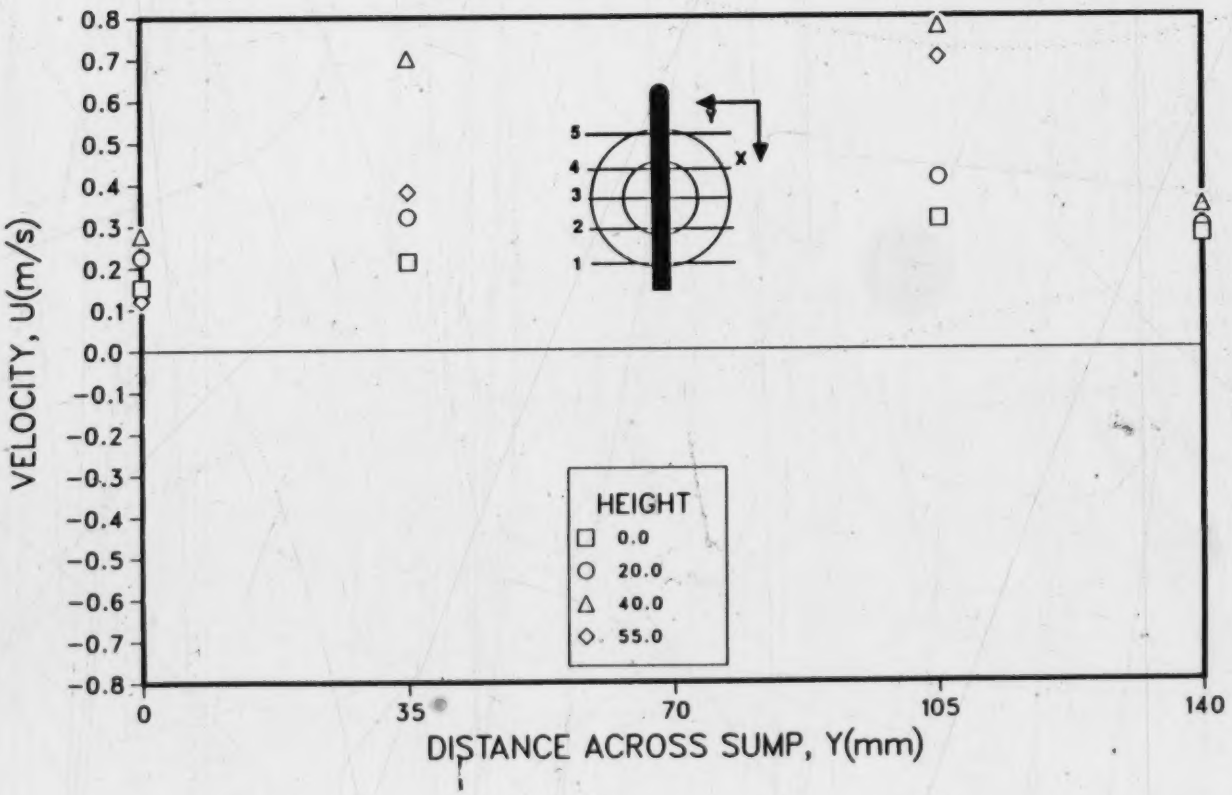

Figure 64. Longitudinal velocity profiles for the area under the north bell, section 5 in the area xubels of figure 47. Location shown in small inset figure.

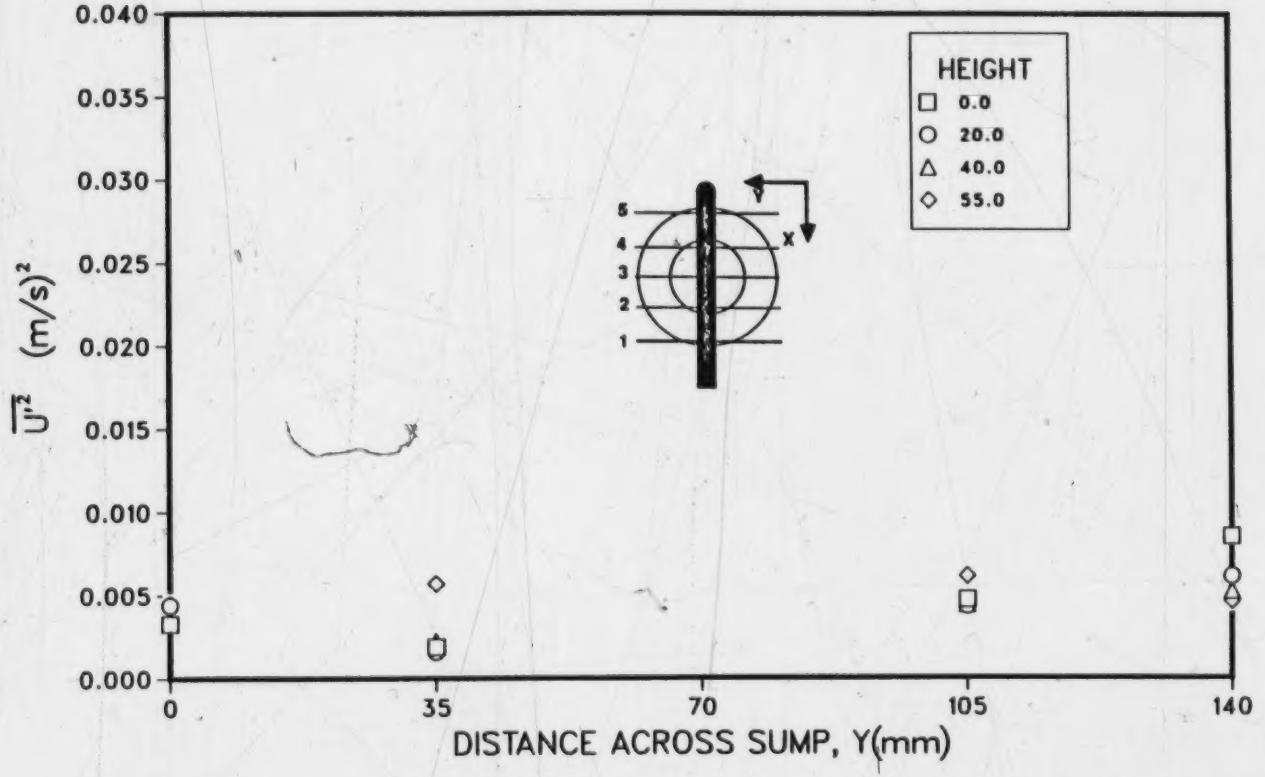

Figure 65. Longitudinal turbulent velocity fluctuations for the area under the north bell, section 1 in the area xubels of figure 47. Location shown in small inset figure.

The turbulence for the area under the intake is approximately the same size as the areas of low turbulence under the intakes of the unimproved sump. The vertical scale for the plots of turbulence in the improved sump have been exaggerated to show the variations that exist. The centre of the sump has the highest turbulence levels, as is the case in the unimproved sump, but the turbulence here is only slightly higher than in the other sections. If the flow in all radial directions were the same, the turbulence here should not be any higher than anywhere else.

2.7.3 Flow in the Intake Cylinders

The improved flow conditions in the sump are reflected in the large reduction in the swirling flows in the intake pipes. The velocities of the secondary, or swirling flows have been reduced by half over the unimproved sump. The improved conditions in the sump have not eliminated all the circulation problems in the intake however, as can be seen in figures 74 and 75. The swirling motion seems to be damping out as the flow travels along the pipe, although it is not doing so very rapidly.

The flow can be seen to have components in both principal directions, indicating a helical flow up the intake pipe. The swirling component of the flow will change the effective angle of attack of the pump's impeller blades, reducing the efficiency of the machine. The machine's efficiency will be much better than with the unimproved sump

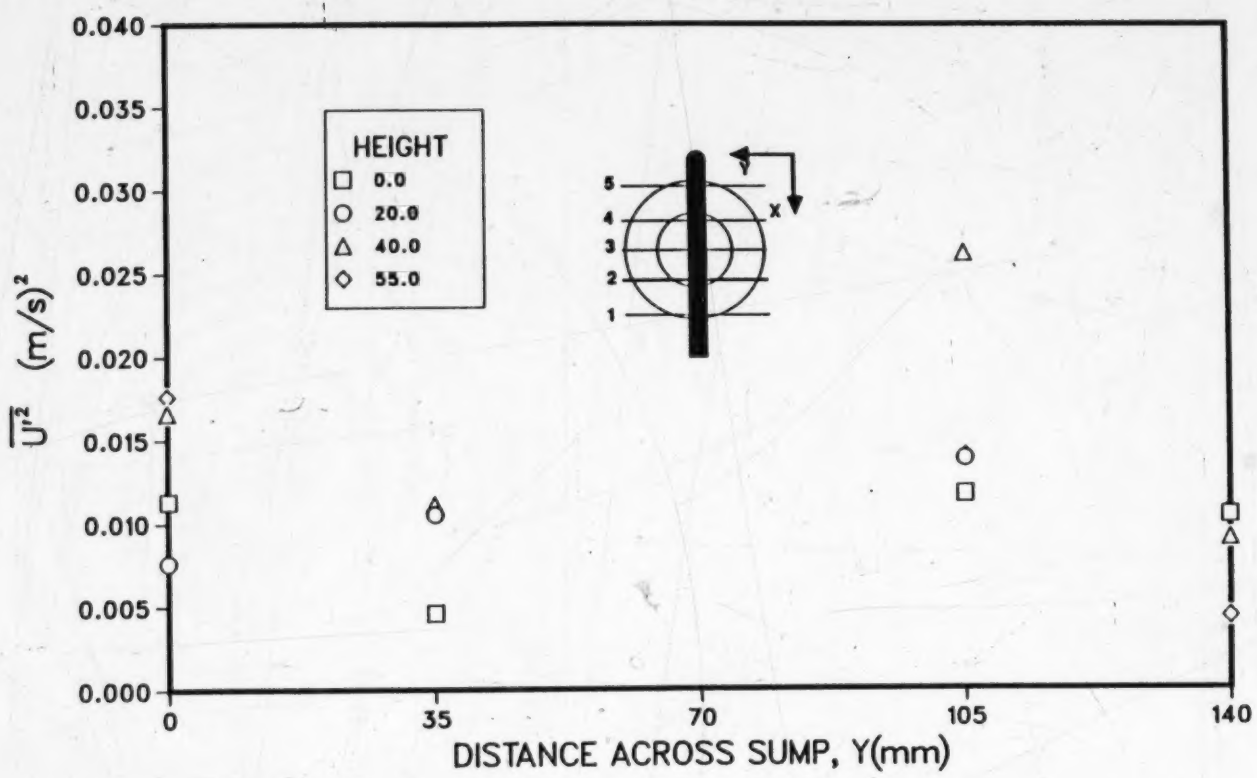

Figure 66. Longitudinal turbulent velocity fluctuations for the area under the north bell, section 2 in the area xubels of figure 47. Location shown in small inset figure.

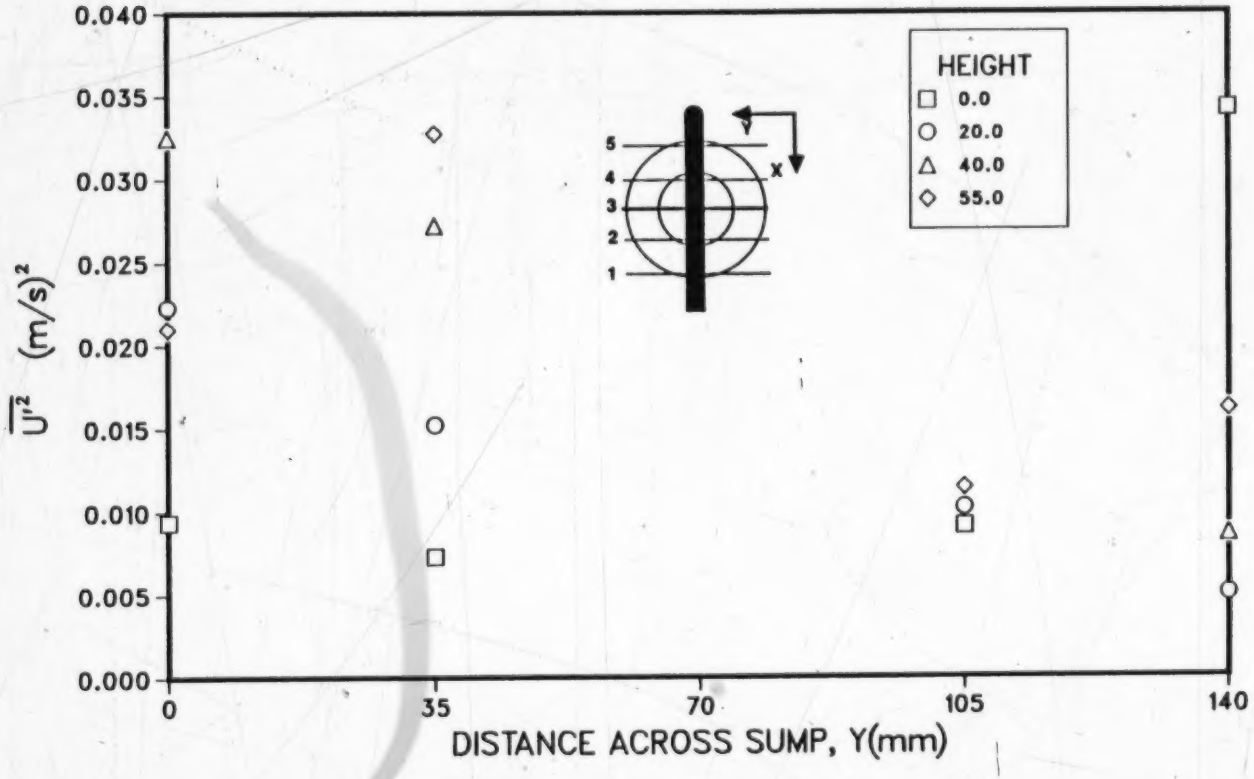

Figure 67. Longitudinal turbulent velocity fluctuations for the area under the north bell, section 3 in the area xubels of figure 47. Location shown in small inset figure.

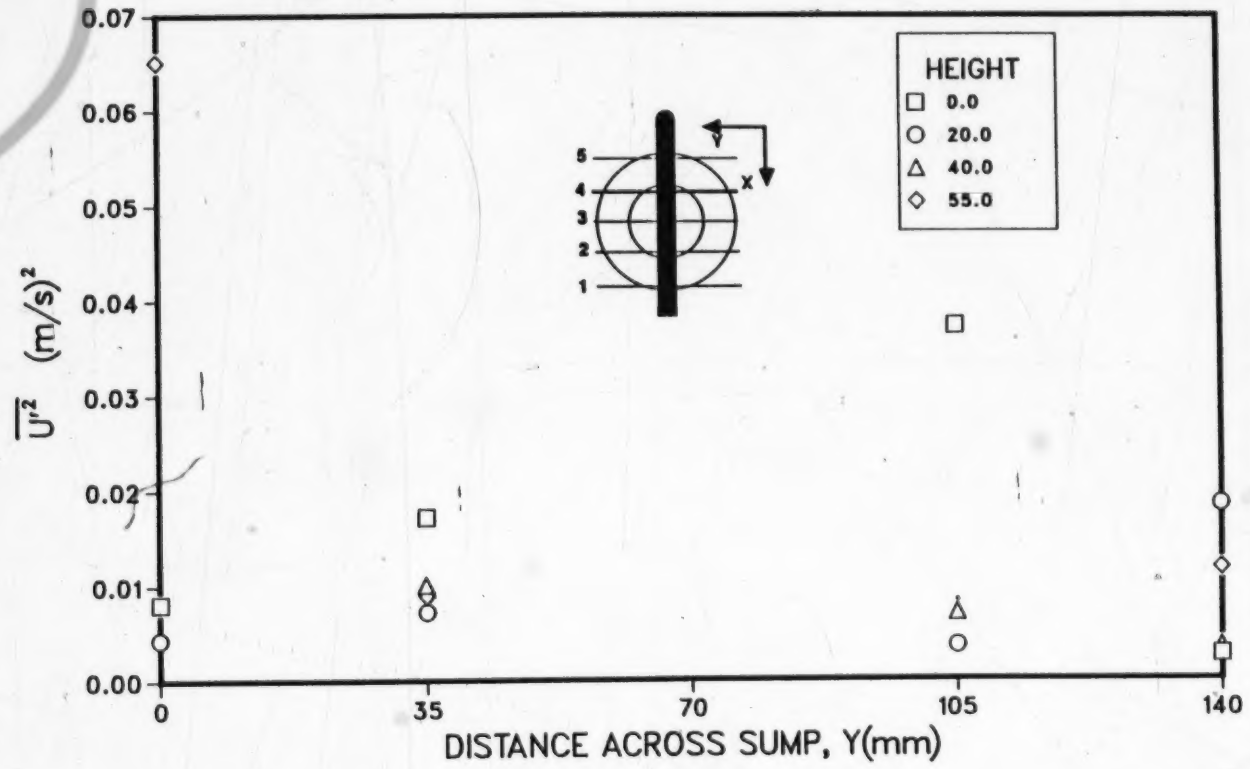

Figure 68. Longitudinal turbulent velocity fluctuations for the area under the north bell, section 4 in the area xubels of figure 47. Location shown in small inset figure.

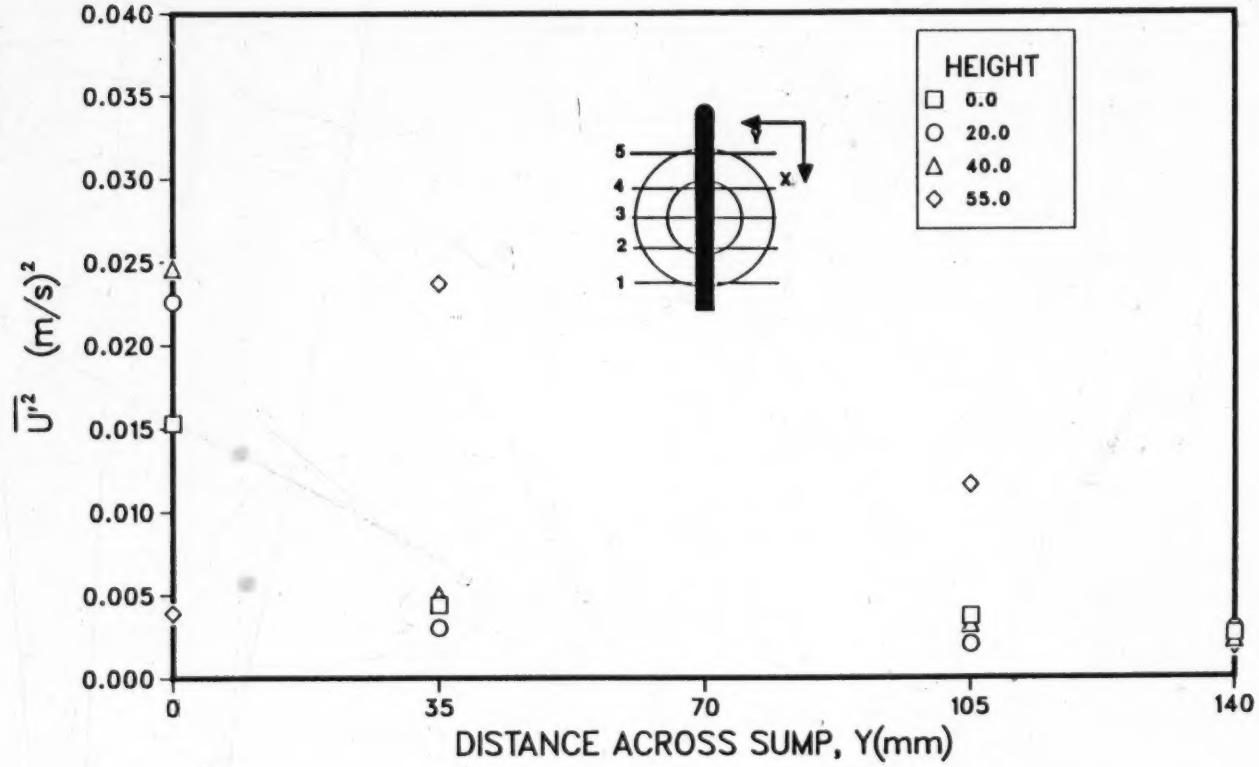

Figure 69. Longitudinal turbulent velocity fluctuations for the area under the north bell, section 5 in the area xubels of figure 47. Location shown in small inset figure.

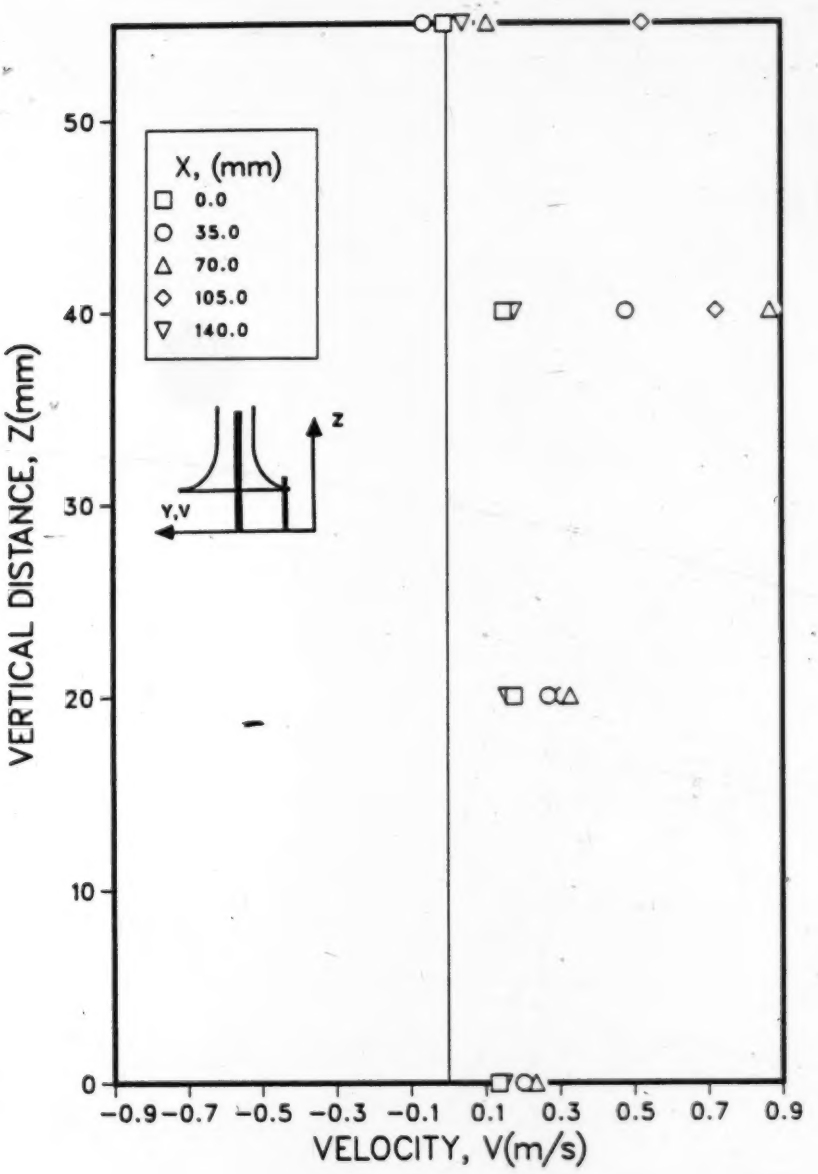

Figure 70. Vertical profiles of the transverse velocity under the north bell of the improved sump, profiles at y = 0 in the area xubels. Location shown in small inset figure.

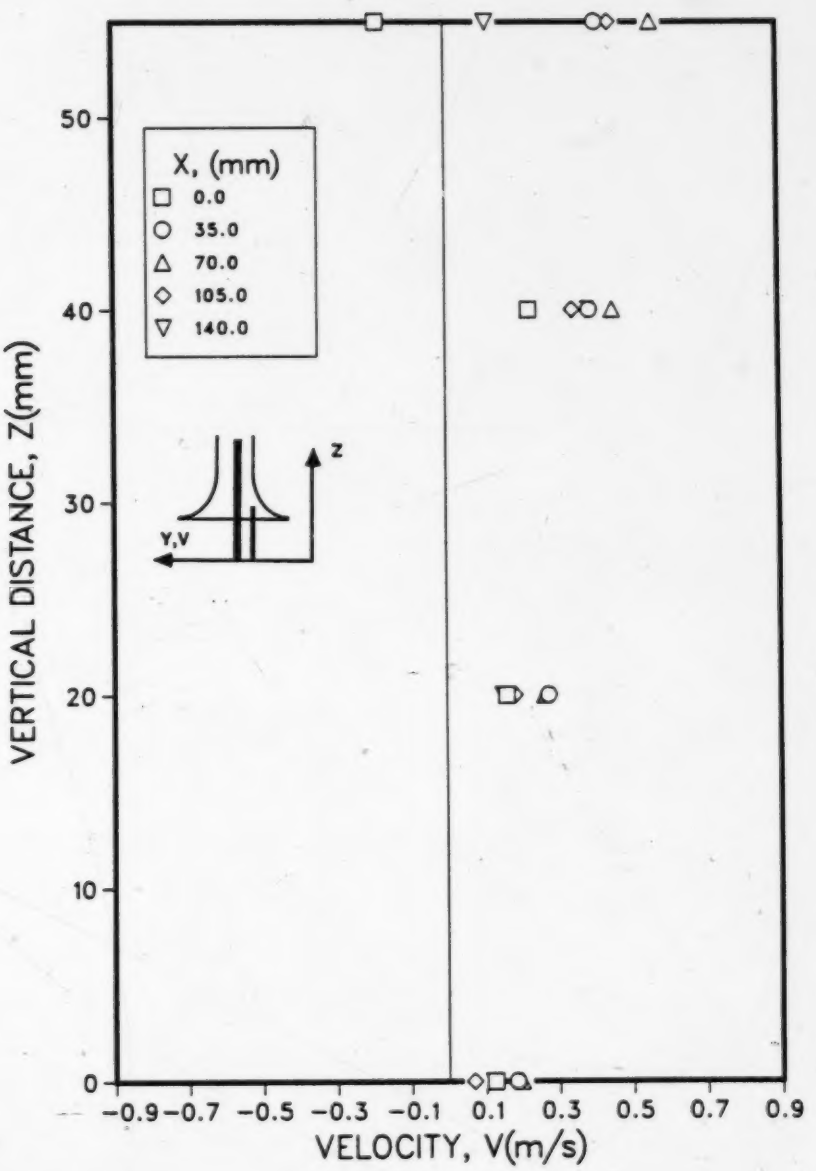

Figure 71. Vertical profiles of the transverse velocity under the north bell of the improved sump, profiles at y = 35 in the area xubels. Location shown in small inset figure.

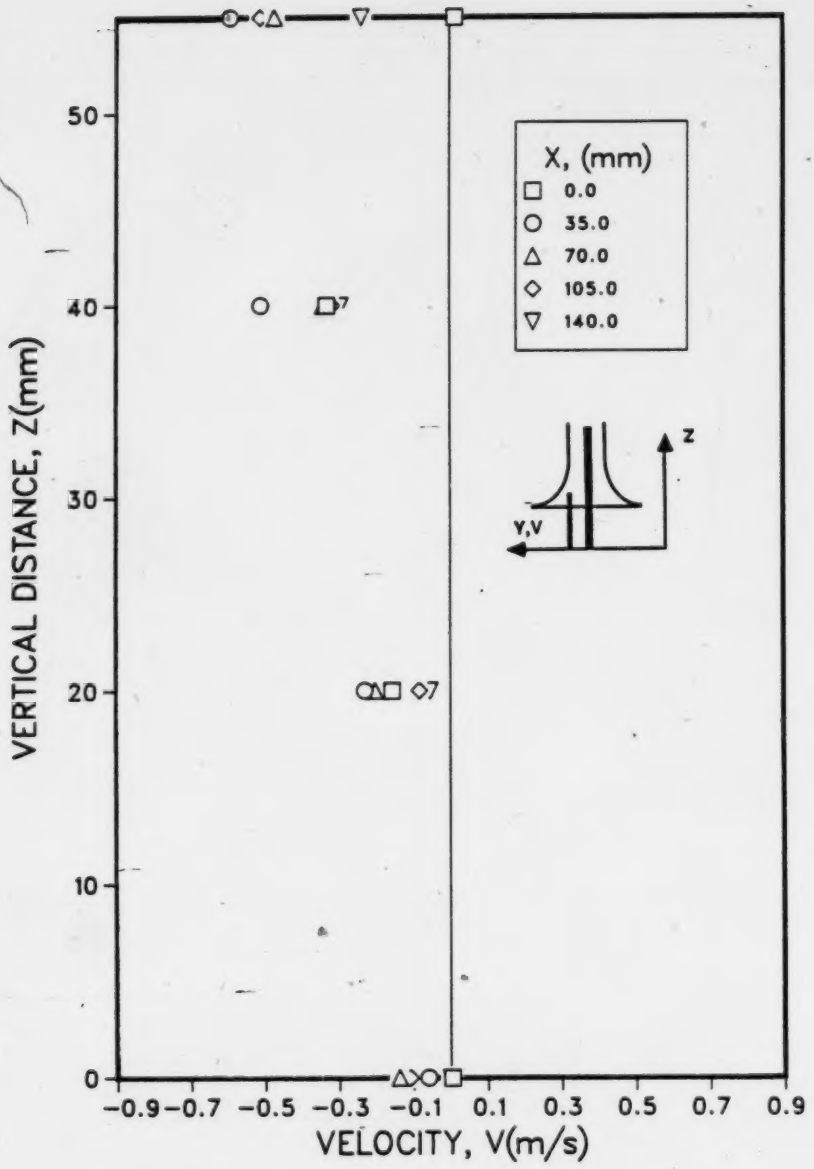

Figure 72. Vertical profiles of the transverse velocity under the north bell of the improved sump, profiles at y = 105 in the area xubels. Location shown in small inset figure.

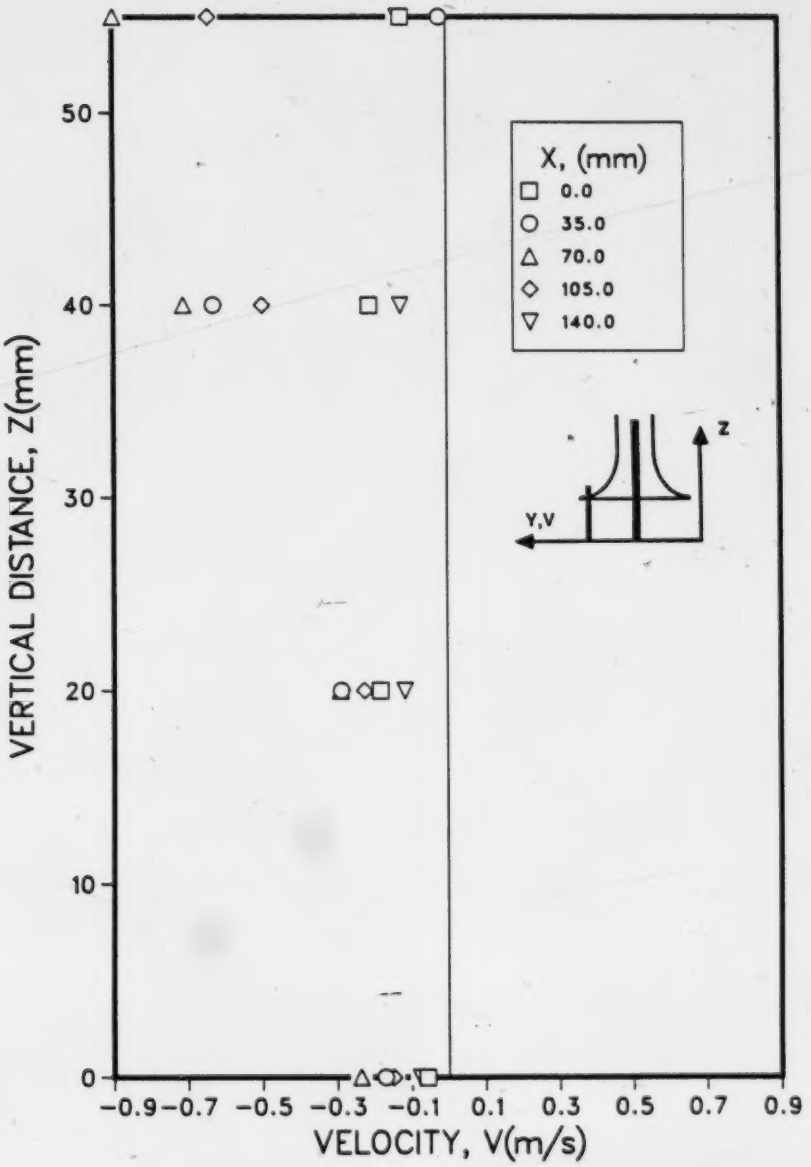

Figure 73. Vertical profiles of the transverse velocity under the north bell of the improved sump, profiles at y = 140 in the area xubels. Location shown in small inset figure.

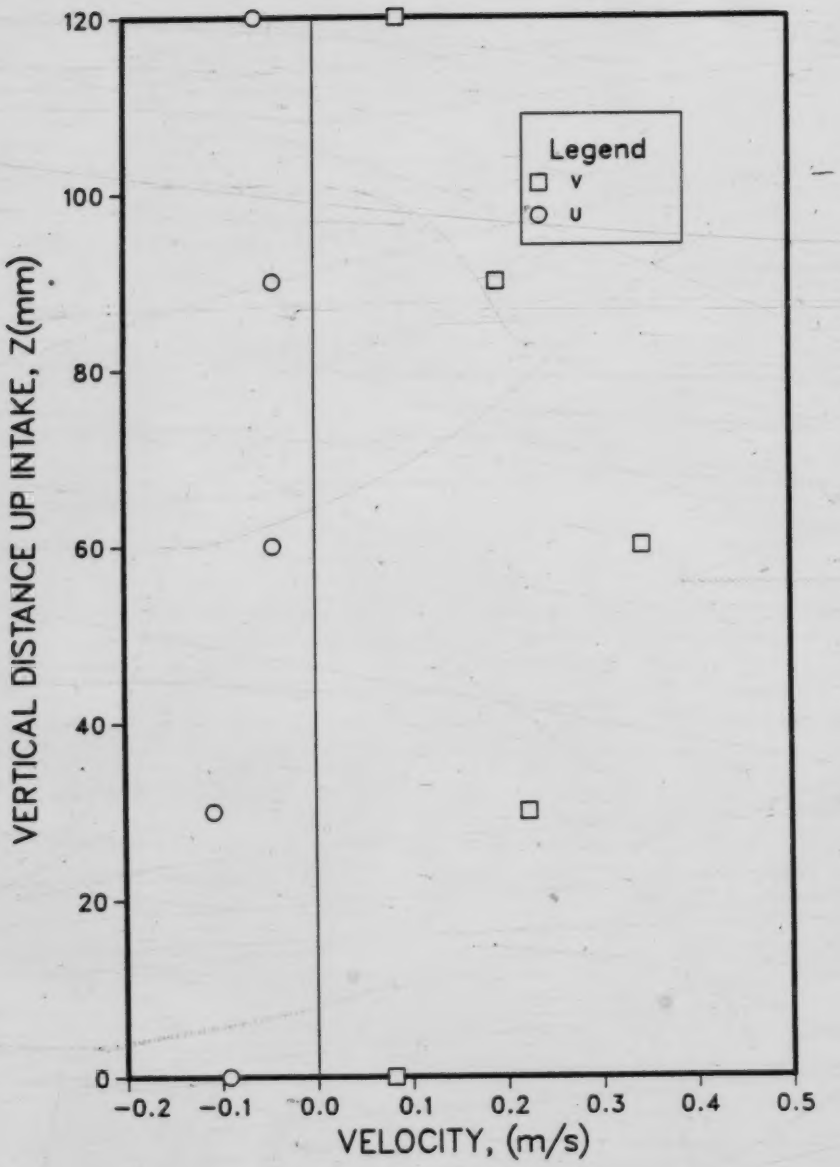

Figure 74. Vertical velocity profiles taken at one quarter of the pipe diameter from the inside wall of the south intake pipe.

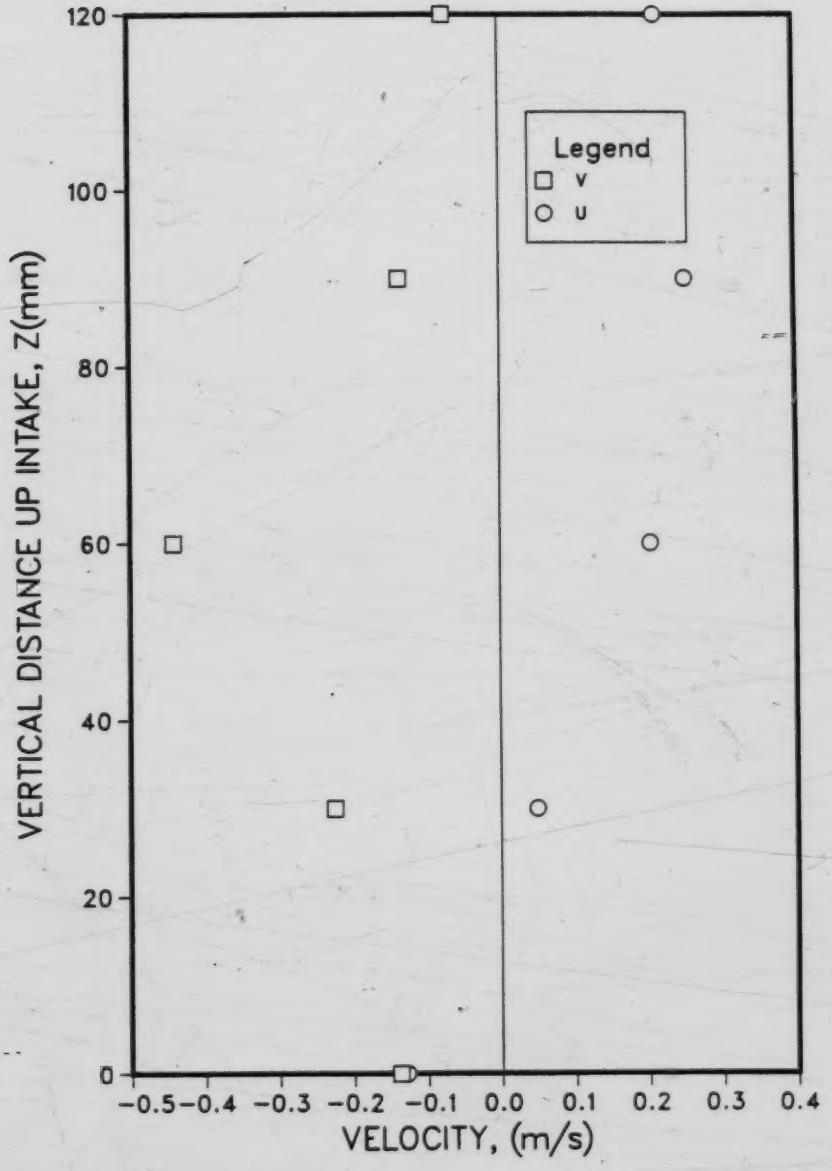

Figure 75. Vertical velocity profiles taken at one quarter of the pipe diameter from the inside wall of the north intake pipe.

however, where there is a much stronger swirl to the flow.

3. Conclusions

3.1 Comparing the Two Sump Designs

The two sump designs studied differed only in the use of flow improvement devices. These devices altered the flow characteristics dramatically and made an acceptable sump out of one that was not acceptable.

The unimproved sump has a large scale circulation pattern that is subject to inversion, as well as unsteady areas in the wake of the two intake cylinders and in the regions of returning flow on the side of the sump. The poor flow conditions result in a strong circulation or secondary flow in the intake pipe that will erode the efficiency of the pump. This circulation pattern can be seen in the plot of the velocity vectors below the intake, figure 77. This data is plotted for a level of 40 mm above the floor because this is where the influence of the intake is greatest, and where the velocities are highest. Strong floor vorticies are always evident below the intake bells.

The flow conditions in the improved sump are vastly better than in the unimproved sump. The flow into the intake bells was almost radial into the intakes as can be seen in figure 78, but there was still some secondary flow in the intake pipe. The maximum velocities in the improved sump are reduced by one quarter over the unimproved design, and the flow pattern is steady. Figure 76 shows the very much more uniform velocity profile across the sump. The improved

design also eliminates some areas of turbulence, such as the area of returning flow and the wake of the intake cylinders, but the wake from the baffles in the expansion region remains as a source of turbulence. Figures 80 through 83 show the actual velocity vectors for the main sump of both designs. The improved flow structure can clearly be seen in these arrow diagrams.

3.2 The Usefulness of LDA measurements in Pump Sump Design

The laser doppler anaemometer offers a superlative method for the investigation of hydraulic sump models. Without altering the flow, the LDA can measure both the velocity and turbulence, essential parameters in the design of efficient sumps. The LDA also allows the direction of the velocity to be determined with accuracy, a feat that can be done only with difficulty using other flow measuring devices. The LDA permits the flow in the sump to be mapped, pointing out troublesome areas. The LDA also allows the secondary flows and the turbulence in the intake pipe itself to be measured, the ultimate test of a sump's performance. The presentation of LDA data in figures such as 77 through 83 can give conclusive proof of the superiority of a sump design, and remove much of the subjectiveness involved in designing a sump.

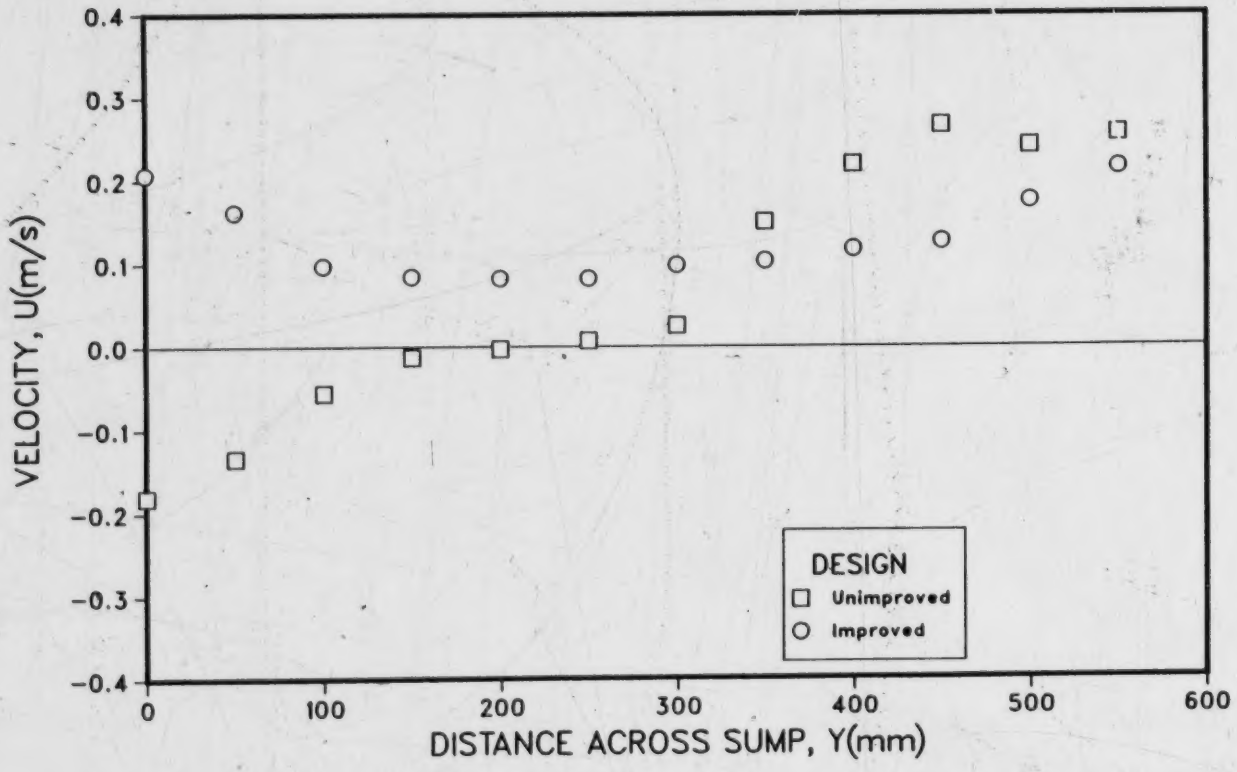

Figure 76. Comparison of velocity profiles in the main sump for the different designs. Note the increased uniformity in the profile for the improved sump. Both profiles are at the third cross section, xsect#3, at a height of 30mm above the floor.

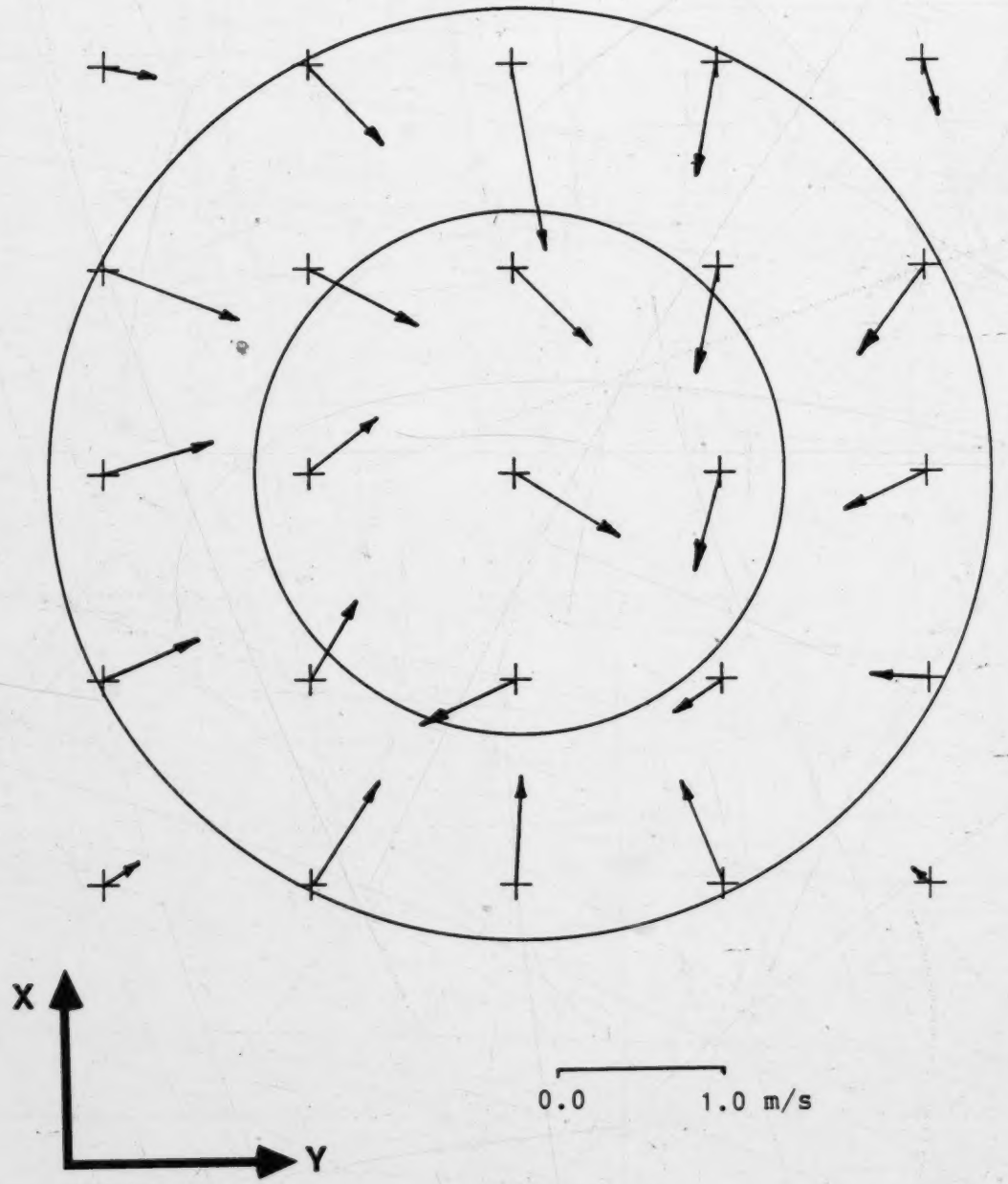

Figure 77. Resultant velocities under the bells of the unimproved sump for the height of 40mm. Arrow length is scaled to the magnitude of the velocity. Note the swirling motion around the centre of the intake.

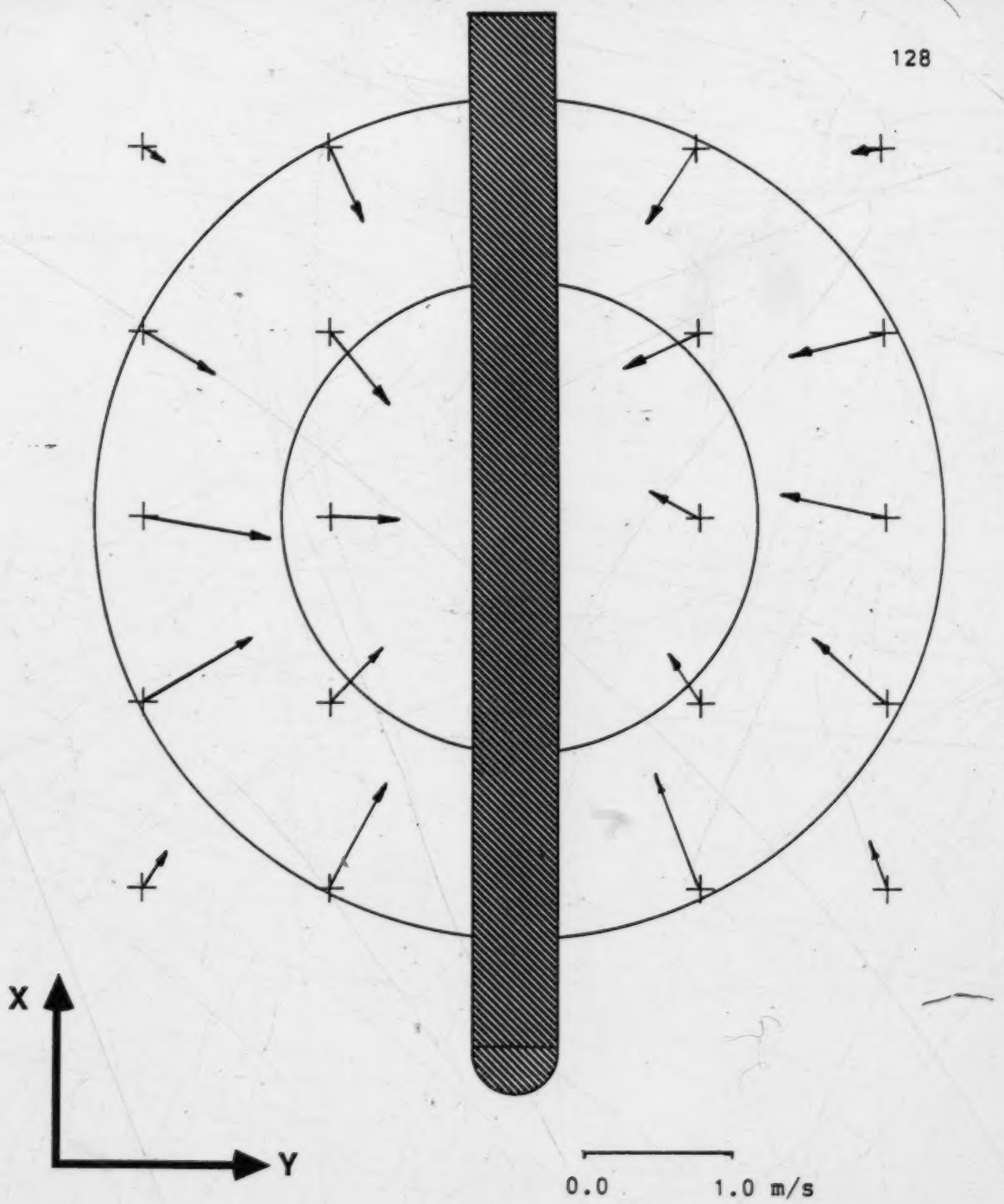

Figure 78. Velocity vectors under the bells of the improved sump for the height of 40mm. Arrow length is scaled to the magnitude of the velocity. Note the almost radial motion of the flow.

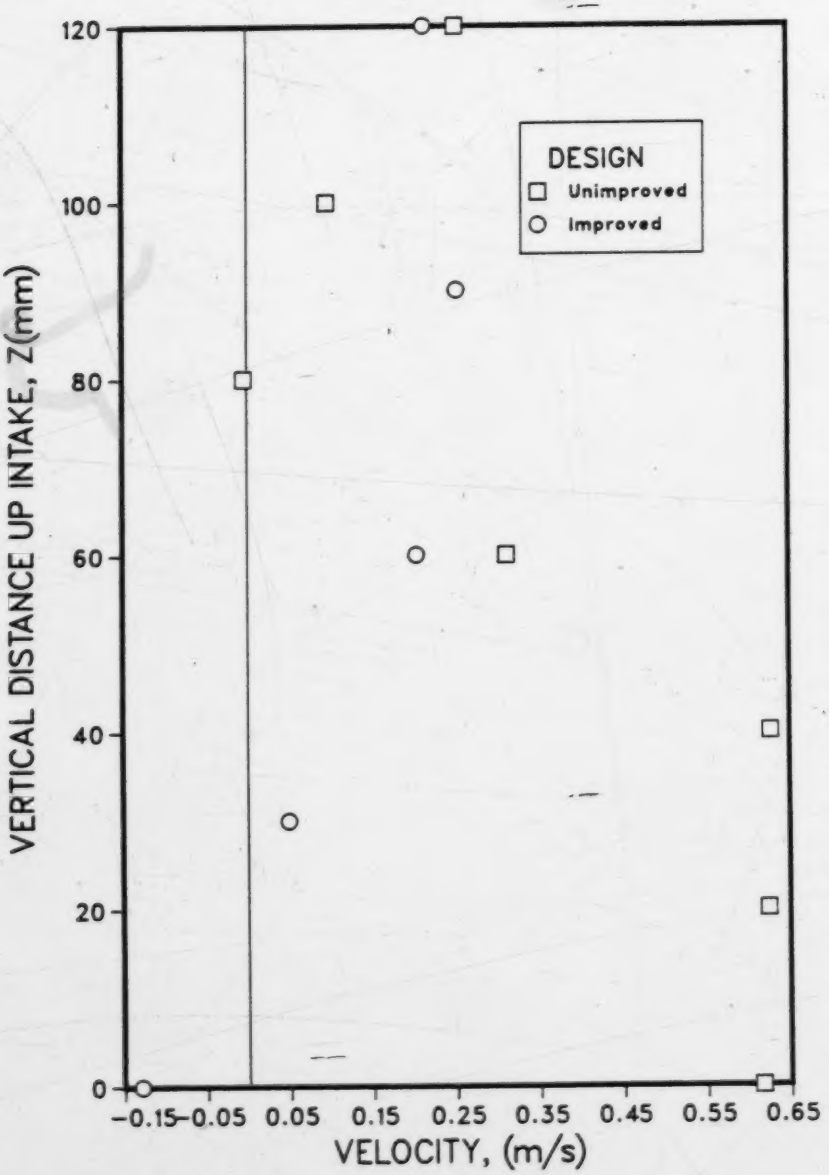

Figure 79. Longitudinal velocities in the horizontal plane of the intake pipe for the two sump designs. Note the smaller velocities in the intake of the improved sump.

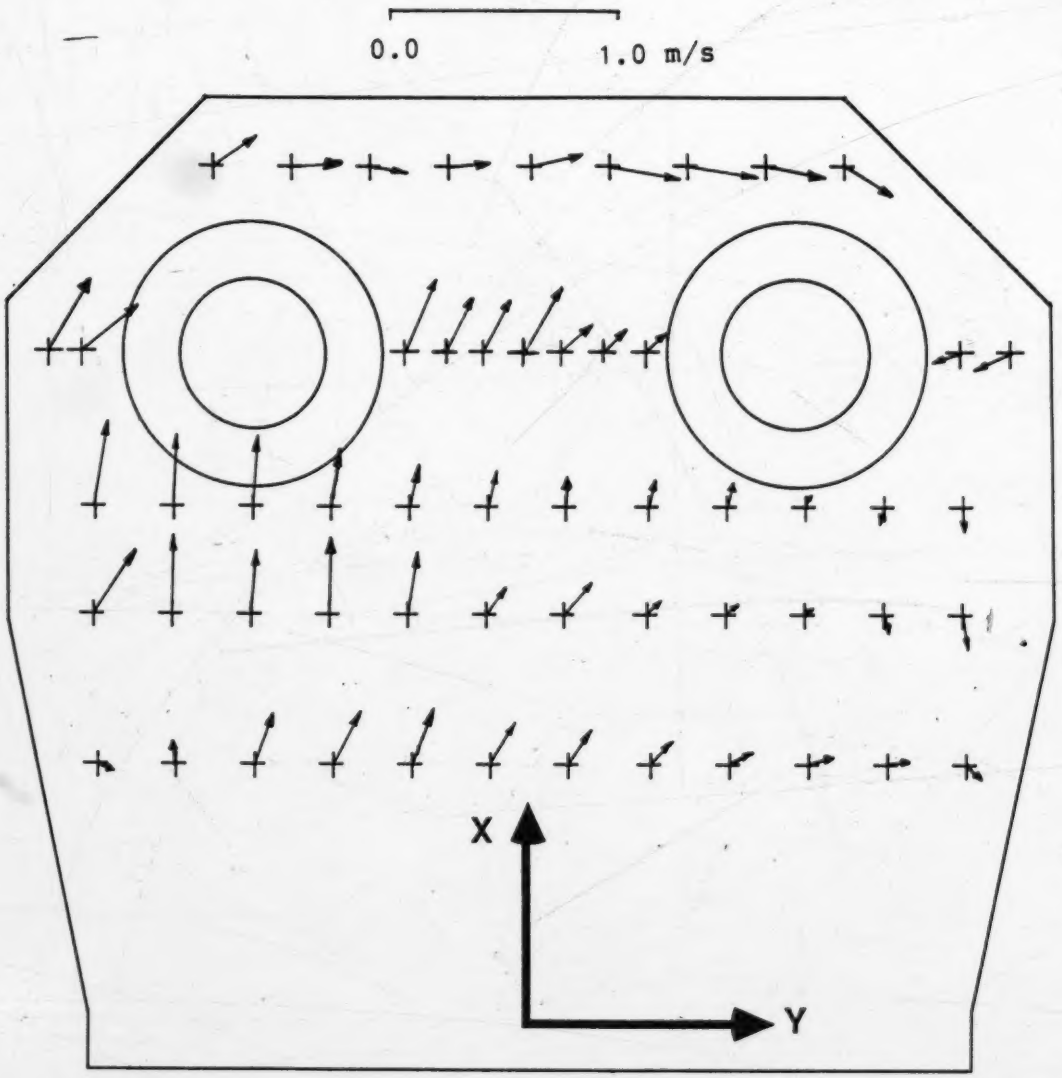

Figure 80. Velocity vectors in the unimproved sump at a height of 90 mm above the floor.

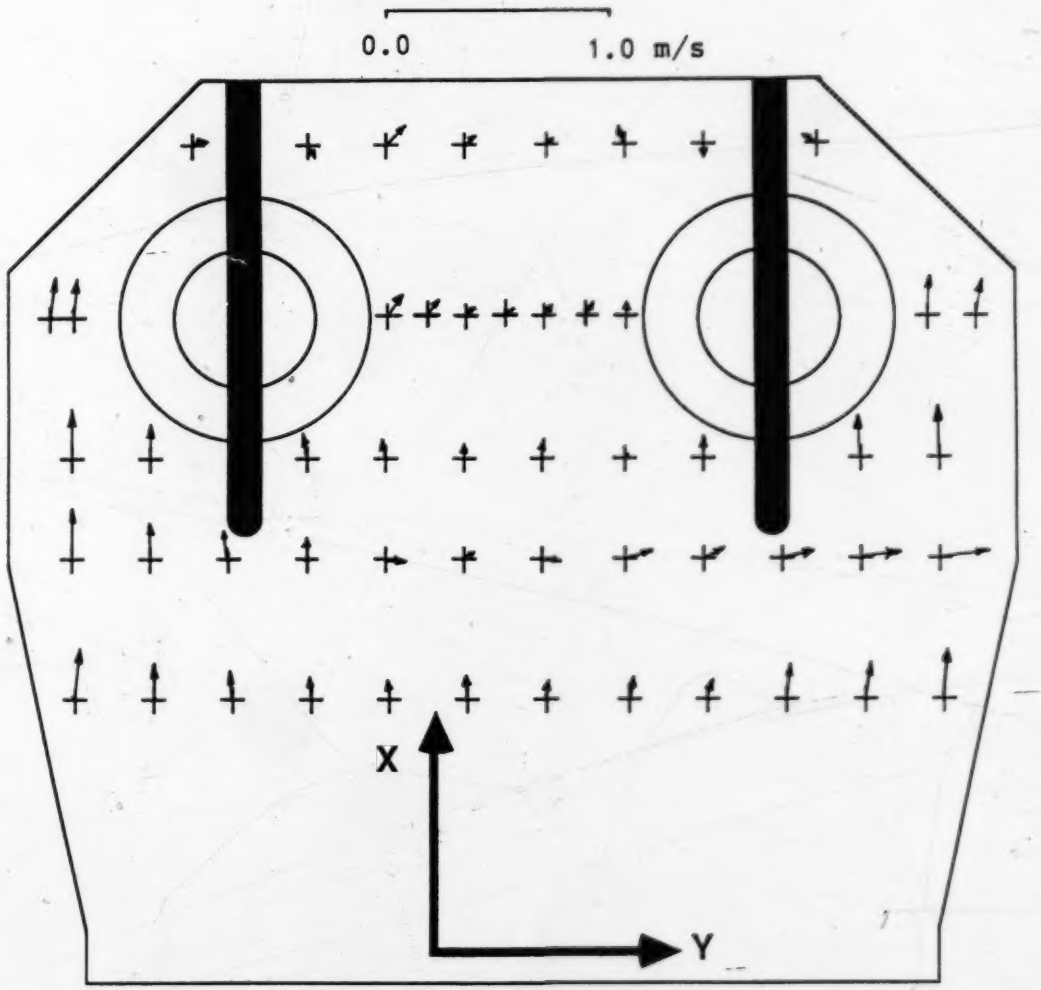

Figure 81. Velocity vectors in the improved sump at a height of 90mm above the floor.

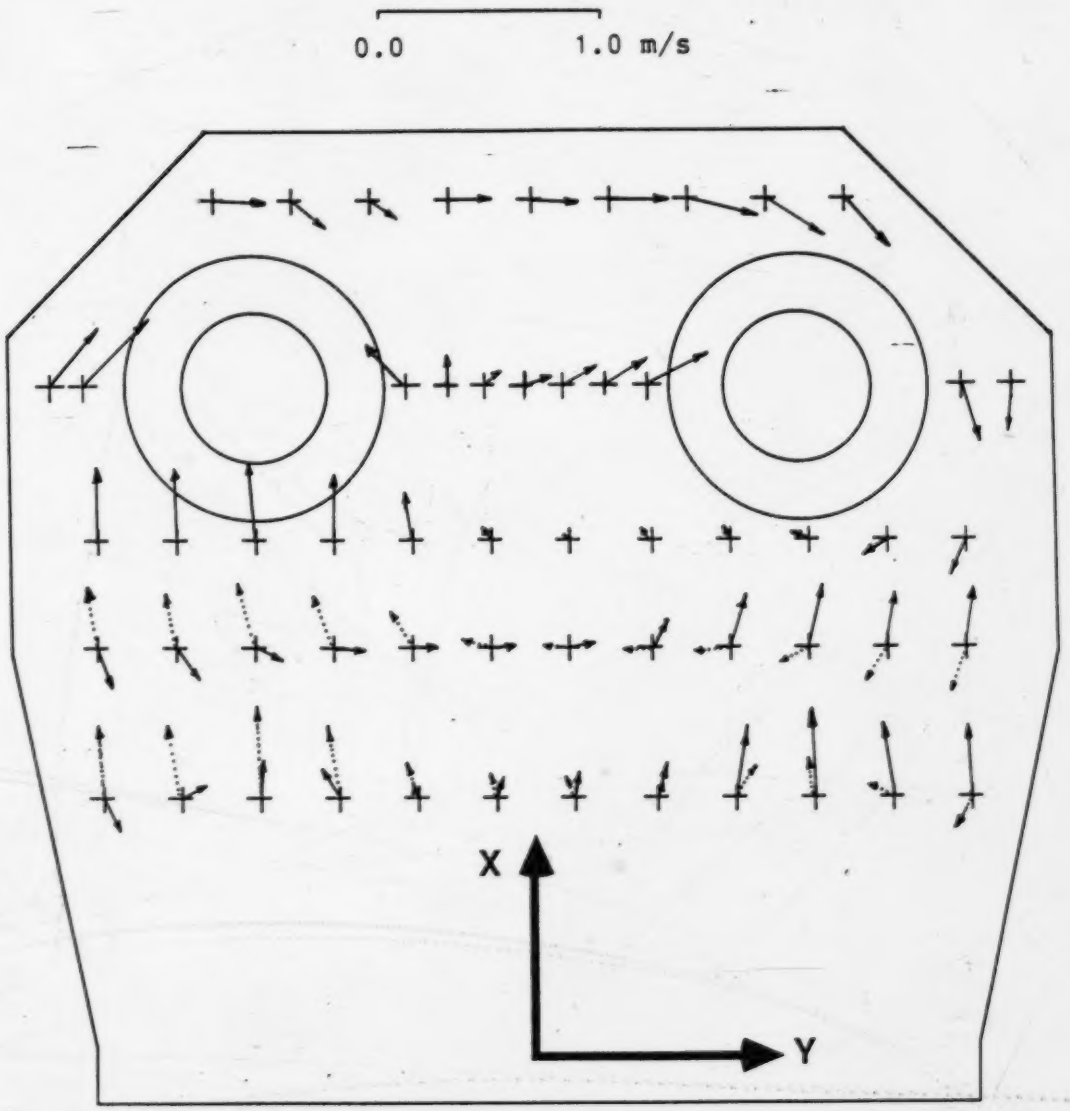

Figure 82. Velocity vectors in the unimproved sump at a height of 30mm above the floor. Note that the bottom two sections were measured at a time when the flow was inverted. For a clearer picture of how the flow would be at one instant of time, dotted arrows give an inverted profile for these sections.

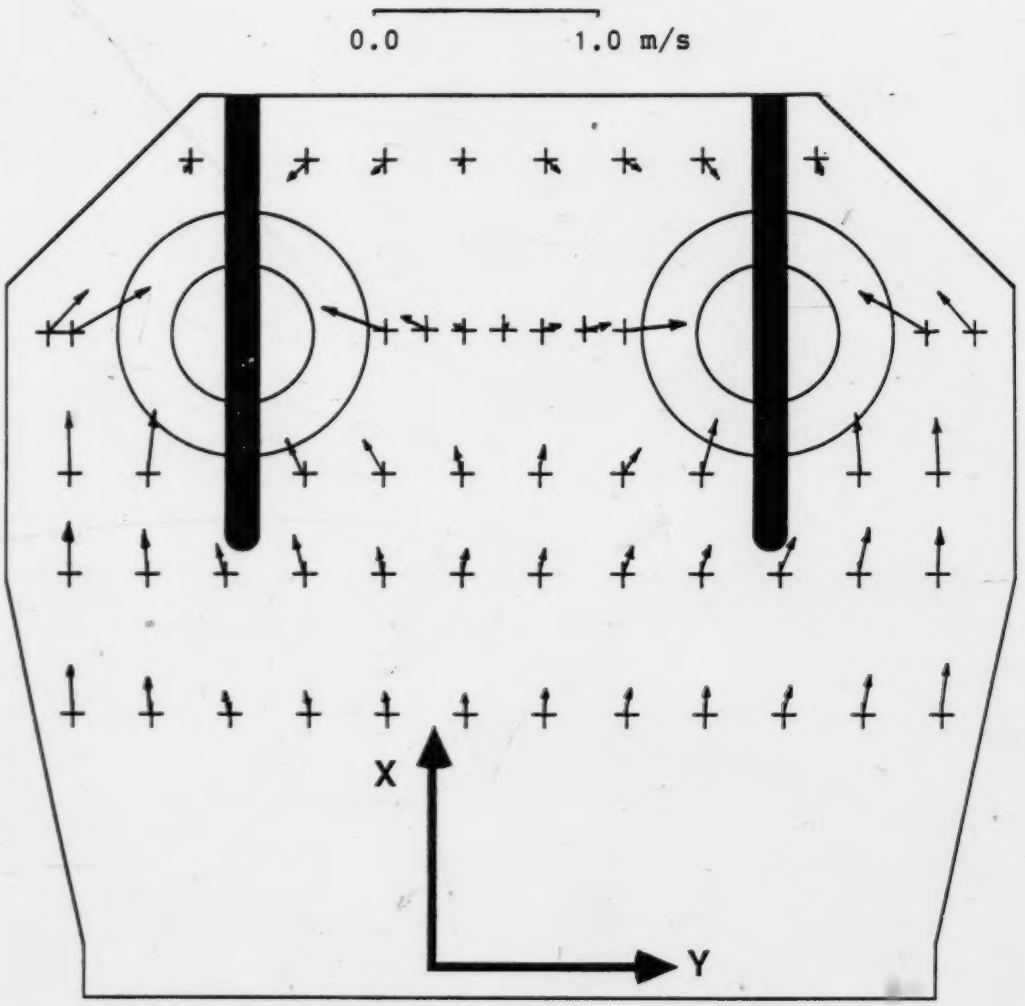

Figure 83. Velocity vectors in the improved sump at a height of 30mm above the floor.

3.3 Recommendations for Further Study

Much work can still be done in the area of pump sump design. The effects of each flow improvement device should be studied individually and in combinations to determine their unique effects on the flow. This will inform designers of the benefits as well as the problems resulting from these devices. Such research will allow designers to know how effective different flow devices are, and to make better choices in designing sumps.

A set of design criteria to fit every possible sump setup without requiring a hydraulic model study is still a long way away. Perhaps if computers become very much faster and more efficient, a numerical solution of sump design problems can be found.

The Laser Doppler Anaemometer can and should play a large role in the study and design of pump sumps. An LDA setup under a pump sump can quickly show the speed and rotation of the flow. A data set taken on a square pattern under the intake bell, such as is done in this study (see figures 77 and 78), could be done for each change in the sump design to illustrate the structure and magnitudes of the flow. Such data will allow the optimum sump design to be chosen on the basis of hard facts rather than subjective dye tests. The empirical methods used to initially design sumps will be here for a long time, but the testing procedures for model sumps can be much improved with the use of Laser Doppler Anaemometry.

4. References

Alexander, L.J.D., Aldworth, G.H., Currie, I.G., Baines, W.D., "Model Test of a Pumping Station Wet Well". Proceedings of the Annual Conference and the 7th Canadian Hydrotechnical Conference of the CSCE. May, 27-31, 1985. Saskatoon, Saskatchewan.

Anwar, H.O., "Flow in a Free Vortex", Water Power April, 1967. pp. 153-161.

Anwar, H.O., "Prevention of Vorticies at Intakes", Water Power, 20(1968) 10, pp. 393-401.

Anwar, H.O. and Amphlett, M.B., "Vorticies at Vertically Inverted Intake". Journal of Hydraulic Research 18 (1980) no. 2.

Anwar, H.O., Weller, J.A., and Amphlett, M.B., "Similarity of Free Vortex at Horizontal Intake". Journal of Hydraulic Research 16 (1978) no. 2.

Babb, A.F., Amorocho, J., and Lomax, C., "Minimum Reynold's Numbers for Physical Model Similarity". Proceedings of the 26th Annual Hydraulics Division Speciality Conference on Verification of Mathematical and Physical Models in Hydraulic Engineering, University of Maryland, August 9-11, 1978. Sponsored by the

Hydraulics Division of the ASCE.

Babb, A.F. and Mih, W.C., "Selection of Model Test Programs with Reference to Viscous and Gravity Force Similtude", IAHR Symposium on Scale Effects in Modelling Hydraulic Structures, Esslingen, FDR. September 3-6, 1984.

Boillat, J.L., Bruschin,, J., and Rolewicz, D., "A Boundary Layer Suction Vortex Supressor". IAHR 1984 Symposium, see Babb and Mih.

Daggett, L.L., and Keulegan, G.H., "Similtude in Free Surface Vortex Formations". Journal of the Hydraulics Division, ASCE Vol. 100, November, 1974, pp. 1565-1581.

Denny, D.F. "An Experimental Study of Air-Entraining Vorticies in Pump Sumps". Proceedings of Institute of Mechanical Engineers, London, England. Vol. 170, Mo. 2, 1956, pp. 107-125.

Dhillon. G.S., Sakhuja, V.S., and Paul, T.C., "Modelling Criteria for Vortex Formation at pipe Intakes", Proceedings of the XIX Congress of the IAHR, New Delhi, February, 1981. Vol. V, pp. 223-234.

Dicmas, J.L., "Effect of Intake Modifications on the Hydraulic Performance of a Mixed Flow Pump". Joint

Symposium on the Design and Operation of Fluid Machinery. Colorado State University, Fort Collins June 1978, pp. 403-412.

Drain, L.E., The Laser Doppler Technique, Chichester, 1980. John Wiley and Sons.

Einstein, H.A. and Li, H., "Steady Vortex Flow in a Real Fluid". La Houille Blanche, No. 4 (1955) pp. 483-497.

Fraser, W.H. and Harrison, N.J., "Hydraulic Problems Encountered in Intake Structures of Vertical Wet-Pit Pumps and Methods Leading to their Solution" Transactions of the ASME, 1953, pp. 643-652.

Fung, L., Rajaratnam, N., and Peterson, A.W., "A Preliminary Study of Drop Structures in the Edmonton Stormwater System". Technical Report WRE 82-12, Department of Civil Engineering, the University of Alberta, December, 1982.

Gordon, J.L., "Vorticies at Intakes", Water Power April, 1970. pp. 137-138.

Haindl, K., "Contribution to Air-Entrainment by a Vortex". Proceedings of the VIII Congress of the IAHR, Paper 16-D, August 1959.

Harshbarger, D.E., Vigander, S., and Hecker, G.E., Discussion of "Air Entrainment in High head Gated Conduits" Journal of the Hydraulics Division, ASCE Vol. 103, December, 1977, pp. 1486-1488.

Hattersley, R.T., "Hydraulic Design of Pump Intakes". Journal of the Hydraulics Division, ASCE. Vol. 95, No. HY2. Proceedings of March, 1965. pp. 223,240.

Hecker, G.E., "Scale Effects in Modelling Vorticies". IAHR 1984 Symposium, see Babb and Mih.

Hecker, G.E. "Model-Prototype Comparison of Free-Surface Vorticies". Journal of the Hydraulics Division, ASCE, No. HY10, vol. 107, October, 1981. pp. 1243-1259.

Iversen, H.W., "Studies of Submergence Requirements of High Specific Speed Pumps". Transactions of the ASME, May, 1953, pp. 634-641.

Jain, S.C. and Kennedy, J.F., "Vortex Flow Drop Structures". IAHR 1984 Symposium, see Babb and Mih.

Jain, A.K., Ranga Raju, K.G. and Garde, R.J., "Vortex Formation at Vertical Pipe Intakes". Journal of the Hydraulics Division, ASCE. Vol.104 September, 1978 pp. 1429-1445.

Jain, A.K., Ranga Raju, K.G. and Garde, R.J., "Air Entrainment in Radial Flow Towards Intakes". Journal of the Hydraulics Division, ASCE. Vol. 104 September, 1978 pp. 1323-1329.

Kells, J.A. (Project Engineer) and Babb, A.F. (Specialist Consultant), "Forty Mile Coulee Project Hydraulic Model Studies". Prepared by Northwest Hydraulics Ltd. for W-E-R Engineering Ltd. in June, 1983.

Kells, J.A., Babb, A.F., and Wise, J.M., "Hydraulic Model of the Fourty Mile Coulee Project". CSCE 1985 Conference, see Alexander, L.J.D.*et al*.

Lewellan, W.S., "A Solution for Three Dimensional Vortex Flows with Strong Circulation". Journal of Fluid Mechanics, 1962 pp. 420-432.

Lugt, H.J., Vortex Flow in Nature and Industry. Wiley and Sons, New York, 1983.

Martins, R., "Vortex Similtude in Hydraulic Models". IAHR 1984 Symposium, see Babb and Mih.

McCorquodale, J.A. "Scale Effects in Swirling Flow". Journal of the Hydraulics Division, ASCE. Vol. 94, No. HY1 January, 1968 pp. 285-300.

Odgaard, A.J., "Fluid Properties and Their Scale Effects in Froude Scaled Hydraulic Models". IAHR 1984 Symposium, see Babb and Mih.

Padmanabhan, M. and Hecker, G.E., "Scale Effects in Pump Sump Models" Journal of Hydraulic Engineering, ASCE vol. 110, no. 11 November, 1984. pp. 1540 - 1556.

Prosser, M.J., "The Hydraulic Design of Pump Sumps and Intakes". BHRA/CIRA publication (1977). Report RR1421, 42p.

Schulthess, "Model tests with Vorticies - El Cajon Project (Honduras)". IAHR 1984 Symposium, see Babb and Mih.

Siervi, De F., Viguier, H.C., Greitzer, E.M. and Tan, C.S. "Mechanisms of Inlet Vortex Formation". 1982 Journal of Fluid Mechanics, vol. 124 pp. 173-207.

Smith, C.D. and Yu, J.N.G. "Use of Baffles in Open Channel Expansions". ASCE Journal of the Hydraulics Division, vol. 92, no. HY2, March, 1966.

Sweeny, C.E., Elder, R.A. and Hay, D., "Pump Sump Design Experience - a Summary". ASCE Annual Conference in Hollywood-by-the-sea, Florida. October 27-31, 1980.

Task Commitee on Intake Vorticies: Closure of the Discussion of Model-Prototype Comparison of Free Surface Vorticies. Journal of the Hydraulics Division, ASCE. Vol. 109 (1983) 3, pp. 487-489.

Toyokura, T. and Kamemoto, K., "Introduction of the JSME Standard to Establish a Set of Basic Rules For Model Testing of Pump Sump Performance". IAHR 1984 Symposium, see Babb and Mih.

Tullis, J.P., "Modelling in Design of Pumping Pits". Journal of the Hydralics Division, ASCE. Vol. 105 September, 1979, pp. 1053-1063.

Venkataratma, S., Dinakar, P.J., Rajan, B.H., "On the Conflicting Modelling Criteria, Causitive Scale Effects and the (In)Compatability of Scale Modelling Vorticies - A Case Study". IAHR 1984 Symposium, see Babb and Mih.

Venkataratma, C.P., Sankara Rao, J.K., Ramanathan, V., and Chauan, A.R., "Experimental Investigations of Scale Effects in Vortex Formation at Intakes". Proceedings of the XIX Congress of the IAHR, New Delhi, February, 1981. Vol. V, pp. 235-241.

Wijdieks, J., "Practice and Criteria for Pump Sump Model Investigation". IAHR 1984 Symposium, see Babb and Mih.

Yildrim, N., and Jain, S.C., "Surface Tension Efect on Profile of a free Vortex". Journal of the Hydraulics Division, ASCE. Vol. 107, no. HY1, January, 1981, pp. 132-136.

5. APPENDIX A: Velocities from the propeller probe.

Velocities taken with a propeller probe at about 5.0cm above the floor

water level: LWL(2) or Prototype elevation 795.8.
Discharge: 12.56 l/s.

Point Location	Frequency (hertz)	Velocity (cm/s)
1	11-23	9.0-15.1
2	12-28	9.5-17.7
3	39-57	23.4-33.0
4	62-80	35.5-45.0
5	37-46	22.4-27.0
6	15-18	11.0-12.5
7	9-13	7.7-10.0
8	9-13	7.7-10.0
9	50-63	29.036.0
10	38-43	22.8-25.3
11	21-26	14.1-16.7
12	30-36	18.7-21.8
13	21-25	14.1-16.2
14	22-25	14.6-16.2
15	67-85	38.0-50.0
16	71-77	40.5-43.0
17		
18	38-41	22.8-24.3
19	20-27	13.6-17.2
20	69-85	39.0-50.0

Velocity Range: 7.0 to 50.0 cm/s

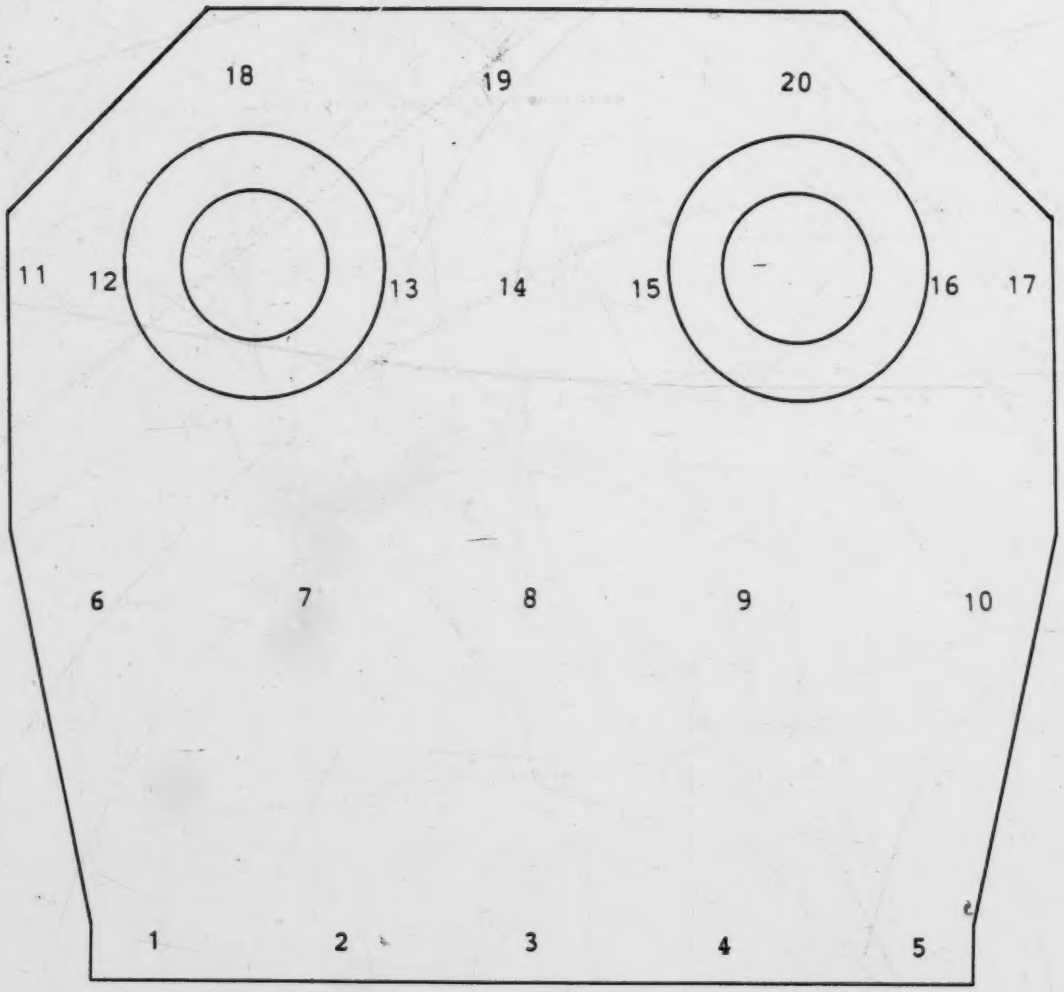

Figure A1. View of sump showing locations where propeller probe velocity measurements were taken.

6. APPENDIX B: Data for the unimproved sump.

Note: All data in units of metres and seconds.

LASER DOPPLER MEASURED VELOCITIES IN UNIMPROVED SUMP

SAMPLE SIZE= 20,000.

LOCATION: CROSS-SECTION IN MAIN BODY OF THE SUMP(XSECT#1).

Z	X	Y	v	u	$\overline{v'^2}$	$\overline{u'^2}$	$\overline{u'v'}$
0.0	0.0	0.0	-0.0083	0.27422	0.00485	0.00706	0.00111
0.0	0.0	50.0	-0.0195	0.30401	0.00632	0.00742	0.00043
0.0	0.0	100.0	-0.044	0.28531	0.00775	0.00938	-0.0012
0.0	0.0	150.0	-0.047	0.22356	0.00831	0.01202	-0.0035
0.0	0.0	200.0	-0.0501	0.06575	0.01117	0.01171	-0.0042
0.0	0.0	250.0	-0.1171	0.02951	0.01153	0.01348	-0.0017
0.0	0.0	300.0	-0.1606	0.02588	0.01065	0.00891	1.9E-05
0.0	0.0	350.0	-0.2082	0.00906	0.00823	0.00568	-0.0009
0.0	0.0	400.0	-0.2364	-0.0327	0.00966	0.00664	-0.0021
0.0	0.0	450.0	-0.2371	-0.104	0.00846	0.00812	-0.0045
0.0	0.0	500.0	-0.1704	-0.1801	0.00492	0.00817	-0.0029
0.0	0.0	550.0	-0.0688	-0.2253	0.00283	0.00671	-0.0003
30.0	0.0	0.0	-0.0002	0.31752	0.00358	0.00788	0.0006
30.0	0.0	50.0	-0.0066	0.31386	0.00689	0.01052	-0.0006
30.0	0.0	100.0	-0.0234	0.33962	0.00758	0.00939	0.00067
30.0	0.0	150.0	0.00835	0.28984	0.02697	0.03526	-0.0146
30.0	0.0	200.0	-0.0285	0.19871	0.01027	0.02081	-0.0036
30.0	0.0	250.0	-0.0415	0.04904	0.00874	0.01422	-0.0012
30.0	0.0	300.0	-0.0251	0.02041	0.0099	0.0161	0.00233
30.0	0.0	350.0	-0.0387	0.04654	0.00983	0.01396	0.00457
30.0	0.0	400.0	-0.0209	0.04094	0.00896	0.00705	0.00154
30.0	0.0	450.0	-0.0741	0.02854	0.01015	0.00877	-0.0004
30.0	0.0	500.0	-0.104	-0.0687	0.00588	0.00607	-0.0003
30.0	0.0	550.0	-0.0784	-0.1736	0.003	0.00433	-0.001
60.0	0.0	0.0	0.00776	0.31742	0.00847	0.01208	0.00416
60.0	0.0	50.0	0.0088	0.32395	0.00834	0.01049	0.00416
60.0	0.0	100.0	0.07857	0.24313	0.04189	0.04577	0.02558
60.0	0.0	150.0	0.0399	0.28542	0.0154	0.02094	0.00755
60.0	0.0	200.0	0.04832	0.21206	0.00927	0.01752	9.2E-05
60.0	0.0	250.0	0.07223	0.14103	0.061	0.06204	0.03674
60.0	0.0	300.0	0.04356	0.09091	0.00711	0.01229	-0.0011
60.0	0.0	350.0	0.07921	0.06296	0.03058	0.03299	-0.0245
60.0	0.0	400.0	0.05443	0.03917	0.00682	0.0082	0.00173
60.0	0.0	450.0	0.00889	0.02691	0.00616	0.00686	-0.0009
60.0	0.0	500.0	-0.0231	-0.0294	0.00579	0.00847	-0.0007
60.0	0.0	550.0	-0.0436	-0.1457	0.00406	0.0039	-0.0011

90.0	0.0	0.0	0.06656	0.36377	0.0339	0.03676	-0.0222
90.0	0.0	50.0	0.01707	0.31228	0.01556	0.01661	-0.0077
90.0	0.0	100.0	0.02065	0.30647	0.01028	0.01247	-0.0013
90.0	0.0	150.0	0.03906	0.24157	0.00751	0.01484	-0.0019
90.0	0.0	200.0	0.03995	0.18606	0.00785	0.01242	-0.0015
90.0	0.0	250.0	0.03793	0.17335	0.0075	0.0161	-0.0005
90.0	0.0	300.0	0.03414	0.12807	0.00639	0.00946	-3E-05
90.0	0.0	350.0	0.0303	0.11569	0.006	0.01082	-0.0004
90.0	0.0	400.0	0.02662	0.10336	0.00661	0.00901	-0.0014
90.0	0.0	450.0	0.01821	0.03812	0.00649	0.01055	-0.0015
90.0	0.0	500.0	-0.0111	-0.0512	0.00662	0.00863	-0.0013
90.0	0.0	550.0	0.00803	-0.1112	0.02884	0.02978	-0.0261
120.0	0.0	0.0	0.50185	-0.0359	0.1864	0.17634	0.03993
120.0	0.0	50.0	0.21006	0.20464	0.12427	0.12327	0.02438
120.0	0.0	100.0	0.12778	0.21127	0.0655	0.06673	0.04072
120.0	0.0	150.0	0.15919	0.2016	0.0825	0.10247	0.00545
120.0	0.0	200.0	0.17566	0.15681	0.077	0.07537	0.01155
120.0	0.0	250.0	0.18606	0.08454	0.07468	0.07261	0.04247
120.0	0.0	300.0	0.15449	0.10597	0.04858	0.04642	0.01717
120.0	0.0	350.0	0.16312	0.11554	0.05823	0.05763	0.02474
120.0	0.0	400.0	0.11045	0.06423	0.03083	0.02924	-0.0048
120.0	0.0	450.0	0.07806	0.03803	0.02239	0.02405	-0.0114
120.0	0.0	500.0	0.09492	-0.0069	0.03063	0.032	-0.0186
120.0	0.0	550.0	0.23544	0.01548	0.08612	0.08675	-0.0471

LASER DOPPLER MEASURED VELOCITIES IN UNIMPROVED SUMP

SAMPLE SIZE= 20,000.

LOCATION: CROSS-SECTION IN MAIN SUMP AREA(XSECT#2)

Z	X	Y	v	u	$\overline{v'^2}$	$\overline{u'^2}$	$\overline{u'v'}$
0.0	0.0	0.0	0.04337	-0.2307	0.005	0.00792	-0.0022
0.0	0.0	50.0	0.11023	-0.2058	0.00367	0.00463	0.00159
0.0	0.0	100.0	0.15094	-0.1769	0.00693	0.00723	4.9E-05
0.0	0.0	150.0	0.15742	-0.1368	0.00759	0.0071	0.00081
0.0	0.0	200.0	0.15327	-0.0924	0.00651	0.00585	0.0004
0.0	0.0	250.0	0.14384	-0.0458	0.02285	0.02288	-0.0159
0.0	0.0	300.0	0.10274	0.00968	0.02773	0.02943	-0.0139
0.0	0.0	350.0	0.07505	0.04969	0.01348	0.01897	0.00735
0.0	0.0	400.0	0.05389	0.1213	0.01135	0.01918	0.00582
0.0	0.0	450.0	0.04004	0.18826	0.01191	0.0174	0.00463
0.0	0.0	500.0	0.03561	0.26001	0.01267	0.01188	0.00308
0.0	0.0	550.0	0.03357	0.2562	0.00887	0.01554	0.00337
30.0	0.0	0.0	0.06359	-0.1812	0.00668	0.0091	-0.0035
30.0	0.0	50.0	0.08989	-0.1335	0.00375	0.00504	0.00092
30.0	0.0	100.0	0.11435	-0.0557	0.01583	0.01894	-0.0115
30.0	0.0	150.0	0.13213	-0.0132	0.02422	0.02712	-0.0186
30.0	0.0	200.0	0.1124	-0.0031	0.00671	0.0106	0.00042
30.0	0.0	250.0	0.10043	0.00687	0.00802	0.0115	-4E-05
30.0	0.0	300.0	0.10428	0.02543	0.00766	0.01221	0.00085
30.0	0.0	350.0	0.08657	0.14991	0.0103	0.0309	0.0062
30.0	0.0	400.0	0.07306	0.21867	0.01199	0.02783	0.00549
30.0	0.0	450.0	0.06613	0.26558	0.01088	0.01914	0.00326
30.0	0.0	500.0	0.03822	0.24126	0.00925	0.01402	0.00252
30.0	0.0	550.0	0.0428	0.25594	0.00784	0.01233	0.00042
60.0	0.0	0.0	0.1028	-0.1309	0.02931	0.03116	-0.0244
60.0	0.0	50.0	0.08432	-0.0941	0.01195	0.01316	-0.0039
60.0	0.0	100.0	0.07253	-0.0143	0.01921	0.02281	-0.0115
60.0	0.0	150.0	0.0508	0.02306	0.00893	0.01148	0.0019
60.0	0.0	200.0	0.0354	0.03362	0.0117	0.01403	0.00452
60.0	0.0	250.0	0.07001	0.0612	0.04256	0.05164	-0.0011
60.0	0.0	300.0	0.07211	0.02838	0.03548	0.04203	0.02712
60.0	0.0	350.0	0.11658	0.04744	0.05921	0.06543	0.04525
60.0	0.0	400.0	-0.0035	0.11948	0.08426	0.08488	0.00917
60.0	0.0	450.0	0.09846	0.16615	0.05298	0.05742	0.03991
60.0	0.0	500.0	0.10179	0.21569	0.04803	0.05222	0.0361
60.0	0.0	550.0	0.11538	0.21366	0.05192	0.05635	0.03713

90.0	0.0	0.0	0.18514	0.27502	0.10745	0.11053	0.02588
90.0	0.0	50.0	0.00932	0.34524	0.01467	0.01601	-0.0038
90.0	0.0	100.0	0.02522	0.28326	0.01334	0.01593	-0.0008
90.0	0.0	150.0	0.01908	0.32567	0.01377	0.01802	0.00343
90.0	0.0	200.0	0.04503	0.26604	0.0204	0.02846	0.00668
90.0	0.0	250.0	0.08412	0.11369	0.03177	0.03643	0.01789
90.0	0.0	300.0	0.11857	0.13163	0.0595	0.06459	-0.0137
90.0	0.0	350.0	0.05961	0.05295	0.01939	0.02245	0.00717
90.0	0.0	400.0	0.04924	0.03631	0.01272	0.01524	-6E-05
90.0	0.0	450.0	0.02157	0.01044	0.02276	0.02314	-0.0162
90.0	0.0	500.0	0.0108	-0.0766	0.01165	0.01161	-0.0049
90.0	0.0	550.0	0.01531	-0.152	0.02849	0.02967	-0.0241
120.0	0.0	0.0	0.07394	0.29612	0.04085	0.0423	0.01505
120.0	0.0	50.0	0.10764	0.35176	0.04878	0.04849	-0.0164
120.0	0.0	100.0	0.05514	0.30508	0.02548	0.02761	0.01136
120.0	0.0	150.0	0.17616	0.15939	0.08616	0.09133	0.07732
120.0	0.0	200.0	0.21577	0.0853	0.09851	0.1047	0.08843
120.0	0.0	250.0	0.31437	-0.0428	0.11339	0.11652	0.09707
120.0	0.0	300.0	0.32727	-0.0706	0.10793	0.1097	0.09332
120.0	0.0	350.0	0.22429	-0.0402	0.07943	0.07625	0.06105
120.0	0.0	400.0	0.16475	0.00781	0.0722	0.07857	0.0159
120.0	0.0	450.0	0.06651	-0.0276	0.01708	0.02111	0.00344
120.0	0.0	500.0	0.03488	-0.0574	0.01416	0.01713	-0.0059
120.0	0.0	550.0	0.19226	-0.0951	0.08995	0.08971	-0.0366

LASER DOPPLER MEASURED VELOCITIES IN UNIMPROVED SUMP

SAMPLE SIZE= 20,000.

LOCATION: CROSS-SECTION IN MAIN SUMP AREA(XSECT#3).

Z	X	Y	v	u	$\overline{v'^2}$	$\overline{u'^2}$	$\overline{u'v'}$
0.0	0.0	0.0	0.07125	-0.186	0.00352	0.00635	-0.0001
0.0	0.0	50.0	0.19783	-0.1302	0.00599	0.00862	0.00226
0.0	0.0	100.0	0.25228	0.00912	0.01193	0.01122	0.00395
0.0	0.0	150.0	0.18583	0.08998	0.01613	0.00919	0.00285
0.0	0.0	200.0	0.10232	0.03927	0.01673	0.01532	-0.0079
0.0	0.0	250.0	0.08771	0.06496	0.01254	0.02226	-0.0023
0.0	0.0	300.0	0.06198	-0.0642	0.00901	0.02259	-0.0002
0.0	0.0	350.0	0.08317	0.02016	0.01304	0.02219	0.0093
0.0	0.0	400.0	0.08745	0.14985	0.01607	0.02086	0.01195
0.0	0.0	450.0	0.01957	0.27354	0.01197	0.01079	0.00445
0.0	0.0	500.0	-0.0378	0.28484	0.0125	0.01193	-0.0012
0.0	0.0	550.0	-0.0326	0.26511	0.00712	0.01073	0.00042
30.0	0.0	0.0	0.06665	-0.1401	0.00337	0.00506	8.4E-05
30.0	0.0	50.0	0.08918	0.04758	0.00632	0.0084	0.00147
30.0	0.0	100.0	0.01412	0.17166	0.00929	0.0054	0.00108
30.0	0.0	150.0	-0.078	0.12458	0.0123	0.01001	-0.0025
30.0	0.0	200.0	-0.016	0.04319	0.01276	0.01158	-0.0003
30.0	0.0	250.0	0.01877	0.06202	0.00872	0.01128	-7E-05
30.0	0.0	300.0	0.01632	0.09929	0.00986	0.01047	0.00287
30.0	0.0	350.0	0.04095	0.14697	0.00833	0.01021	0.00236
30.0	0.0	400.0	0.05161	0.30159	0.01008	0.01234	0.00353
30.0	0.0	450.0	-0.0113	0.38094	0.00867	0.00993	0.00289
30.0	0.0	500.0	-0.0457	0.32534	0.00636	0.00728	0.00072
30.0	0.0	550.0	-0.0159	0.30877	0.00371	0.00592	-0.0008
60.0	0.0	0.0	0.02662	-0.1066	0.00761	0.00821	-0.002
60.0	0.0	50.0	-0.0172	0.00046	0.01074	0.01121	0.00251
60.0	0.0	100.0	-0.0285	-0.0136	0.01827	0.02095	0.00863
60.0	0.0	150.0	-0.0361	0.03645	0.01798	0.02202	0.00557
60.0	0.0	200.0	-0.0025	0.08776	0.02915	0.03346	0.01565
60.0	0.0	250.0	-0.0039	0.08912	0.01708	0.01859	0.0058
60.0	0.0	300.0	0.00481	0.11126	0.01773	0.01913	0.00787
60.0	0.0	350.0	0.01258	0.16781	0.04007	0.04291	0.00046
60.0	0.0	400.0	-0.0219	0.1759	0.03183	0.03417	0.02205
60.0	0.0	450.0	-0.0093	0.16881	0.01628	0.01793	0.00462
60.0	0.0	500.0	0.00755	0.24975	0.01217	0.013	0.00199
60.0	0.0	550.0	0.00565	0.26253	0.01105	0.0138	0.00084

90.0	0.0	0.0	0.07829	-0.0301	0.03984	0.03997	-0.0324
90.0	0.0	50.0	-0.0016	0.06587	0.02921	0.03852	-0.0148
90.0	0.0	100.0	0.088	0.21798	0.02041	0.02242	0.0025
90.0	0.0	150.0	0.12042	0.22457	0.01491	0.01844	0.00199
90.0	0.0	200.0	0.0968	0.24804	0.01943	0.02315	0.00319
90.0	0.0	250.0	0.1084	0.16824	0.02074	0.02347	0.0022
90.0	0.0	300.0	0.09886	0.14224	0.01737	0.01903	-0.0031
90.0	0.0	350.0	0.0966	0.09892	0.01581	0.01688	-0.0037
90.0	0.0	400.0	0.09715	0.05003	0.01231	0.01709	-0.0033
90.0	0.0	450.0	0.11491	0.02968	0.01397	0.01782	-0.0062
90.0	0.0	500.0	0.08374	0.00421	0.01647	0.01631	-0.0086
90.0	0.0	550.0	0.06386	-0.0702	0.03775	0.03742	-0.0327
120.0	0.0	0.0	0.1408	0.3389	0.08768	0.06828	-0.0214
120.0	0.0	50.0	0.05007	0.27446	0.02293	0.02522	-0.0073
120.0	0.0	100.0	0.05981	0.23894	0.01818	0.01978	0.00372
120.0	0.0	150.0	0.11946	0.25764	0.0188	0.02122	0.00595
120.0	0.0	200.0	0.13371	0.20958	0.02467	0.02821	0.00977
120.0	0.0	250.0	0.12386	0.19273	0.02665	0.03043	0.01243
120.0	0.0	300.0	0.1246	0.16385	0.02545	0.02993	0.0071
120.0	0.0	350.0	0.1151	0.10047	0.02301	0.02611	0.00285
120.0	0.0	400.0	0.1258	0.05152	0.02007	0.02389	-0.0026
120.0	0.0	450.0	0.13133	0.02427	0.01384	0.01652	-0.0091
120.0	0.0	500.0	0.12886	0.02649	0.02651	0.02658	-0.018
120.0	0.0	550.0	0.20795	0.05001	0.07166	0.07063	-0.0601

LASER DOPPLER MEASURED VELOCITIES IN UNIMPROVED SUMP

SAMPLE SIZE= 20,000.

LOCATION: BETWEEN INTAKE BELLS.

Z	X	Y	v	u	$\overline{v'^2}$	$\overline{u'^2}$	$\overline{u'v'}$
0.0	0.0	0.0	-0.0836	-0.3128	0.02939	0.05999	0.01056
0.0	0.0	25.0	-0.0362	-0.3048	0.02105	0.04505	0.00776
0.0	0.0	50.0	0.05701	-0.1648	0.02042	0.05103	0.01221
0.0	0.0	75.0	0.09619	-0.1974	0.02429	0.03616	0.01344
0.0	0.0	100.0	0.16283	-0.1604	0.01982	0.03738	0.01034
0.0	0.0	125.0	0.19363	-0.1048	0.02115	0.0429	0.01335
0.0	0.0	150.0	0.23128	-0.0215	0.03575	0.04217	0.02896
30.0	0.0	0.0	-0.1652	0.17469	0.02896	0.04932	0.00374
30.0	0.0	25.0	-0.0014	0.11963	0.01805	0.04066	0.00173
30.0	0.0	50.0	0.06285	0.05311	0.00854	0.02374	0.00054
30.0	0.0	75.0	0.11056	0.0322	0.0071	0.01959	-1E-05
30.0	0.0	100.0	0.138	0.07604	0.0297	0.04774	-0.015
30.0	0.0	125.0	0.1726	0.10494	0.00788	0.01547	0.00213
30.0	0.0	150.0	0.27111	0.13073	0.01329	0.02941	0.00819
60.0	0.0	0.0	0.12958	0.29785	0.01133	0.01452	0.00138
60.0	0.0	25.0	0.10101	0.22909	0.0098	0.01193	0.00054
60.0	0.0	50.0	0.10726	0.15722	0.00936	0.01128	0.00071
60.0	0.0	75.0	0.10618	0.17994	0.0095	0.01202	-0.0003
60.0	0.0	100.0	0.11774	0.11863	0.00818	0.0134	0.00133
60.0	0.0	125.0	0.12047	0.12359	0.00732	0.0117	0.0019
60.0	0.0	150.0	0.09188	0.11595	0.00841	0.0123	0.00304
90.0	0.0	0.0	0.12805	0.30004	0.0073	0.01071	0.00153
90.0	0.0	25.0	0.11878	0.23472	0.00835	0.01193	0.00104
90.0	0.0	50.0	0.12034	0.22109	0.00988	0.01378	0.00177
90.0	0.0	75.0	0.11081	0.196	0.00954	0.01315	0.00135
90.0	0.0	100.0	0.13911	0.12289	0.01436	0.01538	0.00616
90.0	0.0	125.0	0.12234	0.1206	0.01172	0.01454	0.00388
90.0	0.0	150.0	0.10796	0.09582	0.01537	0.01851	0.00804
120.0	0.0	0.0	0.11557	0.28511	0.00875	0.01141	0.00172
120.0	0.0	25.0	0.12941	0.23251	0.01023	0.01237	0.00365
120.0	0.0	50.0	0.12231	0.20341	0.00912	0.01106	0.00189
120.0	0.0	75.0	0.1262	0.16562	0.00949	0.01252	0.00239
120.0	0.0	100.0	0.13274	0.12495	0.01543	0.01649	0.00713
120.0	0.0	125.0	0.14426	0.13236	0.02147	0.02408	0.01424
120.0	0.0	150.0	0.1298	0.10236	0.02171	0.02559	0.01575

LASER DOPPLER MEASURED VELOCITIES IN UNIMPROVED SUMP

SAMPLE SIZE= 20,000.

LOCATION: NEAR BACKWALL OF SUMP

Z	X	Y	v	u	$\overline{v'^2}$	$\overline{u'^2}$	$\overline{u'v'}$
0.0	0.0	0.0	-0.0404	-0.0931	0.0335	0.02428	-0.0168
0.0	0.0	50.0	0.14754	-0.1351	0.01794	0.0062	-0.0022
0.0	0.0	100.0	0.12426	-0.094	0.03028	0.01855	-0.0033
0.0	0.0	150.0	0.17992	-0.0751	0.01275	0.00961	0.00386
0.0	0.0	200.0	0.24824	-0.0631	0.00988	0.01129	0.0021
0.0	0.0	250.0	0.27038	-0.0794	0.00909	0.01253	0.00019
0.0	0.0	300.0	0.32713	-0.1357	0.00801	0.00771	-8E-05
0.0	0.0	350.0	0.26449	-0.1941	0.01026	0.00565	-0.0001
0.0	0.0	400.0	0.1753	-0.2041	0.00988	0.00455	0.00227
30.0	0.0	0.0	0.22797	-0.0139	0.01057	0.01195	-0.0046
30.0	0.0	50.0	0.14835	-0.1245	0.01304	0.00858	8.4E-05
30.0	0.0	100.0	0.1155	-0.085	0.01493	0.01238	0.00347
30.0	0.0	150.0	0.17852	0.00154	0.03201	0.03993	-0.0166
30.0	0.0	200.0	0.19872	-0.0108	0.00829	0.013	0.00333
30.0	0.0	250.0	0.26435	0.00402	0.00813	0.01433	-0.0039
30.0	0.0	300.0	0.30099	-0.0789	0.0054	0.00835	-0.0005
30.0	0.0	350.0	0.25255	-0.1691	0.00764	0.00744	-0.0002
30.0	0.0	400.0	0.18512	-0.2189	0.01071	0.0068	-0.0006
60.0	0.0	0.0	0.18273	0.11393	0.00848	0.01047	-0.0022
60.0	0.0	50.0	0.20941	-0.0125	0.01294	0.01279	0.00046
60.0	0.0	100.0	0.14568	-0.0337	0.03568	0.03845	-0.0057
60.0	0.0	150.0	0.06672	0.10674	0.07193	0.07424	0.03175
60.0	0.0	200.0	0.10031	0.15631	0.06438	0.06749	0.05501
60.0	0.0	250.0	0.24361	0.04119	0.01797	0.02267	0.01221
60.0	0.0	300.0	0.28431	-0.0111	0.01623	0.01941	0.0114
60.0	0.0	350.0	0.24745	-0.0481	0.00747	0.00988	0.00265
60.0	0.0	400.0	0.19014	-0.1482	0.007	0.00765	0.00342
90.0	0.0	0.0	0.18875	0.12793	0.01062	0.01302	-0.0043
90.0	0.0	50.0	0.20993	0.00699	0.0175	0.01681	0.00234
90.0	0.0	100.0	0.15357	-0.0251	0.02146	0.02418	0.00947
90.0	0.0	150.0	0.15705	0.01276	0.01238	0.01828	0.00074
90.0	0.0	200.0	0.21487	0.04878	0.02771	0.03297	0.01738
90.0	0.0	250.0	0.32416	-0.0601	0.05477	0.05685	0.04641
90.0	0.0	300.0	0.31525	-0.0492	0.04279	0.0445	0.03549
90.0	0.0	350.0	0.25085	-0.0481	0.02248	0.0235	0.01518
90.0	0.0	400.0	0.20298	-0.1334	0.01106	0.01114	0.00507
120.0	0.0	0.0	0.18368	0.13566	0.01528	0.01785	-0.0111
120.0	0.0	50.0	0.22453	-0.0273	0.03399	0.03351	0.01666
120.0	0.0	100.0	0.29717	-0.1655	0.07458	0.07545	0.06103
120.0	0.0	150.0	0.25651	-0.0612	0.05534	0.05857	0.04136
120.0	0.0	200.0	0.36303	-0.0959	0.0662	0.06744	0.0555
120.0	0.0	250.0	0.55475	-0.2921	0.06803	0.06627	0.06085
120.0	0.0	300.0	0.5387	-0.2768	0.06905	0.06876	0.06194
120.0	0.0	350.0	0.39615	-0.2032	0.06257	0.06302	0.05631
120.0	0.0	400.0	0.30263	-0.2422	0.0476	0.04768	0.04285

LASER DOPPLER MEASURED VELOCITIES IN UNIMPROVED SUMP

SAMPLE SIZE- 20,000.

LOCATION: SECTION BETWEEN BELL AND SIDEWALL (NORTH SIDE).

Z	X	Y	v	u	$\overline{v'^2}$	$\overline{u'^2}$	$\overline{u'v'}$
0.0	0.0	0.0	-0.0124	-0.0137	0.06925	0.06894	-0.0395
0.0	0.0	15.0	-0.0781	-0.0364	0.10535	0.10746	-0.003
0.0	0.0	30.0	-0.0838	0.09466	0.08812	0.09017	-0.0093
30.0	0.0	0.0	0.07087	-0.2492	0.0588	0.06259	-0.0216
30.0	0.0	15.0	0.01127	-0.2253	0.04755	0.05169	-0.022
30.0	0.0	30.0	-0.0203	-0.2012	0.03953	0.042	-0.0126
60.0	0.0	0.0	-0.0687	0.04678	0.03105	0.04296	-0.012
60.0	0.0	15.0	-0.0349	-0.0892	0.04345	0.04816	-0.0158
60.0	0.0	30.0	-0.0604	-0.1256	0.03916	0.03918	-0.0228
90.0	0.0	0.0	-0.1253	-0.0364	0.03442	0.03888	-0.022
90.0	0.0	15.0	-0.1582	-0.0579	0.04649	0.04599	-0.0354
90.0	0.0	30.0	-0.1604	-0.067	0.04787	0.04818	-0.0415
120.0	0.0	0.0	-0.1695	-0.0021	0.04863	0.05189	-0.0384
120.0	0.0	15.0	-0.2219	-0.0137	0.06439	0.06249	-0.0505
120.0	0.0	30.0	-0.2669	0.00495	0.07211	0.07188	-0.0567

LASER DOPPLER MEASURED VELOCITIES IN UNIMPROVED SUMP

SAMPLE SIZE- 20,000.

LOCATION: BETWEEN BELL AND SIDE OF SUMP (SOUTH SIDE).

Z	X	Y	v	u	$\overline{v'^2}$	$\overline{u'^2}$	$\overline{u'v'}$
0.0	0.0	0.0	0.01872	0.03216	0.08062	0.07944	-0.0086
0.0	0.0	20.0	0.0449	0.03678	0.08446	0.08515	-0.0079
30.0	0.0	0.0	0.21011	0.24884	0.0509	0.05557	-0.0209
30.0	0.0	20.0	0.29608	0.28458	0.05846	0.06085	-0.0286
60.0	0.0	0.0	0.12216	0.3273	0.06563	0.06751	-0.0348
60.0	0.0	20.0	0.06092	0.34704	0.07991	0.08219	-0.0239
90.0	0.0	0.0	0.12401	0.34363	0.08142	0.08113	-0.0479
90.0	0.0	20.0	0.81213	-0.3286	0.09691	0.09493	-0.027
120.0	0.0	0.0	0.18395	0.3075	0.09901	0.10102	-0.0274
120.0	0.0	20.0	0.24773	0.19984	0.11813	0.10542	-0.0185

LASER DOPPLER MEASURED VELOCITIES IN UNIMPROVED SUMP

SAMPLE SIZE= 20,000.

LOCATION: VERTICAL PROFILES INTO INTAKE PIPE(XPIPE AND XUBELS2)

North intake.

Z	X	Y	v	u	$\overline{v'^2}$	$\overline{u'^2}$	$\overline{u'v'}$
0.0	0.0	0.0	-0.048	-0.6159	0.30108	0.15894	-0.0691
20.0	0.0	0.0	-0.1347	-0.6245	0.34748	0.14081	-0.0508
40.0	0.0	0.0	-0.367	-0.6274	0.28595	0.23924	-0.0395
60.0	0.0	0.0	-0.2605	-0.3115	0.29608	0.30092	0.02825
80.0	0.0	0.0	-0.3978	0.00372	0.27206	0.41844	0.05255
100.0	0.0	0.0	-0.0704	-0.0956	0.2558	0.35002	0.04461
120.0	0.0	0.0	0.00973	-0.2513	0.21755	0.30609	-0.0102

South intake: run 1.

0.0	0.0	0.0	-0.1774	-0.3454	0.05554	0.0471	0.00242
20.0	0.0	0.0	-0.3044	-0.2738	0.10103	0.04833	0.00494
40.0	0.0	0.0	-0.3817	-0.2925	0.10234	0.07287	-0.0008
60.0	0.0	0.0	-0.3587	-0.3962	0.10967	0.07388	-0.0003
80.0	0.0	0.0	-0.344	-0.3481	0.10107	0.09249	-0.0065
100.0	0.0	0.0	-0.3319	-0.2188	0.09684	0.09323	-0.0044
120.0	0.0	0.0	-0.271	-0.267	0.11783	0.12728	0.02984

South intake: run 2.

0.0	0.0	0.0	-0.1407	-0.0874	0.10218	0.0997	0.05355
20.0	0.0	0.0	-0.5006	-0.3642	0.03099	0.02987	-0.0074
40.0	0.0	0.0	-0.4391	-0.3675	0.03406	0.0382	-0.0043
60.0	0.0	0.0	-0.3327	-0.4176	0.03051	0.03656	0.00266
80.0	0.0	0.0	-0.3038	-0.3477	0.04405	0.05853	0.00286
100.0	0.0	0.0	-0.3056	-0.25	0.04782	0.06464	0.00828
120.0	0.0	0.0	-0.3229	-0.2194	0.04776	0.0661	0.01003

LASER DOPPLER MEASURED VELOCITIES IN UNIMPROVED SUMP

SAMPLE SIZE= 20.000.

LOCATION: GRID PATTERN BELOW INTAKE BELL

Section 1: Section nearest the back wall.

Z	X	Y	v	u	$\overline{v'^2}$	$\overline{u'^2}$	$\overline{u'v'}$
0.0	140.0	0.0	0.32222	-0.1975	0.00786	0.01377	-0.0028
0.0	140.0	35.0	0.3799	-0.2589	0.00732	0.01132	-0.0023
0.0	140.0	70.0	0.30625	-0.355	0.01238	0.00993	-0.0033
0.0	140.0	105.0	0.15702	-0.3785	0.01558	0.0055	0.00053
0.0	140.0	140.0	0.12335	-0.3054	0.01059	0.00581	0.00202
20.0	140.0	0.0	0.35957	-0.131	0.0054	0.01156	-0.0016
20.0	140.0	35.0	0.40981	-0.288	0.00591	0.00826	-0.003
20.0	140.0	70.0	0.26539	-0.4504	0.00931	0.00492	-0.0025
20.0	140.0	105.0	0.13018	-0.4487	0.00963	0.00372	0.0004
20.0	140.0	140.0	0.08595	-0.3249	0.00662	0.00371	0.00163
40.0	140.0	0.0	0.31463	-0.0571	0.00565	0.01203	-0.001
40.0	140.0	35.0	0.47473	-0.491	0.00927	0.00859	-0.0055
40.0	140.0	70.0	0.19925	-1.1203	0.0175	0.01261	-0.0086
40.0	140.0	105.0	-0.1249	-0.685	0.01905	0.01183	0.00431
40.0	140.0	140.0	0.07852	-0.2961	0.01114	0.01221	0.00548
55.0	140.0	0.0	0.24374	0.01389	0.01088	0.01563	0.00551
55.0	140.0	35.0	0.20178	0.1022	0.02355	0.02449	0.01566
55.0	140.0	70.0	0.00652	-0.3364	0.1216	0.18059	0.03154
55.0	140.0	105.0	0.233	0.00664	0.01095	0.01044	0.00428
55.0	140.0	140.0	0.16784	-0.1759	0.01961	0.02074	0.00485

Section 2:

0.0	105.0	0.0	0.35363	-0.1463	0.0236	0.03109	0.01513
0.0	105.0	35.0	0.41004	-0.1775	0.0195	0.02967	0.01004
0.0	105.0	70.0	0.25205	-0.2717	0.04951	0.04787	0.01992
0.0	105.0	105.0	0.01284	-0.4056	0.04038	0.03096	0.02357
0.0	105.0	140.0	-0.1195	-0.264	0.05067	0.04889	0.04126
20.0	105.0	0.0	0.47615	-0.0967	0.00843	0.0156	0.00266
20.0	105.0	35.0	0.53996	-0.171	0.027	0.04602	-0.003
20.0	105.0	70.0	0.39545	-0.4351	0.01829	0.02052	-0.0018
20.0	105.0	105.0	0.1106	-0.581	0.02653	0.0171	0.00931
20.0	105.0	140.0	-0.0441	-0.4511	0.02508	0.02535	0.02067
40.0	105.0	0.0	0.80354	-0.3011	0.00619	0.02398	-0.0029
40.0	105.0	35.0	0.69574	-0.3619	0.0152	0.03364	-0.0002
40.0	105.0	70.0	0.40035	-0.5378	0.01927	0.01815	-0.001
40.0	105.0	105.0	-0.1261	-0.6381	0.03321	0.02911	0.01219
40.0	105.0	140.0	-0.4021	-0.5478	0.05755	0.0591	0.04624
55.0	105.0	0.0	0.0213	0.03098	0.01711	0.01718	-0.0119
55.0	105.0	35.0	0.66918	-0.4524	0.03752	0.03398	-0.0164
55.0	105.0	70.0	0.30278	-0.5884	0.0241	0.0217	-0.0046
55.0	105.0	105.0	-0.4016	-0.5636	0.02788	0.02675	0.01649
55.0	105.0	140.0	-0.7015	-0.4009	0.04125	0.04289	-0.0116

Section 3:

0.0	70.0	0.0	0.2733	0.01885	0.02011	0.04146	0.01603
0.0	70.0	35.0	0.43339	0.26108	0.03739	0.05875	0.01664
0.0	70.0	70.0	0.40548	-0.2447	0.11099	0.11341	0.02379
0.0	70.0	105.0	-0.2066	-0.3902	0.04494	0.045	0.02858
0.0	70.0	140.0	-0.3014	-0.1808	0.07285	0.07385	0.06337
20.0	70.0	0.0	0.37797	0.03687	0.03201	0.04475	0.01866
20.0	70.0	35.0	0.38516	0.31705	0.04663	0.08906	0.03689
20.0	70.0	70.0	0.57197	-0.3564	0.09899	0.11196	-0.039
20.0	70.0	105.0	-0.0139	-0.5935	0.02641	0.02542	0.01137
20.0	70.0	140.0	-0.1353	-0.4217	0.04561	0.0495	0.0381
40.0	70.0	0.0	0.66041	0.19207	0.04245	0.0596	0.0213
40.0	70.0	35.0	0.40227	0.32383	0.06109	0.08381	0.03451
40.0	70.0	70.0	0.64056	-0.3726	0.08418	0.10656	-0.045
40.0	70.0	105.0	-0.1616	-0.6032	0.04227	0.04365	0.01879
40.0	70.0	140.0	-0.503	-0.2391	0.13593	0.14383	0.12078
55.0	70.0	0.0	0.01118	0.051	0.04813	0.03729	0.00994
55.0	70.0	35.0	0.05833	0.26384	0.12246	0.11934	0.01238
55.0	70.0	70.0	0.00604	0.06768	0.11294	0.11149	0.05002
55.0	70.0	105.0	-0.0699	-0.1535	0.07514	0.07008	0.04744
55.0	70.0	140.0	-0.033	0.06424	0.04941	0.05032	0.0254

Section 4:

0.0	35.0	0.0	0.11265	0.12843	0.0325	0.03668	0.02249
0.0	35.0	35.0	-0.0155	0.40528	0.0833	0.06443	0.04793
0.0	35.0	70.0	-0.6744	-0.1012	0.19157	0.29187	0.04206
0.0	35.0	105.0	-0.3815	-0.2961	0.0315	0.04154	0.0179
0.0	35.0	140.0	-0.2523	-0.229	0.02897	0.03471	0.02496
20.0	35.0	0.0	0.20052	0.1706	0.0473	0.06499	0.00015
20.0	35.0	35.0	0.0035	0.45036	0.12466	0.11811	0.09449
20.0	35.0	70.0	-0.5636	-0.4436	0.25082	0.27759	0.08971
20.0	35.0	105.0	-0.2054	-0.427	0.06277	0.06945	0.04707
20.0	35.0	140.0	-0.1476	-0.3182	0.06903	0.07571	0.06229
40.0	35.0	0.0	0.5848	0.24843	0.03407	0.03315	0.01353
40.0	35.0	35.0	0.28271	0.48229	0.0814	0.08384	0.0501
40.0	35.0	70.0	-0.5555	-0.2624	0.21629	0.22334	0.10902
40.0	35.0	105.0	-0.3109	-0.2161	0.11461	0.14681	0.08817
40.0	35.0	140.0	-0.3802	0.01924	0.15391	0.18681	0.14629
55.0	35.0	0.0	0.64573	0.35564	0.06681	0.06328	0.02235
55.0	35.0	35.0	0.56408	0.28825	0.05049	0.06914	0.02332
55.0	35.0	70.0	-0.4883	0.1238	0.26851	0.25696	0.14012
55.0	35.0	105.0	-0.2598	0.18616	0.14217	0.18615	0.10408
55.0	35.0	140.0	0.01477	0.04014	0.02044	0.02055	-0.008

Section S:	Section	farthest	from	back	wall.			
0.0	0.0	0.0	-0.0772	0.13583	0.02844	0.02642	0.01535	
0.0	0.0	35.0	-0.2015	0.17708	0.04986	0.03688	0.017	
0.0	0.0	70.0	-0.3362	0.03446	0.05219	0.06254	0.02273	
0.0	0.0	105.0	-0.3147	-0.1372	0.02237	0.03889	0.00944	
0.0	0.0	140.0	-0.2114	-0.177	0.01182	0.01919	0.00677	
20.0	0.0	0.0	0.08811	0.14799	0.02311	0.02849	0.00971	
20.0	0.0	35.0	-0.0401	0.37819	0.03353	0.02643	0.00831	
20.0	0.0	70.0	-0.192	0.19279	0.08041	0.09212	0.03176	
20.0	0.0	105.0	-0.2205	-0.0171	0.06493	0.07733	0.05069	
20.0	0.0	140.0	-0.1422	-0.1344	0.04996	0.05915	0.04239	
40.0	0.0	0.0	0.21987	0.13821	0.01488	0.01846	0.00777	
40.0	0.0	35.0	0.42426	0.652	0.02782	0.02553	0.01473	
40.0	0.0	70.0	0.03557	0.82776	0.0275	0.02287	0.00455	
40.0	0.0	105.0	-0.255	0.61477	0.04609	0.05317	0.02658	
40.0	0.0	140.0	-0.1029	0.08502	0.03327	0.03806	0.0233	
55.0	0.0	0.0	0.10553	-0.0027	0.01579	0.01769	0.00515	
55.0	0.0	35.0	0.06704	0.02227	0.10999	0.10564	-0.0131	
55.0	0.0	70.0	-0.1262	0.15569	0.05399	0.06138	0.05204	
55.0	0.0	105.0	0.00701	0.03579	0.03017	0.03057	0.00205	
55.0	0.0	140.0	0.03621	0.01277	0.02724	0.02843	0.01437	

7. APPENDIX C: Data for the improved sump.

Note: All data in units of metres and seconds.

LASER DOPPLER MEASURED VELOCITIES IN IMPROVED SUMP.

SAMPLE SIZE: 20000.

LOCATION: SECTION JUST IN FRONT OF BELLS (SECTION #1).

Z	X	Y	v	u	$\overline{v'^2}$	$\overline{u'^2}$	$\overline{u'v'}$
0	0	0	-0.0037	0.18662	0.00385	0.00453	0.00157
0	0	50	0.01893	0.28481	0.00566	0.00392	0.00195
0	0	150	-0.0638	0.14633	0.0023	0.00211	0.00113
0	0	200	-0.1558	0.14145	0.07395	0.07424	-0.0725
0	0	250	-0.02	0.03466	0.00427	0.00615	-0.0013
0	0	300	0.03608	0.03363	0.00276	0.0072	-0.001
0	0	350	0.07134	0.11582	0.00255	0.00385	-0.0001
0	0	400	0.0631	0.13006	0.00629	0.00602	0.00017
0	0	500	-0.0211	0.25138	0.00239	0.00194	0.00051
0	0	550	-0.0148	0.20144	0.0021	0.00269	0.00022
30	0	0	-0.0086	0.27213	0.03322	0.03388	-0.03
30	0	50	0.03153	0.27813	0.00282	0.00253	0.00056
30	0	150	-0.0682	0.15686	0.00203	0.00178	0.00095
30	0	200	-0.0833	0.14751	0.03581	0.0349	-0.0323
30	0	250	-0.0191	0.08177	0.00209	0.00215	-9E-05
30	0	300	0.01897	0.10424	0.01921	0.02042	-0.0177
30	0	350	0.0748	0.10504	0.00192	0.00284	-0.0006
30	0	400	0.06394	0.23749	0.00244	0.00235	-0.0003
30	0	500	-0.0197	0.28506	0.00252	0.00254	0.0003
30	0	550	-0.008	0.24579	0.00162	0.00257	-7E-05
60	0	0	0.00507	0.2186	0.00321	0.00421	0.00093
60	0	50	0.00176	0.18375	0.00465	0.00461	0.00189
60	0	150	-0.018	0.09323	0.00343	0.00416	0.00016
60	0	200	-0.0288	0.09017	0.00221	0.00264	0.00026
60	0	250	-0.0036	0.0563	0.00253	0.00341	-0.0003
60	0	300	0.02334	0.04328	0.01253	0.01749	-0.0119
60	0	350	0.06594	0.10591	0.00237	0.00431	-0.0011
60	0	400	0.03094	0.12497	0.00236	0.00308	-0.0003
60	0	500	0.01563	0.21466	0.00294	0.00244	-0.0006
60	0	550	0.00801	0.22859	0.00211	0.00295	-0.0005

90	0	0	0.00218	0.21749	0.00312	0.00534	0.00037
90	0	50	-0.0026	0.14995	0.00376	0.00447	0.00161
90	0	150	-0.0126	0.10794	0.02613	0.02542	-0.0214
90	0	200	-0.0081	0.0711	0.0024	0.00285	-0.0001
90	0	250	0.0006	0.05275	0.00311	0.0041	4.3E-05
90	0	300	0.01203	0.08504	0.00246	0.00247	-0.0002
90	0	350	0.00879	0.05009	0.00385	0.00533	-0.001
90	0	400	0.0041	0.09901	0.00482	0.00486	-0.003
90	0	500	-0.0192	0.19269	0.02723	0.02765	-0.0251
90	0	550	-0.0008	0.22339	0.00304	0.00405	-0.0001
120	0	0	-0.0035	0.18443	0.00589	0.00697	-0.0022
120	0	50	0.00143	0.1541	0.00636	0.00735	-0.0015
120	0	150	0.01845	0.10297	0.02208	0.02279	-0.0147
120	0	200	0.00478	0.07621	0.00483	0.00644	-0.0005
120	0	250	-0.0028	0.01982	0.00558	0.0076	-0.0003
120	0	300	0.00933	0.0416	0.00445	0.00643	-0.0012
120	0	350	0.00561	0.08771	0.00717	0.00811	0.00239
120	0	400	-0.0348	0.09144	0.00509	0.00549	-0.0018
120	0	500	-0.005	0.15541	0.00588	0.00636	-0.0033
120	0	550	0.00158	0.22976	0.01886	0.02039	0.0007

LASER DOPPLER MEASURED VELOCITIES IN IMPROVED SUMP.

SAMPLE SIZE: 20000.

LOCATION: SECTION IN MAIN SUMP (SECTION #2).

Z	X	Y	v	u	$\overline{v'^2}$	$\overline{u'^2}$	$\overline{u'v'}$
0	0	0	-0.0058	0.21448	0.00308	0.00423	0.0011
0	0	50	-0.015	0.1816	0.00345	0.00312	0.00081
0	0	100	-0.026	0.12994	0.00235	0.00213	0.00087
0	0	150	-0.0201	0.09385	0.00285	0.00284	0.00096
0	0	200	-0.0418	0.0634	0.0009	0.00095	-0.0005
0	0	250	-0.0046	0.06131	0.00151	0.00174	-0.0004
0	0	300	0.03988	0.07437	0.00127	0.00326	-0.0004
0	0	350	0.04768	0.08612	0.00767	0.00856	-0.0073
0	0	400	0.02813	0.14067	0.0168	0.01786	-0.0161
0	0	450	0.08498	0.15065	0.00212	0.00171	-0.0008
0	0	500	0.04592	0.1919	0.00251	0.00284	-0.0011
0	0	550	0.01528	0.1716	0.00223	0.00362	0.00027
30	0	0	-0.0021	0.22665	0.00305	0.00444	0.00083
30	0	50	-0.0065	0.18412	0.00295	0.00336	0.0013
30	0	100	-0.0256	0.12187	0.00315	0.00219	0.00099
30	0	150	-0.0228	0.09495	0.00141	0.0021	0.00019
30	0	200	-0.014	0.10364	0.00112	0.00118	-0.0001
30	0	250	0.01289	0.10007	0.00116	0.00199	-0.0003
30	0	300	0.02685	0.105	0.00119	0.00194	-0.0003
30	0	350	0.04532	0.1152	0.00149	0.00193	-0.0007
30	0	400	0.04337	0.11952	0.01372	0.01472	-0.0128
30	0	450	0.06809	0.15277	0.01474	0.01434	-0.0135
30	0	500	0.04464	0.18954	0.00128	0.00184	-0.0004
30	0	550	0.01689	0.20207	0.00159	0.00243	-9E-05
60	0	0	0.01371	0.19709	0.00266	0.00386	0.0002
60	0	50	-0.005	0.16019	0.00301	0.00327	0.00086
60	0	100	-0.01	0.1319	0.00305	0.00281	0.00097
60	0	150	-0.0221	0.09424	0.00197	0.00167	0.00018
60	0	200	-0.0049	0.09546	0.0016	0.00156	1.3E-05
60	0	250	0.00674	0.0601	0.00152	0.00204	-0.0004
60	0	300	0.03858	0.04486	0.0019	0.00274	-0.0005
60	0	350	0.04008	0.09288	0.01268	0.01291	-0.0115
60	0	400	0.04469	0.09893	0.00194	0.00203	-0.0011
60	0	450	0.03982	0.13803	0.00245	0.00239	-0.0012
60	0	500	0.03028	0.18785	0.00216	0.00389	-0.001
60	0	550	0.0192	0.21844	0.00165	0.00307	-0.0002

90	0	0	0.01053	0.20377	0.00731	0.00798	-0.0038
90	0	50	-0.0041	0.15642	0.00328	0.00343	-0.0005
90	0	100	-0.0117	0.11788	0.00252	0.00281	6.6E-05
90	0	150	-0.0042	0.09065	0.00273	0.00239	0.00027
90	0	200	-0.002	0.08904	0.00192	0.00209	-0.0001
90	0	250	0.01252	0.02649	0.00197	0.00411	-0.0004
90	0	300	-0.0031	0.07041	0.00204	0.00235	7.4E-05
90	0	350	0.02726	0.10626	0.01066	0.0113	-0.0094
90	0	400	0.03658	0.08465	0.00184	0.00169	-0.0002
90	0	450	0.02606	0.12795	0.00212	0.00255	-0.0009
90	0	500	0.02056	0.17576	0.00265	0.00327	-0.0009
90	0	550	0.02167	0.21672	0.00189	0.00272	-0.0004
120	0	0	0.05379	0.15497	0.05918	0.06016	-0.0225
120	0	50	0.02325	0.15114	0.0273	0.02842	-0.0189
120	0	100	0.0053	0.12249	0.0087	0.00865	-0.0039
120	0	150	-0.0201	0.08675	0.02034	0.01956	-0.0178
120	0	200	0.00238	0.06937	0.0034	0.00319	-0.0011
120	0	250	0.00819	0.05138	0.00232	0.00536	-0.0001
120	0	300	0.01862	0.08018	0.00194	0.00281	-0.0007
120	0	350	0.01534	0.06199	0.00243	0.00341	0.00022
120	0	400	0.01288	0.09834	0.01567	0.01619	-0.0142
120	0	450	0.00606	0.13787	0.00233	0.0034	-0.001
120	0	500	0.00932	0.17199	0.00227	0.00283	-0.0007
120	0	550	0.00461	0.2059	0.02631	0.02734	-9E-06

LASER DOPPLER MEASURED VELOCITIES IN IMPROVED SUMP.

SAMPLE SIZE: 20000.

LOCATION: SECTION IN MAIN SUMP (SECTION #3).

Z	X	Y	v	u	$\overline{v'^2}$	$\overline{u'^2}$	$\overline{u'v'}$
0	0	0	-0.0719	0.19677	0.02739	0.03026	-0.0237
0	0	50	-0.0401	0.14355	0.00283	0.00401	0.00093
0	0	100	-0.0455	0.12779	0.02807	0.02824	-0.0239
0	0	150	-0.0231	0.06634	0.00137	0.00152	-0.0004
0	0	200	-0.0034	0.06334	0.00171	0.00163	-0.0007
0	0	250	0.00288	0.06893	0.00148	0.00134	-0.0003
0	0	300	0.01442	0.09113	0.00176	0.00231	-0.0005
0	0	350	0.01211	0.06803	0.00161	0.00178	-0.0006
0	0	400	0.01761	0.08561	0.0014	0.00195	-0.0006
0	0	450	0.03712	0.10219	0.00206	0.00188	-0.0008
0	0	500	0.02888	0.13205	0.00247	0.00321	-0.0012
0	0	550	-7E-05	0.18328	0.02669	0.02782	-0.0255
30	0	0	-0.0092	0.20659	0.00284	0.00595	0.00075
30	0	50	-0.013	0.1621	0.00299	0.00409	0.00142
30	0	100	-0.0183	0.09733	0.00212	0.00234	0.00053
30	0	150	-0.0155	0.08379	0.00188	0.00199	0.00027
30	0	200	-0.0078	0.08189	0.00171	0.00135	-0.0001
30	0	250	-9E-05	0.08184	0.00143	0.00193	-0.0004
30	0	300	0.00761	0.09768	0.00149	0.00238	7.3E-05
30	0	350	0.02236	0.10328	0.00162	0.00242	-0.0002
30	0	400	0.00606	0.11717	0.01657	0.01654	-0.0149
30	0	450	0.03592	0.12575	0.00173	0.0024	-0.0007
30	0	500	0.03309	0.175	0.00192	0.00239	-0.0007
30	0	550	0.02913	0.21479	0.00194	0.0039	-0.0004
60	0	0	-0.0115	0.25152	0.00364	0.00606	0.00084
60	0	50	-0.0091	0.15447	0.0079	0.00864	-0.0017
60	0	100	-0.0266	0.11271	0.0026	0.00255	0.00023
60	0	150	-0.0133	0.093	0.00259	0.00237	-5E-05
60	0	200	-0.0173	0.08092	0.00199	0.00222	-0.0003
60	0	250	-0.0268	0.10728	0.02755	0.02768	-0.0258
60	0	300	-0.0254	0.13714	0.03831	0.03876	-0.0358
60	0	350	0.0006	0.10331	0.01754	0.01819	-0.0162
60	0	400	0.01988	0.09391	0.00222	0.00244	-0.0008
60	0	450	0.02487	0.11266	0.00234	0.00203	-0.0009
60	0	500	0.02658	0.13959	0.00295	0.00485	-0.0017
60	0	550	0.02761	0.20885	0.00204	0.00355	-0.0004

90	0	0	0.02285	0.20999	0.03413	0.03521	-0.0169
90	0	50	0.0008	0.16496	0.01518	0.01589	-0.0092
90	0	100	-0.0117	0.11878	0.0078	0.00852	-0.0042
90	0	150	-0.0061	0.09673	0.00518	0.00479	-0.002
90	0	200	-0.0058	0.07541	0.00477	0.00465	-0.0023
90	0	250	-0.0072	0.09836	0.00161	0.00281	-0.0001
90	0	300	0.01174	0.0719	0.00193	0.00207	-0.0003
90	0	350	0.01548	0.09072	0.00207	0.0029	-0.0001
90	0	400	0.0226	0.07493	0.00205	0.00217	-0.0002
90	0	450	0.01639	0.144	0.00804	0.00818	-0.0064
90	0	500	0.02659	0.16468	0.00285	0.00384	-0.0014
90	0	550	0.02332	0.22158	0.00228	0.004	-0.0005
120	0	0	-0.0138	0.04258	0.10499	0.10669	-0.0014
120	0	50	0.02114	0.14877	0.06765	0.06954	-0.0402
120	0	100	0.01037	0.17016	0.01131	0.01186	-0.0037
120	0	150	-0.002	0.09324	0.00351	0.00348	-0.0009
120	0	200	-0.0052	0.06836	0.00308	0.0037	-0.001
120	0	250	-0.0168	0.09832	0.02313	0.02321	-0.0209
120	0	300	0.00232	0.10781	0.01855	0.02067	-0.016
120	0	350	0.02622	0.09081	0.00293	0.00391	-0.0003
120	0	400	0.01794	0.09913	0.00234	0.00277	-0.0003
120	0	450	0.01688	0.13048	0.00291	0.0029	-0.0007
120	0	500	0.00756	0.20255	0.00255	0.00394	-0.001
120	0	550	0.01621	0.2167	0.0055	0.00752	0.00149

LASER DOPPLER MEASURED VELOCITIES IN IMPROVED SUMP

SAMPLE SIZE= 20,000.

LOCATION: BETWEEN INTAKE BELLS.

Z	X	Y	v	u	$\overline{v'^2}$	$\overline{u'^2}$	$\overline{u'v'}$
0	0	0	-0.1852	0.00556	0.00162	0.01171	0.00112
0	0	25	-0.1227	-0.0271	0.00171	0.00978	0.00062
0	0	50	-0.0432	-0.0428	0.00178	0.00705	-0.0005
0	0	75	0.00487	-0.0471	0.00149	0.00786	-0.0007
0	0	100	0.05847	-0.0131	0.00141	0.00772	-5E-05
0	0	125	0.12915	-0.0217	0.00164	0.00756	-0.0007
0	0	150	0.19648	-0.0517	0.0018	0.01034	0.00077
30	0	0	-0.2695	0.10058	0.00215	0.0079	-4E-05
30	0	25	-0.1002	0.05493	0.0018	0.00561	0.00015
30	0	50	-0.0422	0.02458	0.00205	0.00492	0.00035
30	0	75	0.0115	0.01743	0.00245	0.00533	-7E-05
30	0	100	0.05654	0.01355	0.00169	0.00385	-0.0002
30	0	125	0.10647	0.02341	0.00204	0.00486	0.00031
30	0	150	0.26048	0.025	0.00145	0.00385	-0.0007
60	0	0	0.02576	0.09334	0.00436	0.00281	-0.0001
60	0	25	-0.0193	0.05371	0.00496	0.00288	0.00077
60	0	50	0.02368	0.02968	0.00429	0.00363	-0.0018
60	0	75	-0.0032	0.01286	0.00317	0.00369	-0.001
60	0	100	0.04827	0.03682	0.00178	0.00239	-0.0003
60	0	125	0.05184	0.07099	0.01317	0.01391	-0.0125
60	0	150	0.01369	0.04044	0.00592	0.00622	-0.0015
90	0	0	0.05933	0.0841	0.00427	0.00304	0.00084
90	0	25	0.04457	0.05286	0.00573	0.00303	0.001
90	0	50	0.03205	0.02383	0.00471	0.00333	0.00021
90	0	75	0.02585	0.02085	0.00741	0.00337	-0.0006
90	0	100	0.03046	0.03857	0.01462	0.01426	-0.0121
90	0	125	-0.0255	0.05202	0.03222	0.02961	-0.0263
90	0	150	-0.0024	0.04927	0.00474	0.00542	-0.0013
120	0	0	0.06538	0.07942	0.00413	0.00368	0.00119
120	0	25	0.01542	0.03424	0.00569	0.00374	0.00151
120	0	50	0.02141	0.05236	0.00406	0.00387	0.00153
120	0	75	0.03114	0.04407	0.00357	0.00307	0.00048
120	0	100	0.01506	0.03267	0.00712	0.00388	-0.0001
120	0	125	-0.0188	0.04868	0.00483	0.004	-0.0006
120	0	150	-0.0391	0.02768	0.0039	0.0055	0.00024

LASER DOPPLER MEASURED VELOCITIES IN IMPROVED SUMP

SAMPLE SIZE= 20,000.

LOCATION: NEAR BACK WALL OF SUMP.

Z	X	Y	v	u	$\overline{v'^2}$	$\overline{u'^2}$	$\overline{u'v'}$
0	0	0	-0.0166	-0.0573	0.00478	0.003	0.00038
0	0	70	-0.0822	-0.0755	0.00296	0.0024	-0.0008
0	0	120	-0.0507	-0.0476	0.00405	0.005	-0.0022
0	0	170	-0.008	-0.0149	0.00199	0.00395	-0.0011
0	0	220	0.05389	-0.0574	0.00231	0.00217	-0.0011
0	0	270	0.07734	-0.0499	0.00267	0.00358	0.00032
0	0	320	0.06282	-0.0846	0.00356	0.00218	-0.0008
0	0	390	0.02065	-0.0549	0.00412	0.00393	-0.0029
30	0	0	0.04533	-0.0629	0.01773	0.01689	-0.0158
30	0	70	-0.0609	-0.102	0.0022	0.00094	-0.0002
30	0	120	-0.0653	0.00635	0.00379	0.00558	0.00014
30	0	170	-0.0123	-0.014	0.00347	0.00333	0.00035
30	0	220	0.04777	-0.0042	0.00331	0.00298	-0.0001
30	0	270	0.11105	-0.0494	0.0011	0.00137	0.0002
30	0	320	0.07075	-0.1222	0.00217	0.0013	0.00019
30	0	390	-0.0489	-0.0426	0.00222	0.00204	-0.0012
60	0	0	0.06991	-0.0238	0.00188	0.00197	0.00033
60	0	70	0.00021	-0.0948	0.00366	0.00242	0.0001
60	0	120	0.04722	0.05295	0.00553	0.00434	0.00122
60	0	170	-0.0004	-0.0073	0.00254	0.00253	0.0004
60	0	220	0.03526	-0.0008	0.00447	0.0037	-0.001
60	0	270	0.07768	-0.0153	0.00223	0.00321	-0.001
60	0	320	0.00113	-0.1154	0.00355	0.0024	-0.0007
60	0	390	-0.0581	-0.0036	0.00181	0.00247	-0.0007
90	0	0	0.06192	0.00536	0.00463	0.00541	0.00229
90	0	70	0.0265	-0.0528	0.00403	0.00364	0.00086
90	0	120	0.08664	0.0866	0.00574	0.00313	0.00086
90	0	170	0.05322	0.04195	0.00315	0.00232	0.00013
90	0	220	0.02162	0.01803	0.00514	0.00312	-0.0014
90	0	270	-0.0167	0.07337	0.00829	0.007	-0.0052
90	0	320	0.00168	-0.0499	0.00475	0.0064	-0.0013
90	0	390	-0.0588	0.02554	0.00216	0.00261	-0.0007
120	0	0	0.05562	0.0077	0.01084	0.0112	0.00484
120	0	70	0.04574	-0.0289	0.01002	0.00938	-0.0013
120	0	120	0.08537	0.08695	0.00529	0.00355	0.00078
120	0	170	0.08358	0.0364	0.00484	0.00336	0.00105
120	0	220	0.06028	-0.0017	0.00489	0.00319	-0.0013
120	0	270	-0.0231	0.08271	0.02727	0.02762	-0.0244
120	0	320	0.01893	-0.036	0.00837	0.00812	-0.0048
120	0	390	-0.0614	0.02623	0.0052	0.00571	-0.0033

LASER DOPPLER MEASURED VELOCITIES IN IMPROVED SUMP.

SAMPLE SIZE: 20000.

LOCATION: ON S. SIDE OF S. BELL.

Z	X	Y	v	u	$\overline{v'^2}$	$\overline{u'^2}$	$\overline{u'v'}$
0	0	0	0.14138	0.09667	0.00216	0.00697	3E-05
0	0	20	0.19909	0.10253	0.00175	0.00612	-0.0002
30	0	0	0.1764	0.18825	0.00144	0.00498	-0.0006
30	0	20	0.34936	0.19796	0.00157	0.00592	-0.0011
60	0	0	0.04849	0.18357	0.00255	0.0039	0.00023
60	0	20	-0.005	0.1648	0.00309	0.00488	0.00043
90	0	0	0.03485	0.18092	0.00279	0.00415	0.00018
90	0	20	0.01374	0.17647	0.00349	0.00531	0.00157
120	0	0	0.01836	0.16035	0.0177	0.01881	0.01002
120	0	20	0.02591	0.18178	0.00853	0.00983	0.00466

LASER DOPPLER MEASURED VELOCITIES IN IMPROVED SUMP.

SAMPLE SIZE: 20000.

LOCATION: ON N. SIDE OF N. BELL.

Z	X	Y	v	u	$\overline{v'^2}$	$\overline{u'^2}$	$\overline{u'v'}$
0	0	0	-0.1961	0.0785	0.00123	0.00325	-0.0003
0	0	20	-0.1377	0.06784	0.00134	0.00464	-0.0004
30	0	0	-0.2969	0.17899	0.00088	0.00534	0.00085
30	0	20	-0.1557	0.18297	0.00086	0.00257	0.0003
60	0	0	-0.012	0.18464	0.00245	0.00433	-0.0003
60	0	20	-0.0593	0.17644	0.00167	0.00319	-8E-05
90	0	0	-0.0082	0.17473	0.01018	0.01017	-0.0039
90	0	20	-0.024	0.16106	0.0081	0.00963	-0.0057
120	0	0	-0.0289	0.13233	0.02242	0.0225	-0.0011
120	0	20	0.00946	0.04263	0.08255	0.0841	-0.0242

LASER DOPPLER MEASURED VELOCITIES IN IMPROVED SUMP.

SAMPLE SIZE: 20000.

LOCATION: DIRECTLY UNDER INTAKE (#1).

Z	X	Y	v	u	$\overline{v'^2}$	$\overline{u'^2}$	$\overline{u'v'}$
0	0	0	-0.1377	-0.1291	0.00668	0.00706	-0.0004
30	0	0	-0.3248	0.0492	0.01064	0.02207	-0.0047
60	0	0	-0.4416	0.20271	0.02596	0.02833	-0.013
90	0	0	-0.1359	0.25201	0.01372	0.01682	-0.0002
120	0	0	-0.0755	0.21265	0.01784	0.02454	-0.0017

LASER DOPPLER MEASURED VELOCITIES IN IMPROVED SUMP.

SAMPLE SIZE: 20000.

LOCATION: DIRECTLY UNDER INTAKE (#2).

Z	X	Y	v	u	$\overline{v'^2}$	$\overline{u'^2}$	$\overline{u'v'}$
0	0	0	0.08102	-0.0925	0.00735	0.01005	0.00029
30	0	0	0.22272	-0.1083	0.0147	0.01708	-1E-04
60	0	0	0.34387	-0.0441	0.03311	0.03958	-0.0093
90	0	0	0.19169	-0.0432	0.05448	0.05861	-0.0048
120	0	0	0.08773	-0.0824	0.05046	0.05087	-0.0015

LASER DOPPLER MEASURED VELOCITIES IN IMPROVED SUMP.

SAMPLE SIZE: 20000.

LOCATION: SECTION UNDER INTAKE BELL

	Z	X	Y	v	u	$\overline{v'^2}$	$\overline{u'^2}$	$\overline{u'v'}$
1.	0	0	0	0.13452	-0.1341	0.00257	0.00335	0.00075
	0	0	35	0.12522	-0.1912	0.0023	0.00193	8.1E-05
	0	0	105	0.00435	-0.1917	0.00557	0.0047	-0.0026
	0	0	140	-0.0595	-0.1078	0.0065	0.00855	-0.0055
	20	0	0	0.17606	-0.092	0.00466	0.00442	0.00058
	20	0	35	0.16185	-0.2484	0.00185	0.00164	0.00063
	20	0	105	-0.1572	-0.2134	0.00576	0.00432	-0.0025
	20	0	140	-0.1819	-0.0432	0.00424	0.00609	-0.003
	40	0	0	0.15012	-0.1116	0.0038	0.00336	0.00085
	40	0	35	0.22557	-0.4876	0.00471	0.00223	0.00187
	40	0	105	-0.3323	-0.5	0.00524	0.00439	-0.0029
	40	0	140	-0.2101	-0.0256	0.0025	0.00522	-0.0022
	55	0	0	-0.0071	-0.0541	0.01072	0.0045	-0.0015
	55	0	35	-0.184	0.01861	0.00745	0.0057	-0.0011
	55	0	105	0.01389	0.1204	0.01306	0.00605	-0.0057
	55	0	140	-0.1229	0.06568	0.00242	0.00458	-0.0011
2.	0	0	0	0.20099	-0.0896	0.00263	0.01129	0.0024
	0	0	35	0.18369	-0.1713	0.00361	0.00462	0.00031
	0	0	105	-0.0585	-0.1724	0.00854	0.0117	-0.0029
	0	0	140	-0.1717	-0.0689	0.00368	0.01041	-0.0004
	20	0	0	0.26897	-0.1406	0.00479	0.0076	0.00189
	20	0	35	0.27539	-0.2104	0.00863	0.01054	-0.0014
	20	0	105	-0.231	-0.1598	0.01105	0.01382	0.00012
	20	0	140	-0.2868	0.05739	0.00275	0.01049	-0.0004
	40	0	0	0.48013	-0.2846	0.00876	0.01657	0.00225
	40	0	35	0.38987	-0.4797	0.01647	0.01108	0.00561
	40	0	105	-0.5103	-0.2459	0.0159	0.02616	-0.004
	40	0	140	-0.6324	-0.1499	0.00168	0.00903	-0.0017
	55	0	0	-0.0626	0.00543	0.00965	0.01761	0.00483
	55	0	35	0.41126	-0.6996	0.028	0.03212	0.01292
	55	0	105	-0.5929	-0.5926	0.0097	0.01394	-0.0038
	55	0	140	-0.019	0.18277	0.00264	0.00433	-0.0004

	Z	X	Y	v	u	$\overline{v'^2}$	$\overline{u'^2}$	$\overline{u'v'}$
3.	0	0	0	0.23391	0.02315	0.00188	0.00937	0.00074
	0	0	35	0.19581	-0.0087	0.00507	0.00731	-0.0006
	0	0	105	-0.1384	-0.0424	0.00796	0.00913	0.00186
	0	0	140	-0.2371	0.14443	0.03259	0.03421	-0.0306
	20	0	0	0.32786	0.00521	0.00424	0.02226	0.00081
	20	0	35	0.26482	0.06534	0.00746	0.01517	-0.0022
	20	0	105	-0.2034	0.14699	0.00493	0.01018	-0.0012
	20	0	140	-0.2886	0.204	0.00181	0.005	0.00023
	40	0	0	0.86887	-0.1525	0.00331	0.03247	-0.0019
	40	0	35	0.45262	0.01895	0.01906	0.02723	-0.0018
	40	0	105	-0.3407	0.19154	0.01021	0.00913	-0.0009
	40	0	140	-0.7119	0.153	0.00354	0.00863	0.00117
	55	0	0	0.10593	0.00913	0.0351	0.02097	0.01032
	55	0	35	0.56064	-0.0805	0.02632	0.0327	-0.0038
	55	0	105	-0.4727	0.20587	0.00869	0.01136	0.00069
	55	0	140	-0.8987	0.141	0.0069	0.01605	0.00351
4.	0	0	0	0.23144	0.08387	0.00214	0.00812	-0.0024
	0	0	35	0.06808	0.10071	0.01807	0.01715	-0.009
	0	0	105	-0.1089	0.19705	0.03627	0.03723	-0.0299
	0	0	140	-0.1504	0.23838	0.00216	0.00261	0.00047
	20	0	0	0.29959	0.22107	0.00233	0.00432	-0.0017
	20	0	35	0.18386	0.22368	0.00594	0.00715	-0.0028
	20	0	105	-0.0838	0.39282	0.00443	0.00349	0.00033
	20	0	140	-0.2254	0.33367	0.01751	0.01838	-0.0149
	40	0	0	0.72412	0.42964	0.00432	0.00806	-0.0034
	40	0	35	0.34362	0.36136	0.01041	0.01015	-0.0028
	40	0	105	-0.3193	0.49782	0.00609	0.00702	0.00126
	40	0	140	-0.4997	0.44832	0.00233	0.00344	0.00103
	55	0	0	0.52479	0.26737	0.22268	0.06508	0.108
	55	0	35	0.44702	0.47166	0.00925	0.00886	-0.0033
	55	0	105	-0.5119	0.60992	0.00593	0.00748	0.00225
	55	0	140	-0.6432	0.4879	0.01012	0.01173	-0.0047
5.	0	0	0	0.14786	0.15296	0.01329	0.01533	-0.0112
	0	0	35	0.11995	0.21181	0.00437	0.00445	-0.0009
	0	0	105	-5E-05	0.31196	0.00317	0.00367	2.5E-05
	0	0	140	-0.0774	0.27295	0.00339	0.00255	0.00117
	20	0	0	0.15588	0.22508	0.02021	0.02259	-0.02
	20	0	35	0.1521	0.31952	0.00254	0.00298	-0.0008
	20	0	105	-0.0546	0.41133	0.0026	0.00202	4E-05
	20	0	140	-0.1153	0.29158	0.00291	0.00294	0.00167
	40	0	0	0.17905	0.27757	0.0238	0.02465	-0.0231
	40	0	35	0.3822	0.70131	0.00526	0.00496	-0.0023
	40	0	105	-0.2954	0.77628	0.00559	0.0032	0.00082
	40	0	140	-0.1255	0.34266	0.00249	0.00222	0.00057
	55	0	0	0.03973	0.12081	0.00386	0.0039	-0.0015
	55	0	35	0.11431	0.38028	0.0368	0.0237	0.00892
	55	0	105	-0.2389	0.70049	0.01391	0.01155	-0.008
	55	0	140	-0.1298	0.34766	0.00213	0.00182	0.00031